Alma Mater Studiorum – Università di Bologna

DOTTORATO DI RICERCA IN

Scienze della Terra, della Vita e dell'Ambiente

Ciclo XXXI

Settore Concorsuale: 05/C1 - ECOLOGIA

Settore Scientifico Disciplinare: BIO/07 - ECOLOGIA

Growth and shell properties variations in the clam *Chamelea gallina* along a latitudinal gradient of environmental parameters

Presentata da: Arianna Mancuso

Coordinatore Dottorato
Prof. Giulio Viola

Supervisore
Prof. Stefano Goffredo

Esame finale anno 2019

“Look deep into nature,
and then you will understand
everything better”

Albert Einstein

To you,
mammut and paput

ABSTRACT

Important ecological interactions between the organisms and their environment can be prompted by the studies along the latitudinal gradients, where it is possible to explore the varying environmental pressures on both biological and evolutionary processes. Thermal conditions vary with latitude and the ability to understand the relationship between growth and temperature is important because global climate change will be a thermal challenge to most ectotherms. Molluscs are particularly sensitive to different environmental parameters, showing macroscale shell morphology variations in response to environmental parameters. The aim of this thesis is to investigate variations in shell skeletal properties, mineral composition and growth along a latitudinal gradient (~400 km) in the Adriatic Sea (Italian cost) in relation to different environmental parameters. Shell morphology of the most irradiated and warmest populations was characterized by lighter, thinner, more porous and fragile shells, likely affecting the economic aspects of fisheries and the survival of the species. No variation was observed in shell $CaCO_3$ polymorphism (100% aragonite) or in compositional and textural shell parameters, indicating no effect of the environmental parameters on the basic biomineralization processes. Moreover, *C. gallina* showed an increase in shell linear extension and net calcification rates towards South where warmer seawater, low fluctuations in salinity and high diversity of phytoplankton seem to be the most favourable environmental conditions for its growth. Whereas, prolonged exposure to low salinity, eutrophic habitats and the presence of silt and clay in the substrate seem to stress the clams affecting shell growth, and this habitat conditions heavily characterise the northern sites which are under the influence of Po river delta. Because of the importance of *C. gallina* as commercial resource in the Adriatic Sea, variations in shell properties and in growth rates along the latitudinal gradient may have economic implications for fisheries and the observations from this research could help to guarantee the biological and economic sustainability of this resource.

INDEX

Chapter 1

General introduction

The environment plays a key role in growth and development of organisms. There is a strong suggestion that organisms and communities present adaptive and acclimation mechanisms and significant flexibility to respond of environmental changes (Buddemeier & Smith, 1999). Moreover, many organisms have the ability to express different observable phenotypes in response to changes of biotic and abiotic environmental parameters. This process is referred as phenotypic plasticity, which is the ability of organism to produce a range of relatively fit phenotypes by altering morphology, state, movement, life history or behaviour in relation to variations in environmental parameters (DeWitt & Scheiner, 2004; Beldade, Mateus, & Keller, 2011; Gilbert, 2012). The ability of organisms to produce different phenotypes under different environmental parameters in natural populations is a critical issue to understand how species might face future changes.

Calcifying marine organisms (e.g. corals, echinoderms and molluscs) are likely to be among the most susceptible organisms to changing environmental conditions (DeWitt & Scheiner, 2004) including anthropogenic climate change (Laing, Utting, & Kilada, 1987; Levitan, 1991; DeWitt, 1998; Carballo et al., 2006; Harley et al., 2006). These organisms make extensive use of calcium carbonate ($CaCO_3$), one of the most abundant minerals in nature, as a structural and/or protective material through the biomineralization process (Addadi & Weiner, 2014). Morphology, mineralogy and chemistry of biologically formed $CaCO_3$ skeletons are largely dependent on both biology and environmental surroundings, with structural proteins and enzymes that act as keys to controlling internal conditions and that respond to external environmental parameters (Falini et al., 1996). Investigate the effects of environmental conditions on natural populations is also a critical issue to understand how species will can face future changes, predicted by Intergovernmental Panel on Climate change (IPCC). Changes in the calcium carbonate saturation state, with a subsequent decrease in the concentration of available carbonate ions in seawater and higher dissolution rates of $CaCO_3$ (especially its more soluble polymorph aragonite), as well as high-magnesium calcite are expected results of ocean acidification trends (IPCC, 2014; Morse, Andersson, & Mackenzie, 2006; Tyrrell, 2008; Zeebe, 2012). These will

result in a general decrease in the production and accumulation of marine biogenic carbonates, less favourable conditions for biogenic calcification and severe impacts on marine calcifiers and marine biogenic processes, with different calcareous organisms being affected in different ways. Mediterranean corals show a decrease in calcification (Goffredo et al., 2009), abundance (Goffredo et al., 2007) and the stability of population structure (Goffredo et al., 2008) with increasing temperature. Elevated temperatures have been also reported to disrupt the metabolism, growth, fitness and calcification in some gastropod species (Sokolova & Pörtner, 2001; Melatunan et al., 2013; Irie & Morimoto, 2016). Furthermore, in some bivalve species, larvae are found to be more sensitive to increases in temperature than juvenile stages, showing depressed survival, development and growth (Talmage & Gobler, 2011; Barton et al., 2012). Producers of aragonite and high-magnesium calcite are of special concern due to the much higher solubility of these forms (Kleypas et al., 2006; Hall-Spencer et al., 2008; Ries, 2011). Moreover, temperature rise is expected to accompany current ocean acidification with severe impacts already documented for several marine areas (Barnes & Peck, 2008; Coma et al., 2009; Schofield et al., 2010).

Beside ocean acidification and warming, other environmental factors, such as solar radiation, salinity, oxygen and food availability, all can influence energy expenditure in marine organisms, especially in temperate seas, where marine organisms show marked seasonal patterns in growth, reproduction and abundance (Miller, 1995; Reum et al., 2014; Rodolfo-Metalpa et al., 2008; Przeslawski, Byrne, & Mellin, 2015; Cole et al., 2016). To study the effect of environmental conditions on marine organisms, latitudinal gradients are useful natural laboratories, influencing variations in solar radiation and sea surface temperature and allowing to examine long-term effects on populations of the same species, adapted to different environmental conditions (Jansen et al., 2007; Watson et al., 2012).

Molluscs and environment

Molluscs are among the most diverse and abundant animal groups, inhabiting many aquatic and terrestrial environments. They are important ecosystem engineers, helping to structure aquatic bottom environments and providing habitat, protection and food to a wide array of other taxa. Molluscs have been historically important to humans in many ways and are today an economically important group worldwide. As major calcareous organisms with an extensive fossil record, they can provide important information on past climate events and oceanic changes, thus, increasing our understanding of predicted future changes (Fortunato, 2016).

During the course of evolution, organisms used the most common mineral to build their skeletons, thus avoiding extra costs (Knoll, 2003; Murdock & Donoghue, 2011; Marin, 2012). Mollusc shells originated during the so-called "aragonite seas" and most species kept using aragonite as the major polymorph, even though ocean chemistry changed and biomineralization became costlier (Bengtson & Morris, 1992; Porter, 2010). Molluscs biomineralize $CaCO_3$ in the form of both calcite and aragonite and many species add Mg-calcite in different percentages (Chave, 1954; Addadi et al., 2006; Furuhashi et al., 2009; Marin, 2012). There are some important differences in the way molluscs deposit shell biominerals in relation to the environment isotopic contents. Whereas most aquatic species build their shells in isotopic equilibrium with the surrounding water, land species use oxygen from ingested water and carbon from both respiratory CO_2 and food plant source for their shells (Grossman & Ku, 1986; McConnaughey, 1989; Carré et al., 2006). Molluscs species that deposit biominerals not in oxygen isotope equilibrium with the surrounding seawater, may control their shell isotopic contents raising the question of the so called "vital effects" (Chave, 1954; Ziveri et al., 2003; Carré et al., 2006). Vital effects are defined as biological processes, such as metabolism or physiology, overriding environmental signals, as recorded in geochemical signatures in biominerals (Weiner & Dove, 2003; Pérez-Huerta & Andrus, 2010). The ability to build

skeletons from $CaCO_3$ polymorphs and Mg-calcite makes molluscs very sensitive to changes in ocean chemistry with possible dramatic consequences for this group and the aquatic systems where they live(Gaylord et al., 2011; Doney et al., 2012; Gazeau et al., 2013).

Due to their high diversity, abundance, constant presence across wide latitudinal gradients and good preservation in the fossil record and archaeological deposits, molluscs can serve as a potential recorder of environmental changes in most oceanic regions (Richardson, 2001; Hallmann et al., 2013; Prendergast et al., 2013). Mollusc growth patterns and isotopic composition can be used to document short-term ecological changes (Witbaard, 1996; Carroll, Romanek, & Paddock, 2006) as well as long-term temporal registry of the conditions at the time of deposition (Davenport, 1938; Dettman et al., 2004; Schoene & Surge, 2012).

The bivalve *Chamelea gallina*

Chamelea gallina (Linnaeus 1758) is a common infaunal clam of the Veneridae family (Bivalvia: Lamellibranchiata: Veneridae), locally known in Italy as "vongola" or "lupino". *C. gallina* is distributed from the Portuguese south coast to the Mediterranean, including the Black Sea (Backeljau et al., 1994; Poppe & Goto, 1993). In particular, it is abundant in the Adriatic sea, where it inhabits well-sorted fine sand biocoenosis at 3-7 m depth and has a considerable economical relevance for fishery(Froglia, 1989; Ramón & Richardson, 1992).

Between 1970 and 1980, the development of clam fisheries based on hydraulic dredges led to an over-exploitation of this resource with a dramatic decrease in clam population density associated with a reduction in the number of clams over 25 mm long, the minimum legal marketable size, although the maximum length recorded for this species is about 50 mm(Froglia, 1989). In Italy, in the late 1970s the fishery yielded 80,000-100,000 metric tons, however currently it does not exceed 20,000 metric tons (Romanelli, Cordisco, & Giovanardi, 2009). *Chamelea gallina* appears to exhibit density-dependent growth

rate and mortality: years of exceptional recruitment may lead the following year to very poor stocks of large individuals due to juvenile mortality, or to very large stocks of small individuals due to growth inhibition and resource competition. It has been reported that a proportion of the population reaches maturity by the end of the first year of age (18-19 mm) and all individuals are ready to reproduce within the second year (Morello et al., 2005). Recently, there is growing concern for the survival of bivalve communities, because large inter-annual fluctuations in stock abundance, periodic recruitment failure and irregular mortality events threaten the biological and economic sustainability of this fishery, especially in the Adriatic Sea (Ramón & Richardson, 1992; Romanelli et al., 2009).

In the Adriatic Sea, the fishery is divided into Districts (Compartimenti Marittimi) and for each District a fixed number of dredgers are licensed to operate. Reduction in catches spurred the Italian government to impose a number of management regulations on gear characteristics (technical measures), the number of fishing days per year (fishing effort or inputs) and individual catch quota per day (catches or outputs). Within the scope of general regulations issued by the Italian Directorate for Fisheries, the local Consortium of Clam Fishermen can add additional rules such as diminishing the daily individual quota or imposition of a rotation of the fishing areas inside the District. The scientific advice for such regulations is based mainly on resource assessment surveys conducted once per year by scientific institutions (e.g., Laboratory of Marine Biology and Fishery of Fano, University of Bologna and ISMAR-CNR, Institute of Marine Sciences of the National Research Council). These surveys provide an estimate of relative abundance of the resource at sea in terms of biomass and an estimate of the size-distribution of the clam populations. Morello (2011) presented the outcomes of fishery-independent surveys conducted in the Ancona (AN) and S. Benedetto (SB) Maritime Districts from 1984 to 2001 to assess the *C. gallina* stock. The study revealed a considerable year-to-year fluctuations and the results are indicative of a resource and fleet heavily dependent on stochastic substantial recruitment events. Large recruitment events followed by significant natural mortality episodes and the paucity of older individuals may suggest a shift in the allocation of energy, from growth to reproduction.

C. gallina reaches sexual maturity at sizes between 13 and 18 mm (European Parliament study-PECH Committee on the Clam Fishery sector; Scarcella & Cabanelas, 2016). Until January 2017, the European Union Council Regulation 850/98 set the minimum landing size (MLS) for *C. gallina* at 25 mm for the Mediterranean Council Regulation 1967/2006. As consequence, the Turkish clam with a minimum legal size of 17 mm generated market competition which derived in socioeconomic impact for the Adriatic Sea clam fisheries sector. The management measure based on MLS has often generated controversy in the sector having requested in several occasions a reduction in the legal size based on new scientific studies indicating lower sizes of sexual maturity. Recently, according to article 15 comma 10 Reg. EU 1380/13, MLS has been reduced to 22 mm in the Adriatic Sea. This size is ~22% higher that the size at first maturity (18 mm) and it is thus in line with the sexual maturity to ensure sustainability of resource.

Studies on this species are of critical importance for developing appropriate management strategies for one of the most important economic sectors of southern EU countries. The Food and Agriculture Organization of the United Nations (FAO) reports a mean annual total catch of about 60,000 tons (2004-2013) in the Atlantic, Mediterranean and Black Sea, with the largest catches in Italy (22,000 tons) and Turkey (33,000 tons).

REFERENCES

Addadi, L., Joester, D., Nudelman, F., & Weiner, S. (2006). Mollusk shell formation: A source of new concepts for understanding biomineralization processes. *Chemistry - A European Journal 12(4),* 980-987

Addadi, L., & Weiner, S. (2014). Biomineralization: Mineral formation by organisms. *Physica Scripta 89(9), 098003*

Backeljau, T., Bouchet, P., Gofas, S., & Bruyn, L. De. (1994). Genetic variation, systematics and distribution of the venerid clam Chamelea gallina. *Journal of the Marine Biological Association of the United Kingdom*, *74*(01), 211

Barnes, D. K. A., & Peck, L. S. (2008). Vulnerability of Antarctic shelf biodiversity to predicted regional warming. *Climate Research 37(2-3),* 149-163

Barton, A., Hales, B., Waldbusser, G. G., Langdon, C., & Feely, R. A. (2012). The Pacific oyster, *Crassostrea gigas* , shows negative correlation to naturally elevated carbon dioxide levels: Implications for near-term ocean acidification effects. *Limnology and Oceanography*, *57*(3), 698–710

Beldade, P., Mateus, A. R. A., & Keller, R. A. (2011). Evolution and molecular mechanisms of adaptive developmental plasticity. *Molecular Ecology 20(7),* 1347-1363

Bengtson, S., & Morris, S. C. (1992). Early Radiation of Biomineralizing Phyla (pp. 447–481). Springer, Boston, MA

Buddemeier, R. W., & Smith, S. V. (1999). Coral adaptation and acclimatization: A most ingenious paradox. *American Zoologist 39(1),* 1-9*.*

Carballo, J. L., Ávila, E., Enríquez, S., & Camacho, L. (2006). Phenotypic plasticity in a mutualistic association between the sponge *Haliclona caerulea* and the calcareous macroalga *Jania adherens* induced by transplanting experiments. I: Morphological responses of the sponge. *Marine Biology 148(3),* 467

Carré, M., Bentaleb, I., Bruguier, O., Ordinola, E., Barrett, N. T., & Fontugne, M. (2006). Calcification rate influence on trace element concentrations in aragonitic bivalve shells: Evidences and mechanisms. *Geochimica et Cosmochimica Acta*, *70*(19), 4906–4920

Carroll, M., Romanek, C., & Paddock, L. (2006). The relationship between the hydrogen and oxygen isotopes of freshwater bivalve shells and their home streams. *Chemical Geology 234(3-4),* 211-222

Chave, K. E. (1954). Aspects of the biogeochemistry of Magnesum 1. Calcareous marine organisms. *The Journal of Geology 62(3),* 266-283

Cole, V. J., Parker, L. M., O'Connor, S. J., O'Connor, W. A., Scanes, E., Byrne, M., &

Ross, P. M. (2016). Effects of multiple climate change stressors: ocean acidification interacts with warming, hyposalinity, and low food supply on the larvae of the brooding flat oyster *Ostrea angasi*. *Marine Biology 163(5),* 125

Coma, R., Ribes, M., Serrano, E., Jimenez, E., Salat, J., & Pascual, J. (2009). Global warming-enhanced stratification and mass mortality events in the Mediterranean. *Proceedings of the National Academy of Sciences, pnas-0805801106*

Davenport, C. B. (1938). Growth lines in fossil Pectens as indicators of past climates. *Journal of Paleontology*.

Dettman, D. L., Flessa, K. W., Roopnarine, P. D., Schöne, B. R., & Goodwin, D. H. (2004). The use of oxygen isotope variation in shells of estuarine mollusks as a quantitative record of seasonal and annual Colorado River discharge. *Geochimica et Cosmochimica Acta 68(6),* 1253-1263

DeWitt, T. J. (1998). Costs and limits of phenotypic plasticity: Tests with predator-induced morphology and life history in a freshwater snail. *Journal of Evolutionary Biology 11(4),* 465-480

DeWitt, T. J., & Scheiner, S. M. (2004). *Phenotypic plasticity : functional and conceptual approaches*. Oxford University Press

Doney, S. C., Ruckelshaus, M., Emmett Duffy, J., Barry, J. P., Chan, F., English, C. A., … Talley, L. D. (2012). Climate Change Impacts on Marine Ecosystems

Falini, G., Albeck, S., Weiner, S., & Addadi, L. (1996). Control of aragonite or calcite polymorphism by mollusk shell macromolecules. *Science 271(5245),* 67-69

Fortunato, H. (2016). Mollusks: Tools in Environmental and Climate Research. *American Malacological Bulletin 33*(2), 310–324

Froglia, C. (1989). Fisheries with hydraulic dredges in the Adriatic Sea. J. Caddy (Ed). Marine invertebrate fisheries. J. wiley, pp. 507-524

Furuhashi, T., Schwarzinger, C., Miksik, I., Smrz, M., & Beran, A. (2009). Molluscan shell evolution with review of shell calcification hypothesis. *Comparative Biochemistry and Physiology - B Biochemistry and Molecular Biology 154(3),* 351-371

Gaylord, B., Hill, T. M., Sanford, E., Lenz, E. A., Jacobs, L. A., Sato, K. N., … Hettinger, A. (2011). Functional impacts of ocean acidification in an ecologically critical foundation species. *Journal of Experimental Biology 214(15),* 2586-2594

Gazeau, F., Parker, L. M., Comeau, S., Gattuso, J. P., O'Connor, W. A., Martin, S., … Ross, P. M. (2013). Impacts of ocean acidification on marine shelled molluscs. *Marine Biology 160(8),* 2207-2245

Gilbert, S. F. (2012). Ecological developmental biology: Environmental signals for

normal animal development. *Evolution and Development 14(1),* 20-28

Goffredo, S., Caroselli, E., Mattioli, G., Pignotti, E., Dubinsky, Z., & Zaccanti, F. (2009). Inferred level of calcification decreases along an increasing temperature gradient in a Mediterranean endemic coral. *Limnology and Oceanography 54*(3), 930-937

Goffredo, S., Caroselli, E., Mattioli, G., Pignotti, E., & Zaccanti, F. (2008). Relationships between growth, population structure and sea surface temperature in the temperate solitary coral *Balanophyllia europaea* (Scleractinia, Dendrophylliidae). *Coral Reefs*, *27*(3), 623–632

Goffredo, S., Caroselli, E., Pignotti, E., Mattioli, G., & Zaccanti, F. (2007). Variation in biometry and population density of solitary corals with solar radiation and sea surface temperature in the Mediterranean Sea. *Marine Biology 152(2),* 351-361

Grossman, E. L., & Ku, T. L. (1986). Oxygen and carbon isotope fractionation in biogenic aragonite: Temperature effects. *Chemical Geology: Isotope Geoscience Section 59,* 59-74

Hall-Spencer, J. M., Rodolfo-Metalpa, R., Martin, S., Ransome, E., Fine, M., Turner, S. M., … Buia, M. C. (2008). Volcanic carbon dioxide vents show ecosystem effects of ocean acidification. *Nature 454(7200),* 96

Hallmann, N., Burchell, M., Brewster, N., Martindale, A., & Schöne, B. R. (2013). Holocene climate and seasonality of shell collection at the Dundas Islands Group, northern British Columbia, Canada-A bivalve sclerochronological approach. *Palaeogeography, Palaeoclimatology, Palaeoecology 373,* 163-172

Harley, C. D. G., Hughes, A. R., Hultgren, K. M., Miner, B. G., Sorte, C. J. B., Thornber, C. S., … Williams, S. L. (2006). The impacts of climate change in coastal marine systems. *Ecology Letters 9(2),* 228-241

IPCC. (2014). *Climate Change 2014*. *Climate Change 2014: Synthesis Report*

Irie, T., & Morimoto, N. (2016). Intraspecific variations in shell calcification across thermal window and within constant temperatures: Experimental study on an intertidal gastropod Monetaria annulus. *Journal of Experimental Marine Biology and Ecology 483*, 130–138

Jansen, J. M., Pronker, A. E., Kube, S., Sokolowski, A., Sola, J. C., Marquiegui, M. A., … Hummel, H. (2007). Geographic and seasonal patterns and limits on the adaptive response to temperature of European Mytilus spp. and *Macoma balthica* populations. *Oecologia 154(1),* 23-34

Kleypas, J., Feely, R., Fabry, V., Langdon, C., Sabine, C., & Robbins, L. (2006). Impacts of Ocean Acidification on Coral Reefs and Other Marine Calcifiers : A Guide for Future Research. Report of a workshop held 18-20 April 2005, St. Petersburg

FL, sponsored by NSF, NOAA and the U.S. Geological Survey

Knoll, A. H. (2003). Biomineralization and Evolutionary History. *Reviews in Mineralogy and Geochemistry 54(1),* 329-356

Laing, I., Utting, S. D., & Kilada, R. W. S. (1987). Interactive effect of diet and temperature on the growth of juvenile clams. *Journal of Experimental Marine Biology and Ecology 113(1),* 23-38

Levitan, D. R. (1991). Skeletal changes in the test and jaws of the sea urchin *Diadema antillarum* in response to food limitation. *Marine Biology 111(3),* 431-435

Marin, F. (2012). The formation and mineralization of mollusk shell. *Frontiers in Bioscience 4(1099),* 125

McConnaughey, T. (1989). ^{13}C and ^{18}O isotopic disequilibrium in biological carbonates: I. Patterns. *Geochimica et Cosmochimica Acta 53(1),* 151-162

Melatunan, S., Calosi, P., Rundle, S., Widdicombe, S., & Moody, A. (2013). Effects of ocean acidification and elevated temperature on shell plasticity and its energetic basis in an intertidal gastropod. *Marine Ecology Progress Series*, *472*, 155–168

Miller, M. W. (1995). Growth of a temperate coral: Effects of temperature, light, depth, and heterotrophy. *Marine Ecology Progress Series 122,* 217-225

Morello, E. B., Froglia, C., Atkinson, R. J. A., & Moore, P. G. (2005). Hydraulic dredge discards of the clam (*Chamelea gallina*) fishery in the western Adriatic Sea, Italy. *Fisheries Research 76(3),* 430-444

Morello, E., Martinelli, M., Antolini, B., Gramitto, M., Arneri, E., & Froglia, C. (2011). Population dynamics of the clam, *Chamelea gallina*, in the Adriatic Sea (Italy). *Marine Research at CNR*, 1907–1921.

Morse, J. W., Andersson, A. J., & Mackenzie, F. T. (2006). Initial responses of carbonate-rich shelf sediments to rising atmospheric pCO_2 and "ocean acidification": Role of high Mg-calcites. *Geochimica et Cosmochimica Acta 70(23),* 5814-5830

Murdock, D. J. E., & Donoghue, P. C. J. (2011). Evolutionary origins of animal skeletal biomineralization. In *Cells Tissues Organs 194(2-4),* 98-10*2*

Nudelman, F., Gotliv, B. A., Addadi, L., & Weiner, S. (2006). Mollusk shell formation: Mapping the distribution of organic matrix components underlying a single aragonitic tablet in nacre. *Journal of Structural Biology 153(2),* 176-187

Pérez-Huerta, A., & Andrus, C. F. T. (2010). Vital effects in the context of biomineralization. In *Workshop on Biominerals and Biomineralization Processes* (pp. 35–45). Sociedad Española de Mineralogía Madrid.

Poppe, GT and Goto, Y. (1993). European Seashells, vol. 2. *Verlag Christa Hemmen, Wiesbaden*, 221.

Porter, S. M. (2010). Calcite and aragonite seas and the de novo acquisition of carbonate skeletons. *Geobiology 8(4),* 256-277

Prendergast, A. L., Azzopardi, M., O'Connell, T. C., Hunt, C., Barker, G., & Stevens, R. E. (2013). Oxygen isotopes from *Phorcus (Osilinus) turbinatus* shells as a proxy for sea surface temperature in the central Mediterranean: A case study from Malta. *Chemical Geology 345,* 77-86

Przeslawski, R., Byrne, M., & Mellin, C. (2015). A review and meta-analysis of the effects of multiple abiotic stressors on marine embryos and larvae. *Global Change Biology 21(6),* 2122-2140

Ramón, M., & Richardson, C. A. (1992). Age determination and shell growth of *Chamelea gallina* (Bivalvia: Veneridae) in the western Mediterranean. *Marine Ecology Progress Series 15-23*

Reum, J. C. P., Alin, S. R., Feely, R. A., Newton, J., Warner, M., & McElhany, P. (2014). Seasonal carbonate chemistry covariation with temperature, oxygen, and salinity in a fjord estuary: Implications for the design of ocean acidification experiments. *PLoS ONE 9(2),* e89619

Richardson, C. A. (2001). Molluscs as archives of environmental change. *Oceanography and Marine Biology*.

Ries, J. B. (2011). Skeletal mineralogy in a high-CO_2 world. *Journal of Experimental Marine Biology and Ecology 403(1),* 54-64

Rodolfo-Metalpa, R., Peirano, A., Houlbrèque, F., Abbate, M., & Ferrier-Pagès, C. (2008). Effects of temperature, light and heterotrophy on the growth rate and budding of the temperate coral *Cladocora caespitosa*. *Coral Reefs 27(1),* 17-25

Romanelli, M., Cordisco, C. A., & Giovanardi, O. (2009). The long-term decline of the *Chamelea gallina* L . (Bivalvia : Veneridae) clam fishery in the Adriatic Sea : is a synthesis possible ? *Acta Adriatica 50*(2), 171-205

Scarcella Giuseppe, C. A. M. (2016). Research for PECH Committee - The Clam Fisheries Sector in the EU - The Adriatic Sea Case - Think Tank

Schoene, B., & Surge, D. M. (2012). Treatise Online no. 46: Part N, Revised, Volume 1, Chapter 14: Bivalve sclerochronology and geochemistry. *Treatise Online*

Schofield, O., Ducklow, H. W., Martinson, D. G., Meredith, M. P., Moline, M. A., & Fraser, W. R. (2010). How do polar marine ecosystems respond to rapid climate change? *Science 328(5985),* 1520-1523

Sokolova, I., & Pörtner, H. O. (2001). Temperature effects on key metabolic enzymes in *Littorina saxatilis* and *L. obtusata* from different latitudes and

shore levels. *Marine Biology*, *139*(1), 113–126.

Talmage, S. C., & Gobler, C. J. (2011). Effects of Elevated Temperature and Carbon Dioxide on the Growth and Survival of Larvae and Juveniles of Three Species of Northwest Atlantic Bivalves. *PLoS ONE*, *6*(10), e26941

Tyrrell, T. (2008). Calcium carbonate cycling in future oceans and its influence on future climates. *Journal of Plankton Research 30(2),* 141-156

Watson, S. A., Peck, L. S., Tyler, P. A., Southgate, P. C., Tan, K. S., Day, R. W., & Morley, S. A. (2012). Marine invertebrate skeleton size varies with latitude, temperature and carbonate saturation: Implications for global change and ocean acidification. *Global Change Biology 18(10),* 3026-3038

Weiner, S., & Dove, P. M. (2003). An Overview of Biomineralization Processes and the Problem of the Vital Effect. *Reviews in Mineralogy and Geochemistry*, *54*(1), 1–29

Witbaard, R. (1996). Growth variations in *Arctica islandica* L. (Mollusca): a reflection of hydrography-related food supply. *ICES Journal of Marine Science*, *53*(6), 981–987

Zeebe, R. E. (2012). History of Seawater Carbonate Chemistry, Atmospheric CO_2 , and Ocean Acidification. *Annual Review of Earth and Planetary Sciences 40,* 141-165

Ziveri, P., Stoll, H., Probert, I., Klaas, C., Geisen, M., Ganssen, G., & Young, J. (2003). Stable isotope 'vital effects' in coccolith calcite. *Earth and Planetary Science Letters*, *210*(1–2), 137–149

Chapter 2

Shell properties of commercial clam *Chamelea gallina* are influenced by temperature and solar radiation along a wide latitudinal gradient

Published in Scientific Reports

SCIENTIFIC REPORTS

OPEN

Shell properties of commercial clam *Chamelea gallina* are influenced by temperature and solar radiation along a wide latitudinal gradient

Received: 20 June 2016
Accepted: 11 October 2016
Published: 02 November 2016

Francesca Gizzi[1], Maria Giulia Caccia[1], Ginevra Allegra Simoncini[1], Arianna Mancuso[1,2], Michela Reggi[3], Simona Fermani[3], Leonardo Brizi[4,5], Paola Fantazzini[4,5], Marco Stagioni[2], Giuseppe Falini[3], Corrado Piccinetti[2] & Stefano Goffredo[1]

Phenotype can express different morphologies in response to biotic or abiotic environmental influences. Mollusks are particularly sensitive to different environmental parameters, showing macroscale shell morphology variations in response to environmental parameters. Few studies concern shell variations at the different scale levels along environmental gradients. Here, we investigate shell features at the macro, micro and nanoscale, in populations of the commercially important clam *Chamelea gallina* along a latitudinal gradient (~400 km) of temperature and solar radiation in the Adriatic Sea (Italian cost). Six populations of clams with shells of the same length were analyzed. Shells from the warmest and the most irradiated population were thinner, with more oval shape, more porous and lighter, showing lower load fracture. However, no variation was observed in shell $CaCO_3$ polymorphism (100% aragonite) or in compositional and textural shell parameters, indicating no effect of the environmental parameters on the basic processes of biomineralization. Because of the importance of this species as commercial resource in the Adriatic Sea, the experimentally quantified and significant variations of mass and fracture load in *C. gallina* shells along the latitudinal gradient may have economic implications for fisheries producing different economical yield for fishermen and consumers along the Adriatic coastline.

Organisms are able to modulate their developmental trajectory and alter gene-expression patterns in response to abiotic (such as temperature or photoperiod) or biotic (such as those emanating from predators, conspecifics or food) environmental cues[1]. Environmental parameters influence the organism, producing a non-pathological phenotype, appropriate for that environment. An enduring puzzle in evolutionary biology is to understand how individuals and populations adjust to changing environments. Intraspecific phenotypic variation is believed to arise from divergent selection pressures between different environments[2], from environment-independent phenotype generation, as well as from potentially non-adaptive effects of the environment on phenotype[2]. Thus, a particular environment can elicit different phenotypes from the same genotype[1]. The ability of organisms to produce different phenotypes under different environmental parameters in natural populations is a critical issue to understand how species might face future changes.

Phenotype plasticity is the ability of an organism to produce a range of relatively fit phenotypes, by altering morphology, movement, behavior or rate of biological activity in response to fluctuations in environmental parameters[3]. Considering the existing effects of anthropogenic activities on the environment, organisms exhibiting higher phenotypic plasticity might cope better to broad scale disturbances, such as climate change[4].

[1]Marine Science Group, Department of Biological, Geological and Environmental Sciences, University of Bologna, Via F. Selmi 3, I-40126 Bologna, Italy, European Union. [2]Laboratory of Fisheries and Marine Biology at Fano, University of Bologna, Viale Adriatico 1/N, I-61032, Fano (PU), Italy, European Union. [3]Department of Chemistry "Giacomo Ciamician", University of Bologna, Via F. Selmi 2, I-40126 Bologna, Italy, European Union. [4]Department of Physics and Astronomy, University of Bologna, Viale Berti Pichat 6/2, 40127 Bologna, Italy, European Union. [5]Museo Storico della Fisica e Centro Studi e Ricerche Enrico Fermi, Piazza del Viminale 1, Roma, Italy, European Union. Correspondence and requests for materials should be addressed to G.F. (email: giuseppe.falini@unibo.it) or C.P. (email: corrado.piccinetti@unibo.it) or S.G. (email: s.goffredo@unibo.it)

Calcifying marine organisms (e.g. corals, echinoderms and mollusks) are likely to be among the most susceptible organisms to changing environmental parameters[3] and show morphological variations of the skeleton/shell related to bottom topography, sediment characteristics, hydrodynamic processes[5], and especially pH and temperature[6]. These organisms make extensive use of calcium carbonate ($CaCO_3$), one of the most abundant minerals in nature, as a structural and/or protective material through the biomineralization process[7]. Morphology, mineralogy and chemistry of biologically formed $CaCO_3$ skeletons are largely dependent on both biology and environmental surroundings, with structural proteins and enzymes that act as keys to controlling internal conditions and that respond to external environmental parameters[8]. Mollusks are able to exert an exquisite biological control on the biomineralization process by determining which type of $CaCO_3$ polymorph precipitates through the control of intra-skeletal macromolecules[8]. It is well known that the intra-crystalline skeletal organic matrix (OM) plays a major role in biomineralization and as in all biominerals, mollusk shells also contain OM that rarely exceeds 5% weight of the total shell[9].

Environmental factors, such as solar radiation, food availability, oxygen, salinity and temperature, all influence energy expenditure in marine organisms, especially in temperate seas, where marine organisms show marked seasonal patterns in growth, reproduction and abundance. Solar radiation (SR) and sea surface temperature (SST), are widely used as monitoring parameters for ecological studies and generally influences the demography and skeletal properties of marine calcifying organisms, including sponges[10] and non-zooxanthellate coral[11,12]. The effects of SST on calcification and growth have been deeply studied on several calcifying marine organisms, including mollusks[6,13–16], but no study investigated the effect of SR on calcification and growth of bivalve mollusks.

To study the effect of SR and SST on marine organisms, latitudinal gradients are useful natural laboratories, influencing variations in SR and SST and allowing to examine long-term effects on populations of the same species, adapted to different environmental conditions[6,17]. Several studies on bivalves were performed along latitudinal gradients, focusing on biodiversity[18], growth rate, body size and lifespan[15,16], but no one investigated the shell variation at multiscale level. Mollusk shell morphology is particularly sensitive to environmental parameters, varying in relation to depth[19], current[20], wave exposure[21], bottom type, sediment[19,22], pH and temperature[6]. The quagga mussel *Dreissena bugensis* shows plasticity in shell morphology in relation to depth: deep ones presents a more laterally flattened shell and a more oval shape than those from shallow water habitats[19]. The clam *Mya arenaria* from sandy bottoms shows a longer and narrower shape, compared to a rounder shape when grown in gravel[22]. Shell shape of the limpet *Lottia gigantea* changes as a function of intertidal zonation and related environmental factors, such as resistance to desiccation, thermal stress and wave impact, by developing high spiraled and heavily ridged shells which may reduce the likelihood of reaching elevated body temperatures[21]. Growth in length and height of the shells of the cockle, *Cerastoderma edule*, cease in winter when mean water temperatures fell to 5 °C[14]. Bivalve growth is not very affected by water temperature variations between 10° and 20 °C, but decreases at low temperatures (below 10 °C) or high temperatures (above 20 °C)[13]. High temperature influences key processes that can impair calcification in bivalves, and together with food availability plays an essential role in mollusk shell growth[23].

The observed phenotypic plasticity of many marine calcifying organisms in relation to environmental parameters makes them potentially ideal models for studying such plastic responses and associated trade-offs in the face of global climate change.

The clam *Chamelea gallina* (Linnaeus 1758) is a common infaunal bivalve of the Mediterranean Sea, where it inhabits well-sorted fine sand biocoenosis at 3–7 m depth and has a considerable economical relevance for fishery[24,25]. In the 1970s the development of clam fisheries based on hydraulic dredges led to an over-exploitation of the resource with a dramatic decrease in clam population density associated with a reduction in the number of clams over 25 mm long, the minimum legal marketable size, although the maximum length recorded for this species is about 50 mm[24]. In Italy, in the late 1970s the fishery yielded 80,000-100,000 metric tons, however currently it does not exceed 20,000 metric tons[26]. Recently, there is growing concern for the survival of bivalve communities because large inter-annual fluctuations in stock abundance, periodic recruitment failure and irregular mortality events threaten the biological and economic sustainability of this fishery, especially in the Adriatic Sea[25,26]. Thus, studies on this species are of critical importance for developing appropriate management strategies for one of the most important economic sectors of southern EU countries. The Food and Agriculture Organization of the United Nations (FAO) reports a mean annual total catch of about 60,000 tons (2004–2013) in the Atlantic, Mediterranean and Black Sea, with the largest catches in Italy (22,000 tons) and Turkey (33,000 tons).

Several studies demonstrated that changes in abiotic environmental factors, such as temperature, salinity and oxygen strongly influence immune parameters of *C. gallina*, making it more susceptible to infection and diseases[27].Water temperature has a dominant role also in shell growth of *C. gallina*[25,28]. Temperatures below 10 °C strongly slow or inhibit shell growth, whereas values above 28 °C reduce energy absorption and increase energy expenditure via respiration, thus suppressing shell growth[25,28]. Calcification of *C. gallina* seems to be related to temperature and food conditions, showing widely spaced growth bands during winter-spring, while narrow growth increments are deposited in summer-autumn[25].

Several studies have been reported on variations of shell biometry in response to environmental parameters[6,19,20,22,29], however few studies comparatively analyzed shell features at the micro and nanoscale level along environmental gradients[30–33]. The present study aimed to investigate the phenotypic response to the environment of shell features of *C. gallina* at different scales of observation, in six populations along a latitudinal gradient.

Results

Environmental parameters. SR and SST both varied among sites (Kruskal–Wallis test, $df = 5$, and $p < 0.001$; Table 1) and correlated negatively with latitude (Supplementary Fig. S1). The Monfalcone site, located in the Gulf of Trieste, has a higher SST than typically expected for this latitude[34].

Code	Latitude (°)	n	SR (W m^{-2})		SST (°C)	
			mean (SE)	Range	mean (SE)	Range
MO	45.7	1447	159.4 (2.5)	154.4–164.4	16.96 (0.19)	16.58–17.35
CH	45.2	1447	160.8 (2.5)	155.8–165.7	16.47 (0.19)	16.09–16.84
GO	44.8	1447	163.8 (2.6)	158.7–168.8	16.54 (0.19)	16.17–16.92
CE	44.2	1447	165.2 (2.5)	160.2–170.2	17.05 (0.20)	16.65–17.45
SB	43.1	1447	172.4 (2.5)	167.4–177.4	17.90 (0.19)	17.52–18.28
CA	41.9	1447	180.4 (2.6)	175.4–185.5	18.60 (0.17)	18.27–18.93

Table 1. Environmental parameters. Mean annual values for solar radiation (SR) and sea surface temperature (SST) from 2011 to 2014, of the sites. n = number of collected data; SE = standard error. Values for each population, in decreasing order of latitude: MO (Monfalcone), CH (Chioggia), GO (Goro), CE (Cesenatico), SB (San Benedetto), CA (Capoiale).

Code	n	Length (mm) mean (CI)	Height (mm) mean (CI)	Width (mm) mean (CI)	Thickness (mm) mean (CI)	Mass (g) mean (CI)	Volume (cm3) mean (CI)
MO	40	26.85 (0.40)	22.28 (0.27)	7.41 (0.13)	1.60 (0.05)	2.15 (0.07)	0.77 (0.03)
CH	40	26.14 (0.41)	21.45 (0.32)	6.39 (0.09)	1.33 (0.06)	1.66 (0.07)	0.59 (0.02)
GO	40	26.06 (0.47)	21.29 (0.39)	6.69 (0.13)	1.26 (0.05)	1.59 (0.08)	0.57 (0.03)
CE	40	26.52 (0.49)	21.49 (0.39)	6.47 (0.15)	1.17 (0.04)	1.57 (0.09)	0.56 (0.03)
SB	40	26.39 (0.45)	21.71 (0.32)	6.44 (0.11)	1.14 (0.04)	1.52 (0.07)	0.54 (0.02)
CA	40	26.40 (0.51)	21.42 (0.42)	6.13 (0.12)	1.06 (0.03)	1.41 (0.08)	0.51 (0.03)
K-W		NS	***	***	***	***	***

Table 2. Shell biometric parameters. Macroscale level. Average of biometric parameters at each site. n = number of samples; CI = 95% confidence interval. Populations are arranged in order of decreasing latitude: MO (Monfalcone), CH (Chioggia), GO (Goro), CE (Cesenatico), SB (San Benedetto), CA (Capoiale). K-W = Kruskal-Wallis equality-of-populations rank test, NS = not significant, ***$p < 0.001$.

Code	n	Micro-density (g cm^{-3}) mean (CI)	Bulk density (g cm^{-3}) mean (CI)	Apparent porosity (%) mean (CI)
MO	40	2.80 (0.010)	2.72 (0.010)	2.86 (0.149)
CH	40	2.82 (0.010)	2.72 (0.012)	3.30 (0.317)
GO	40	2.81 (0.012)	2.70 (0.013)	3.87 (0.261)
CE	40	2.81 (0.003)	2.70 (0.011)	4.04 (0.342)
SB	40	2.82 (0.006)	2.70 (0.008)	3.98 (0.343)
CA	40	2.80 (0.004)	2.68 (0.008)	4.20 (0.312)
K-W		NS	***	***

Table 3. Shell biometric parameters. Macro- and microscale levels. Micro-density, bulk density and apparent porosity of the sites in decreasing order of latitude. n = number of samples; CI = 95% confidence interval. Populations are arranged in order of decreasing latitude: MO (Monfalcone), CH (Chioggia), GO (Goro), CE (Cesenatico), SB (San Benedetto), CA (Capoiale). K-W = Kruskal-Wallis equality-of-populations rank test, ***$p < 0.001$.

Shell biometric parameters. Clam biometric parameters (length, height, width, mass, volume, micro-density, bulk density and apparent porosity) were homogeneous between left and right valves, thus data from both valves were pooled for following analyses. Since only clams of commercial size (25–30 mm) were considered in this study, shell length was homogeneous among populations (Table 2). Shell macroscale biometric data, height, width, mass and volume (with the exception of length), bulk density and apparent porosity were significantly different among sites, thus correlations analyses between SR or SST and clam parameters were performed (Tables 2 and 3; Figs 1 and 2). Micro-density did not differ among sites (Table 3). Width, mass, volume, correlated negatively with SR and SST, while shell height correlated only with SR (Fig. 1). Bulk density and apparent porosity correlated negatively and positively, respectively, with both SR and SST (Fig. 2). All parameters were more highly correlated with SR than with SST (Figs 1 and 2). Differences found in *C. gallina* shells among populations were related to tri-dimensional shell biometric parameters (height, width, mass, volume, bulk density and apparent porosity). To check if differences at bi-dimensional level occurred among populations, the bi-dimensional shell shape parameters (perimeter, area, aspect ratio, solidity, circularity and roundness), in addition with length and height, were analysed using multivariate statistical analysis (PCA). No differences were found among populations (see Supplementary Information; Supplementary Fig. S2a,b).

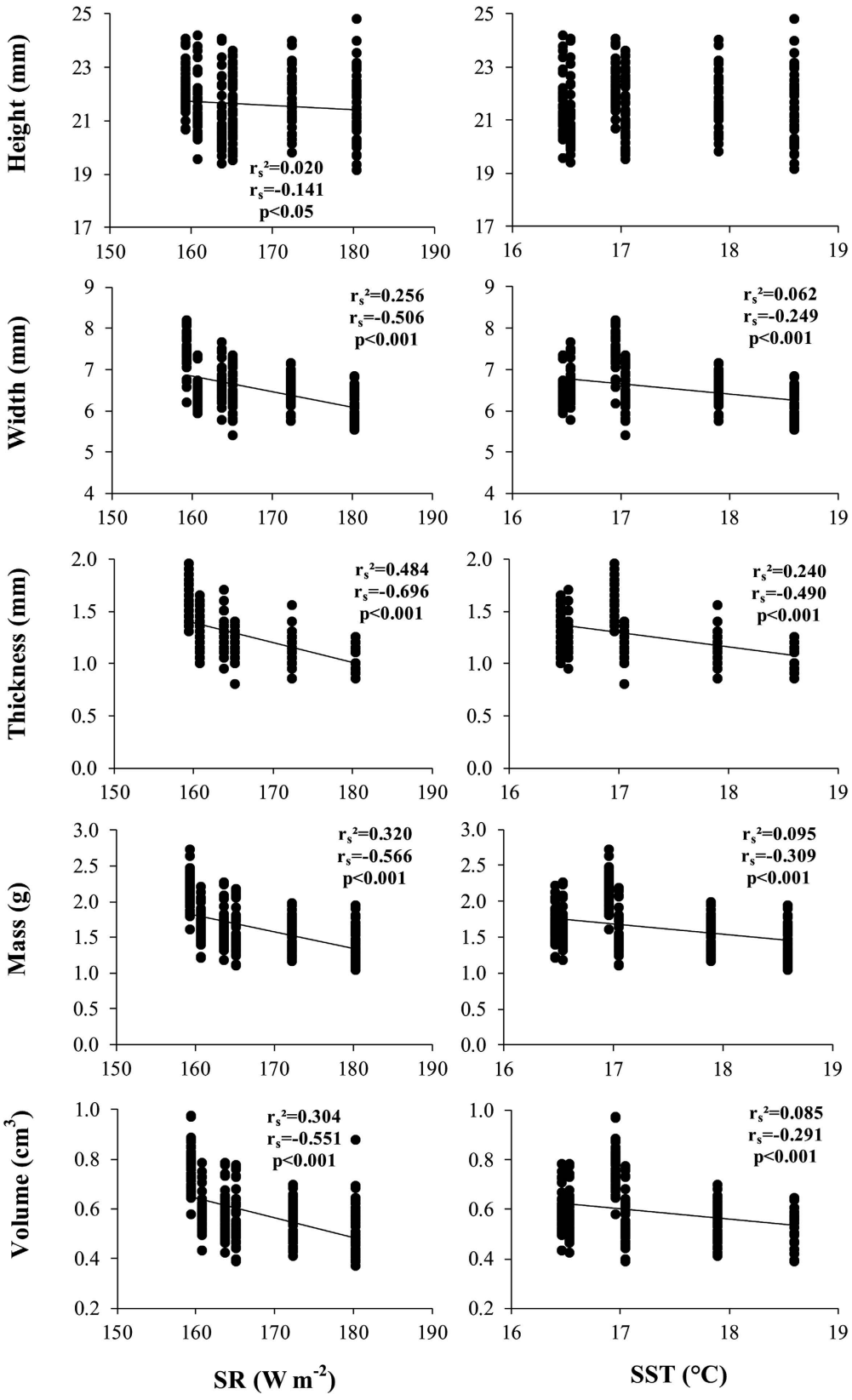

Figure 1. Shell biometric parameters. Macroscale level. Variation in the biometric parameters of *C. gallina* with environmental variables (SR and SST). r_s = Spearman's determination coefficient. n = 40 in each population. Mean values for each population are listed in Table 2.

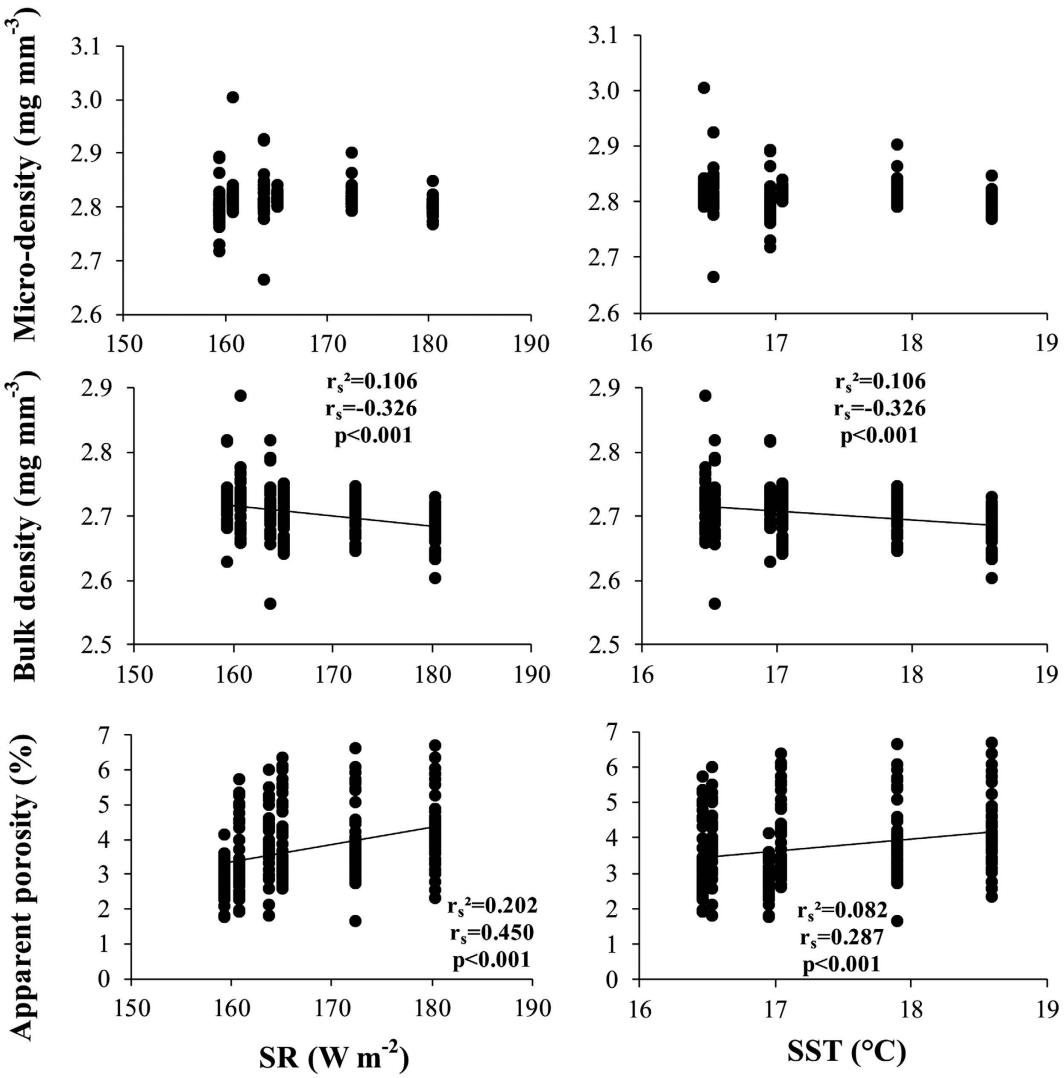

Figure 2. Shell biometric parameters. Macro- and microscale levels. Variation in the shell parameters of *C. gallina* with environmental variables (SR and SST). r_s = Spearman's determination coefficient. n = 40 in each population. Mean values for each population are listed in Table 3.

Shell microstructure. The scanning electron microscopy observations (Supplementary Fig. S3a,b) showed that the microstructure of *C. gallina* shell contains two main layers, according to what observed in most venerids[35]. In the outer layer compound prisms are observed (Supplementary Fig. S3c). They are formed by the compact assembly of grains (Supplementary Fig. S3f). The inner layer is homogeneous and is formed of irregular granules (Supplementary Fig. S3e). Among these grains, having a size around 1 μm, layers of materials are dispersed (Supplementary Fig. S3h). A middle layer, which represents the transition zone between the inner layer and the outer one, is characterized by the presence of granules (Supplementary Fig. S3d), bigger than the ones observed in the inner layer (around 3 μm), from which the prisms start their structure. The granules observed in the outer and inner layer are quite similar in size and shape (Supplementary Fig. S3f,h). All populations revealed the same pattern at each considered magnification.

Shell mechanical and mineral features. Mechanical tests showed differences among populations for Young's modulus and fracture load (Table 4), and both parameters correlated negatively with SR and SST (Fig. 3).

The analysis of the inorganic phase was obtained from the results of X-ray powder diffraction patterns (XRD) and Fourier transform infrared spectroscopy (FTIR) data. Both techniques showed that shells from all populations were composed of pure aragonite and no other mineral phase was detected (Supplementary Figs S4 and S5). Full width at half maximum (FWHM) calculated for the (111) peak of each diffraction pattern was different among populations but not correlated with SR and SST (Supplementary Table S1). In FTIR spectra the bands at 1484 cm^{-1} (ν_3) 859 cm^{-1} (ν_2) and 712 cm^{-1} (ν_4), typical of aragonite, did not shift among samples (Supplementary Table S1; Fig. S5). The wavenumber of the ν_2 band is a function of the content of Sr within the aragonitic sample[36]; accordingly a Sr content of about 8000 ppm can be estimated in each shell, independently from the collection site.

Code	n	Young's modulus (kN mm^{-1}) mean (CI)	Maximum Load (kN), mean (CI)
MO	14	2.50 (0.54)	0.13 (0.02)
CH	30	2.80 (0.16)	0.15 (0.01)
GO	28	2.35 (0.18)	0.11 (0.01)
CE	21	2.61 (0.13)	0.13 (0.02)
SB	28	2.30 (0.19)	0.11 (0.02)
CA	20	2.18 (0.29)	0.09 (0.01)
K-W		***	***

Table 4. Shell mechanical properties. Young's modulus (kN mm^{-1}) and Maximum load (kN) mean value for each population. n = number of samples; CI = 95% confidence interval. Values for each population, in decreasing order of latitude: MO (Monfalcone), CH (Chioggia), GO (Goro), CE (Cesenatico), SB (San Benedetto), CA (Capoiale). K-W = Kruskal-Wallis equality-of-populations rank test, ***$p < 0.001$.

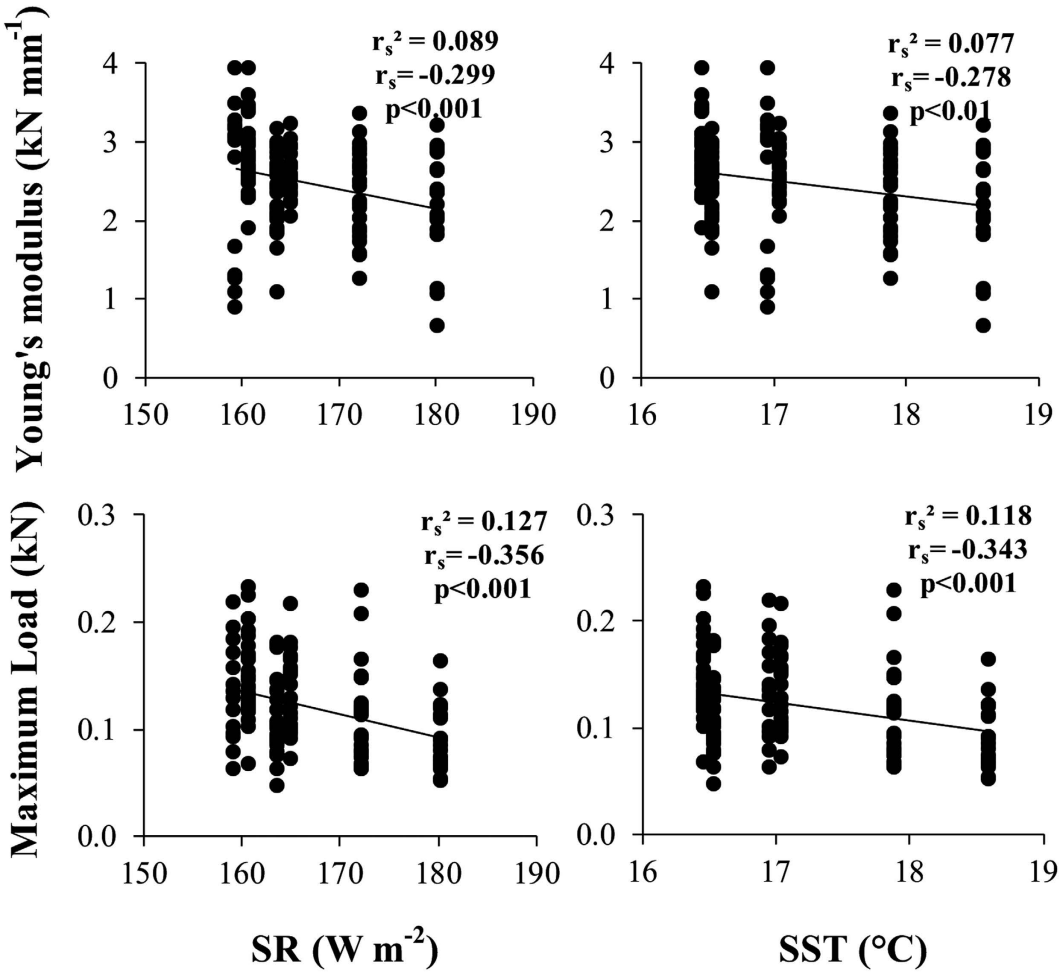

Figure 3. Shell mechanical properties. Variation in mechanical properties of *C. gallina* with environmental variables (SR and SST). r_s = Spearman's determination coefficient. Samples number and mean values for each population are listed in Table 4.

A series of successive grindings of the powder from a shell sample for each population was carried out, following a reported procedure to generate the grinding curve, a qualitative estimation of the atomic order[37]. The bands heights were measured and the height ratios ν_4/ν_3 and ν_2/ν_3 were calculated. All the ratio values fitted in a curve in the ν_4/ν_3 vs ν_2/ν_3 graph (Supplementary Fig. S6). The obtained curve was compared with other curves fitted from data from different marine calcifying organisms (Phyla: Cnidaria, Anellida and Mollusca) and from geogenic and synthetic aragonite[37] (Supplementary Fig. S6). The curve fitted from *C. gallina* data was located between those of geogenic and synthetic aragonite, along with the other biogenic aragonite samples (Supplementary Fig. S6).

The content of intra-skeletal OM, as weight percentage, was measured by thermogravimetric analysis (TGA; Supplementary Fig. S7). It was in average below 2% in all samples and homogeneous among populations (Supplementary Table S2); an equivalent result to that obtained from several other mollusk[38].

Discussion

The main aim of this study was to investigate the effect of SR and SST on shell features at macro (biometry), micro (texture) and nanoscale (atomic order and composition) levels, in natural populations of the common clam *C. gallina* along a latitudinal gradient in the Western Adriatic Sea, as a case study to gain further insight on the relationship between phenotype and environment in calcifying marine organisms. The possible relationships between growth rate and SR and SST were not considered in this study. Further investigation will be necessary to better understand how bivalves' growth respond to changes in SR and SST.

At macroscale level, shells of the same length of *C. gallina* were affected by increasing SR and SST, presenting lighter, thinner, more oval shaped, more macro-porous and less resistant to fracture valves in the warmer and more irradiated populations. Previous studies show that the shells of many mollusks species are affected along latitudinal gradient due to decreasing SST[6,39]. A possible explanation could be that at low SST, $CaCO_3$ is more soluble and seawater is less saturated, increasing energetic costs of shell formation[40]. Moreover, it was shown that low SST directly reduces growth[41] and development[42]. Conversely, in this study *C. gallina* seemed to be negatively affected in shell biometry by high SST, showing an opposite trend. The effect of temperature on physiology of *C. gallina* has been studied in specimens exposed to different temperature by Moschino and Marin[28]. They investigated the scope for growth balancing the processes of energy acquisition (i.e. feeding, digestion) with the energy expenditure (i.e. respiration, excretion) and providing an instantaneous measure of the energy state[28]. Specimens of *C. gallina* exposed to high summer temperatures (28 °C), show a reduced energy absorption and an increased energy expenditure via respiration, negatively affecting the energy balance[28] and probably growth, as found during summer season (temperature > 27 °C) in specimens from the eastern coast of Spain[25]. A drop in metabolism was recorded in the snail *Littorina saxatilis* exposed to elevated temperatures, with negative consequences in growth and fitness[43]. Moreover, oxygen depletion due to high temperatures may produce detrimental effects on the physiological performance of clams, as observed in the bivalve *Ruditapes decussatus*[44]. *C. gallina* seems to have relatively low tolerance to high temperatures in comparison with other bivalve species, showing a great influence in the overall physiological responses and heavy stress conditions when exposed to high temperatures, demonstrating that temperature could be a tolerance limit for this species[28].

Despite *C. gallina* being an infaunal bivalve, all macroscale (biometric) parameters of this species seemed to be more correlated with SR than SST. SR could have no direct effect on this species, but the SR latitudinal gradient is related to other abiotic and/or biotic parameters not investigated in this study, such as phytoplankton density and its distribution. Food concentration is one of the major factors influencing the growth of suspension feeding bivalves[45]. SR affects the growth, survival and distribution of phytoplankton[46], which represent the food source for higher trophic organisms, such as bivalves. Phytoplankton distribution in the Adriatic Sea is characterized by the relative influence of northern Italian rivers and by the influence of Mediterranean waters on the southern Italian coasts, showing a generally decreasing trend of nutrient concentration from North to South[47]. The northern Adriatic, influenced by Italian rivers outlets, was marked by low diversity but high density of phytoplankton; the southern Adriatic influenced by Mediterranean waters, exhibited high diversity but low density of phytoplankton[47]. The lower presence of phytoplankton density in southern Adriatic, could cause feeding deficits and consequently a reduction of available energy for clam to invest in shell construction, which could explain the reduction in weight, thickness and the higher porosity and fragility of shells.

Differences found in SST and SR along the gradient could also influence the type and/or density of predators. Predation is an important factor associated with morphological plasticity in bivalves, which can exhibit induced responses based on the capture techniques of the predators[48]. Bivalves' principal defense is their strong calcareous shell, and among shell characteristics, thickness is the most influential factor for shell strength. The increased of bivalve shell thickness can thus reduce the success of many predators[49]. The blue mussel *Mytilus edulis* exposed to high predation density shows a thicker and more robust shell than those exposed to lower predation[49]. Similar results, showing an increase in shell thickness in response to predators, were found in several mollusks species[48–50]. Experimental works on gastropods show that shell thickening in response to predators could be partly due to avoidance behavior, resulting in lower growth rates partly due to direct result of increased shell deposition in the presence of predators[50].

The observed phenotypic changes found in *C. gallina* could occur by genetic or plasticity variations, as found in other bivalves[48], and could be explained by SST difference, nutrient concentration and/or density of predators along the latitudinal gradient. Increased porosity, decreased stiffness (Young's modulus) and reduced thickness of *C. gallina* shells, with increasing SR and SST, lower the shell's fracture load. Resistance to breakage generally increases as the square of the shell thickness increases[39], and the breaking resistance doubles with an increase of 41% in thickness, thus providing a good return in shell strength for each unit of shell thickening[6]. The warmer and more irradiated populations of *C. gallina* showed reduced shell stiffness and fracture load, leading to a modified shell resistance, with a lower load fracture and damage susceptibility that may affect the survival of the species.

Because of the importance of this species as a commercial resource in the Adriatic Sea, those variations in macroscale parameters found in *C. gallina* shells could have economic implications for its fishery. More porous and less resistant to load fracture shells, found in warmer and more irradiated populations, are less resistant to breakage and could be more damaged during fishing with hydraulic dredges, with a larger amount of clams discarded from the trade. This could mean a higher catch effort for fishermen with a loss in economic yield.

In addition, the lower clam mass due to thinner and more porous shells in the southern populations, requires a major number of clams to obtain the same quantitative in kilograms compared to northern populations.

Moreover, the northern populations could allocate a higher energy fraction to reinforce their shells at the expense of a lower somatic growth[29]. Contrarily, the warmer and more irradiated populations could allocate most of their assimilated energy towards somatic growth, compensating the negative aspect of shell variations with an increase in edible mass per catch and per kilogram, with a potential positive economical yield both for consumers and fishermen. Further analysis on edible animals may be necessary to understand if environmental parameters can affect the growth of soft tissue.

Despite the reported differences at the macroscale level, at the microscale and nanoscale levels, all populations of *C. gallina* showed the same skeletal features along the latitudinal gradient of SR and SST. The shells were always made of aragonite, as seen in other mollusks[51–53]. That aragonite always showed the same extent of atomic order[37], evaluated by the grinding curve methodology. Indeed, grinding curves from *C. gallina* samples revealed that the aragonitic atomic order does not vary among populations along the SR an SST gradient. Those curves of *C. gallina* samples were close to that from the mollusk *Vermetus triqueter* shell and other aragonitic marine organisms (Cnidaria, *Balanophyllia europaea*, Anellida *Protula tubularia*). All of them were located between the synthetic, high order, and geogenic, low order, aragonìte curves[37] (Supplementary Fig. S4). The invariance in nanoscale skeletal features is also confirmed by the constancy of shell chemical composition in the content Sr (FTIR data) and OM (TGA data). This is in agreement with what expected for *C. gallina*, a calcifying organism having a high degree of biological control over biomineralization, as other mollusks[7,38].

Electron microscopy observations, at the micro(nano)scale level, showed that valves of *C. gallina* were characterized by two different aragonite structures: an external prismatic layer and an internal granular one, separated by a transition zone. The basic particles composing both layers were similar in shape, spheroidal, and size, below 1 μm. This was observed throughout the whole valve section, independently from the shell collection site. This constancy among all populations, suggests no difference among the aragonite "building blocks" at the micro and nanoscale level, a data that fits well with the results from spectroscopic (atomic order) and diffractometric (texture) measurements at nanoscale level.

Shell micro-density (density of the $CaCO_3$ biomineral that composes the shell) did not change along the gradient. This information, together with the homogeneous amount of OM and Sr among populations, indicates that also other micro-skeletal parameters affecting micro-density, as occluded porosity and content of non crystalline $CaCO_3$, did not change. The latter being linked to shell elasticity, a parameter at the macroscale level, constant along all populations of samples.

The constancy of OM content in *C. gallina* under different environmental conditions represents an important result, which adds relevance to the long recognized key role of OM in biomineral skeleton formation[7,8,54–56]. This despite the fact that still little information is known on varying OM content and composition in relation to environmental parameters.

As indicated by all micro and nanoscale analyses, the biomineral remained the same in all analyzed samples, indicating that the "building blocks" produced by the biomineralization process are substantially unaffected by the SR and SST variations among the different populations along the latitudinal gradient. Also the organization, morphology and packing, of the constituent mineral crystals were the same along the gradient. This constancy, as already discussed, has to be related to the high degree of biological control exerted by *C. gallina* over the calcification process, able to overcome environmental stresses[7,8].

Conclusions

Differences found in shell parameters of the clam *C. gallina* along the latitudinal gradient could be the outcome of phenotypic plasticity or a genetic adaptation of the populations subjected to different environmental parameters. Environmental parameters could directly affect shell morphology, such as temperature, or indirectly, influencing nutrient concentration and/or predator density. Shell morphology of the most irradiated and warmest populations was characterized by lighter, thinner, more porous and fragile shells, likely affecting the economic aspects of fisheries and the survival of the species. At the same time, populations of *C. gallina* did not show significant variations of structural parameters at the microscale and nanoscale level. The type of $CaCO_3$ polymorph, the atomic order of the mineral skeletal phase and the percentage of organic matrix content were unaltered along the latitudinal gradient, indicating no effects of SR and SST on the building blocks produced by the biomineralization process of the clam shells.

Materials and Methods

Ethics Statement. This study was carried out following the fundamental ethical principles. According to the European normative that regulates minimum fishing size of *Chamelea gallina* (25 mm, Council Regulation (EC) No. 1967/2006), only clams of commercial size with minimum length of 25 mm were collected for this study.

Collection and processing of specimens. Between August 2013 and April 2015, specimens of *C. gallina* of commercial size (25–30 mm), were collected from six sites along a latitudinal gradient in the Adriatic Sea from 45°42′N to 41°55′N (Supplementary Fig. S8).

Clams were sampled for each site using hydraulic dredges on soft bottoms in the subtidal zone at 3–7 m depth.

For each collected clam, the bivalve flesh was removed with a scalpel and the shell was cleaned with a toothbrush and washed with distilled water. The right and left valves were then separated, labeled and dried at 37 °C for one night to remove any moisture that may affect measurements.

Shell biometric parameters. Clam shell length (maximum distance on the anterior-posterior axis), height (maximum distance on the dorsal-ventral axis; Fig. 4) and bi-dimensional shell shape parameters, were obtained with ImageJ software[57] after data capture of each shell shape with a scanner (Acer Acerscan Prisa 620 ST 600 dpi,

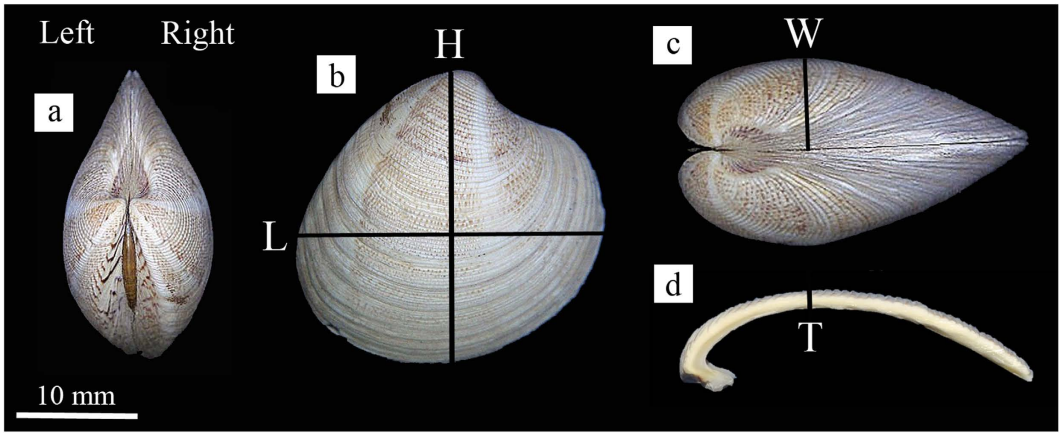

Figure 4. Shell parameters. (**a**) Frontal orientation; by placing the umbo upwards can be distinguished the valve left from the right one; (**b**) Lateral orientation, L = length, H = height; (**c**) cross-sectional orientation, W = width; (**d**) cross-section, T = thickness.

0.04 mm/px). Bi-dimensional shell shape parameters, obtained from shell outline, were perimeter (the length of the outer contour of the shell), area (the space enclosed by the outer contour), aspect ratio (defined as length/height), solidity (area/convex area enclosed by the convex hull), circularity (with a value of 1 indicating a perfect circle and the value approaches 0 indicating an increasingly elongated shape) and roundness (the inverse of aspect ratio).Width (maximum distance on the lateral axis) and thickness (Fig. 4) of the valve were measured with a pair of calipers (±0.05 mm) and dry shell weight was measured using an analytical balance (±0.1 mg). Thickness was measured in the middle of each valve. Volume and shell density parameters were measured by means of the buoyant weight techniques, using a density determination kit Ohaus Explorer Pro balance (±0.1 mg; Ohaus Corp., Pine Brook, NJ, USA).

Measurements required for calculating shell parameters were:

ρ	density of the fluid medium (in this case, double distilled water: 0.99823 g cm^{-3} at 20 °C and 1 atm).
DW	dry mass of the shell.
SW	saturated mass of the shell = mass of the shell plus mass of the water enclosed in its pores. To obtain this measurement, shells were placed in a desiccator connected to a mechanical vacuum pump for about 1 h in order to suck out all of the water and air from the pores. Still under vacuum conditions, the dry shells were soaked by gradually pouring distilled water inside the desiccator. The shell was taken out of the water, quickly blotted with a paper towel to remove surface water, and weighed in air three times, making sure that no water droplets were left on the weighing platform, which would lead to an overestimation.
BW	buoyant mass of the shell = mass of the shell fully saturated with water minus mass of the water displaced by it. The fully water saturated shell was slowly lowered onto the underwater weighing pan, ensuring that no air bubbles adhered to its surface. The buoyant mass measurements were repeated three times and the average was considered for statistical analysis. This simple and nondestructive method has been widely used with great success to examine various calcifying organisms, such as corals[58] and marine mollusks[59].

$$V_{BIOMINERAL} = \frac{DW - BW}{\rho} \quad \text{matrix volume} = \text{volume of the shell, excluding the volume of its pores.} \tag{1}$$

$$V_{PORES} = \frac{SW - DW}{\rho} \quad \text{pore volume} = \text{volume of the pores in the shell.} \tag{2}$$

$$V_{TOT} = V_{MATRIX} + V_{PORES} \quad \text{total volume} = \text{volume of the shell including its pores.} \tag{3}$$

Additionally, the following skeletal parameters were calculated:

$$\textbf{Micro}-\textbf{density}(\text{matrix density}) = \mathrm{DW/V_{MATRIX}} \tag{4}$$

$$\textbf{Bulk}-\textbf{density} = \mathrm{DW/V_{TOT}} \tag{5}$$

$$\textbf{Porosity} = (V_{PORES}/V_{TOT})x\ 100 \quad (6)$$

Shell mechanical properties. To test for shell mechanical properties, compression tests were conducted using a universal testing machine equipped with a force transducer (Instron) of 1 kN maximum capacity. Thirty shell samples were randomly selected from each population and were brought to fracture load using a 3 cm diameter compression platen at a downward speed of 0.5 mm min^{-1}. The Young's modulus (kN mm^{-1}) and the required force to fracture (Maximum load, kN) were recorded using the software Instron (Series IX).

Ten samples from each population were randomly selected and used for the following analyses. The valves were treated with a 5% sodium hypochlorite solution for three days to completely remove any trace of external skeletal organic tissue, and with a 1 M sodium hydroxide solution for one day to hydrolyze residual proteic materials from the shell surface. Samples were then rinsed with distilled water and dried at room temperature for one day. Subsequently, the left valve was sectioned with a dremel (300 series, Dremel System) from the umbo to the ventral margin. One half of each shell was finely ground in a mortar to obtain a homogenous powder to be used for diffractometric and spectroscopic analyses. A transversal section of about 3 mm in width was cut from the mid remaining shell for scanning electron microscope (SEM) observations (Supplementary Fig. S5a).

Diffractometric measurements. XRD analyses were performed on five randomly selected specimens for each populations, preparing a thin, compact layer of powdered sample in a silica background signal free holder. Diffraction patterns for each sample were collected using an X'Celerator detector fitted on a PANalytical X'Pert Pro diffractometer, using Cu-Kα radiation generated at 40 kV and 40 mA. Data were collected within the 2θ range from 15° to 60° with a step size ($\Delta 2\theta$) of 0.02° and a counting time of 1200 s. Fixed anti-scatter and divergence slits of 1/16° were used with 10 mm beam mask and all scans were carried out in 'continuous' mode. The XRD patterns were analyzed using the X'Pert HighScore Plus software (PANalytical) and the FWHM was measured for the peak (111) of each diffraction pattern.

Spectroscopic measurements. FTIR analyses were performed on the same powder samples used for XRD. FTIR analyses were carried out using a FTIR Nicolet 380 Spectrometer (Thermo Electron Corporation) working in the range of wave-numbers 4000–400 cm^{-1} at a resolution of 2 cm^{-1}. Sample disks were obtained mixing a small amount (1 mg) of finely ground sample with 100 mg of KBr and applying a pressure of 670.2 MPa to the mixture using a hydraulic press. For each spectrum, characteristic $CaCO_3$ active vibrational modes ν_2, ν_3 and ν_4 bands were identified and their intensities were measured. To compare atomic order among the six populations, for a sample of each population the intensity of the ν_2 and ν_4 bands were normalized to the ν_3 band and then graphed after successive grinding processes[37]. To understand if there were differences in the atomic order within crystals, the plotted curves of *C. gallina* were compared with grinding curves of other calcifying marine organisms (*Balanophyllia europaea, Protula tubularia, Vermetus triqueter*) and geogenic and synthetic aragonite[37].

Evaluation of OM content. TGA was performed to estimate the OM content of each shell, using an SDT Q600 instrument (TA Instruments). Powdered samples (5–10 mg) from 5 to 10 valves for each site were placed in a ceramic crucible. The analyses were performed under a nitrogen flow of 100 mL/min with a first heating ramp from 30 to 120 °C at 10 °C min^{-1} heating rate, an isothermal at 120° for 5 min, and a second heating ramp from 120 to 600 °C, at 10 °C min^{-1} heating rate.

Skeletal micro-textural analyses. SEM observations were carried out on a subset of individuals from Chioggia and Capoiale (characterized respectively by lowest and highest SST values), to obtain representative information on the textural characteristics of *C. gallina* shell. Skeletal features were investigated on the transversal valve sections. Each section was etched with an acetic acid solution (1% *v*/*v*) for 1 minute to remove debris and artifacts from cutting. Samples were coated with a gold layer (5 nm) and analyzed with a SEM Hitachi S4000.

Environmental parameters. SR (W m^{-2}) and SST (°C) data were obtained for each site from the Euro-Mediterranean Center on Climate Change (CMCC http://oceanlab.cmcc.it/afs/) data banks. Mean annual SR and SST were calculated from daily values measured from July 2011 to June 2015 (number of daily values = 1447 for each site), to enclose the almost full lifespan of two-three years for each sample.

Statistical analyses. Levene's test was used for testing homogeneity of variance and Kolmogorov-Smirnov's test was used for testing normality of variance for both environmental and shell parameters. One-way analysis of variance (ANOVA) was used to test the significance of the differences among sites for environmental variables and shell parameters. When assumptions for parametric statistics were not fulfilled, the non-parametric Kruskal-Wallis equality-of-populations rank test was used instead. Student's t test was used to compare the mean right and left valve shell parameters (length, width, height, thickness, mass, volume, micro-density, bulk density and porosity) in each site. Spearman's rank correlation coefficient was used to calculate the significance of the correlations between shell parameters and environmental parameters. Spearman's rank correlation coefficient is an alternative to Pearson's correlation coefficient; it is useful for data that are non-normally distributed and do not meet the assumptions of Pearson's correlation coefficient[60]. All analyses were computed using PASW Statistics 22.0 (Apache Computer Software Foundation, Forest Hill, USA). Principal component analysis (PCA) was used to test the bi-dimensional shell shape among populations using R Studio software (see Supplementary Information).

References

1. Gilbert, S. F. Ecological developmental biology: developmental biology meets the real world. *Dev. Biol.* **233,** 1–12 (2001).
2. Schluter, D. *The Ecology of Adaptive Radiation* (Oxford Univ. Press, Oxford, UK, 2000).
3. DeWitt, T. J. & Scheiner, S. M. *Phenotypic Plasticity: Functional and Conceptual Approaches*. (Oxford Univ. Press, Oxford, UK, 2004).
4. Pigliucci, M., Murren, C. J. & Schlichting, C. D. Phenotypic plasticity and evolution by genetic assimilation. *J. exp. Boil.* **209,** 2362–2367 (2006).
5. Vogel, S. *Life in Moving Fluids: The Physical Biology of Flow* (Princeton Univ. Press, Princeton, New Jersey, 1996).
6. Watson, S. A. *et al.* Marine invertebrate skeleton size varies with latitude, temperature and carbonate saturation: implications for global change and ocean acidification. *Global Change Biol.* **18,** 3026–3038 (2012).
7. Lowenstam, H. A. & Weiner, S. *On Biomineralization* (Oxford Univ. Press, Oxford, UK, 1989).
8. Falini, G., Albeck, S., Weiner, S. & Addadi, L. Control of aragonite or calcite polymorphism by mollusk shell macromolecules. *Science* **271,** 67–69 (1996).
9. Carter, J. G. Environmental and biological controls of bivalve shell mineralogy and microstructure in *Skeletal Growth of Aquatic Organisms* (eds Rhoads, D. C. & Lutz, R. A.) 69–113 (Plenum Press, New York and London, 1980).
10. Di Camillo, C. G. *et al.* Temporal variations in growth and reproduction of *Tedania anhelans* and *Chondrosia reniformis* in the North Adriatic Sea. *Hydrobiologia*. **687,** 299–313 (2012).
11. Caroselli, E. *et al.* Relationships between growth, population dynamics, and environmental parameters in the solitary non-zooxanthellate scleractinian coral *Caryophyllia inornata* along a latitudinal gradient in the Mediterranean Sea. *Coral Reefs*. **35,** 507–519 (2016).
12. Caroselli, E. *et al.* Environmental implications of skeletal micro-density and porosity variation in two scleractinian corals. *Zoology* **114,** 255–264 (2011).
13. Bayne, B. L., Widdows, J. & Thompson, R. J. Physiological integrations. In *Marine Mussels: Their Ecology and* Physiology (ed. Bayne, B. L.) Ch. 7, 261-292 (Cambridge University Press, Cambridge, 1976).
14. Jones, A. M. Structure and growth of a high-level population of *Cerastoderma edule* Lamellibranchiata). *J. Mar. Biol. Ass. UK* **59,** 277–287 (1979).
15. Hummel, H. *et al.* Growth in the bivalve *Macoma balthica* from its northern to its southern distribution limit: a discontinuity in North Europe because of genetic adaptations in Arctic populations? *Comp. Biochem. Physiol. A*. **120,** 133–141 (1998).
16. Roy, K., Jablonski, D. & Martien, K. K. Invariant size-frequency distributions along a latitudinal gradient in marine bivalves. *Proc. Natl. Acad. Sci. USA* **97,** 13150–13155 (2000).
17. Jansen, J. M. *et al.* Geographic and seasonal patterns and limits on the adaptive response to temperature of European Mytilus spp. and *Macoma balthica* populations. *Oecologia*. **154,** 23–34 (2007).
18. Roy, K., Jablonski, D. & Valentine, J. W. Dissecting latitudinal diversity gradients: functional groups and clades of marine bivalves. *Proc. R. Soc. B. Biol. Sci*. **267,** 293–299 (2000).
19. Claxton, W. T., Wilson, A. B., Mackie, G. L. & Boulding, E. G. A genetic and morphological comparison of shallow and deepwater populations of the introduced dreissenid bivalve *Dreissena bugensis*. *Can. J. Zool.* **76,** 1269–1276 (1998).
20. Fuiman, L. A., Gage, J. D. & Lamont, P. A. Shell morphometry of the deep sea protobranch bivalve *Ledella pustulosa* in the Rockall Trough, North-East Atlantic. *J. Mar. Biol. Ass. UK* **79,** 661–671 (1999).
21. Denny, M. W. & Blanchette, C. A. Hydrodynamics, shell shape, behavior and supervisorship in the owl limpet *Lottia gigantean*. *J. Exp. Biol*. **203,** 2623–2639 (2000).
22. Newell, C. R. & Hidu, H. The effects of sediment type on growth rate and shell allometry in the soft shelled clam *Mya arenaria*. L. *J. Exp. Mar. Biol. and Ecol*. **65,** 285–295 (1982).
23. Laing, I. Effect of temperature and ration on growth and condition of king scallop (*Pecten maximus*) spat. *Aquaculture* **183,** 325–334 (2000).
24. Froglia, C. Clam fisheries with hydraulic dredges in the Adriatic Sea in *Marine Invertebrates Fisheries: Their Assessment and Management* (ed. Caddy, J. F.) 507–524 (Wiley, New York, 1989).
25. Ramón, M. & Richardson, C. A. Age determination and shell growth of *Chamelea gallina* (Bivalvia: Veneridae) in the western Mediterranean. *Mar. Ecol. Prog. Ser*. **89,** 15–23 (1992).
26. Romanelli, M., Cordisco, C. A. & Giovanardi, O. The long term decline of the *Chamelea gallina* L. (Bivalvia: Veneridae) clam fishery in the Adriatic Sea: is a synthesis possible? *Acta Adriat*. **50,** 171–205 (2009).
27. Matozzo, V. & Marin, M. G. Bivalve immune responses and climate changes: is there a relationship. *Invert. Surviv. J*. **8,** 70–7 (2011).
28. Moschino, V. & Marin, M. G. Seasonal changes in physiological responses and evaluation of "well-being" in the Venus clam *Chamelea gallina* from the Northern Adriatic Sea. *Comp. Bioch. Physiol*. **145A,** 433–440 (2006).
29. Valladares, A., Manríquez, G. & Suárez-Isla, B. A. Shell shape variation in populations of *Mytilus chilensis* (Hupe 1854) from southern Chile: a geometric morphometric approach. *Mar. Biol.* **157,** 2731–2738 (2010).
30. Lee, S. W., Kim, Y. M., Kim, R. H. & Choi, C. S. Nano-structured biogenic calcite: a thermal and chemical approach to folia in oyster shell. *Micron*. **39,** 380–386 (2008).
31. Lee, S. W., Kim, G. H. & Choi, C. S. Characteristic crystal orientation of folia in oyster shell, *Crassostrea gigas*. *Mater. Sci. Eng. C*. **28,** 258–263 (2008).
32. Lee, S. W. *et al.* Mechanical characteristics and morphological effect of complex crossed structure in biomaterials: Fracture mechanics and microstructure of chalky layer in oyster shell. *Micron*. **42,** 60–70 (2011).
33. Li, C. *et al.* Mechanical robustness of the calcareous tubeworm *Hydroides elegans*: warming mitigates the adverse effects of ocean acidification. *Biofouling*. **32,** 191–204 (2016).
34. Mauri, E., Poulain, P. M. & Notarstefano, G. Spatial and temporal variability of the sea surface temperature in the Gulf of Trieste between January 2000 and December 2006. *J. Geophys. Res. Oceans* **113** (2008).
35. Popov, S. V. Composite prismatic structure in bivalve shell. *Acta Palaeontol. Pol.* **31,** 3–28 (1986).
36. Dauphin, Y. Microstructures des coquilles de Céphalopodes: la partie apicale de Belopterina (Coleoidea). *Bull. Mus. Natl. Hist. Nat. Sect.* C. **8,** 53–75 (1986).
37. Suzuki, M., Dauphin, Y., Addadi, L. & Weiner, S. Atomic order of aragonite crystals formed by mollusks. *Cryst. Eng. Comm*. **13,** 6780–6786 (2011).
38. Cusack, M., Dauphin, Y., Chung, P., Pérez-Huerta, A. & Cuif, J. P. Multiscale structure of calcite fibres of the shell of the brachiopod *Terebratulina retusa*. *J. Struct. Biol*. **164,** 96–100 (2008).
39. Vermeij, G. J. *A Natural History of Shells* (Princeton University Press, New Jersey, 1993).
40. Clarke, A. Temperature and extinction in the sea: a physiologist's view. *Paleobiology*. **19,** 499–518 (1993).
41. Heilmayer, O., Brey, T. & Pörtner, H. O. Growth efficiency and temperature in scallops: a comparative analysis of species adapted to different temperatures. *Funct. Ecol.* **18,** 641–647 (2004).
42. Peck, L. S., Powell, D. K. & Tyler, P. A. Very slow development in two Antarctic bivalve molluscs, the infaunal clam, *Laternula elliptica* and the scallop *Adamussium colbecki*. *Mar. Biol.* **150,** 1191–1197 (2007).
43. Sokolova, I. M. & Pörtner, H. O. Physiological adaptations to high intertidal life involve improved water conservation abilities and metabolic rate depression in *Littorina saxatilis*. *Mar. Ecol. Prog. Ser.* **224,** 171–186 (2001).
44. Sobral, P. & Widdows, J. Influence of hypoxia and anoxia on the physiological responses of the clam *Ruditapes decussatus* from southern Portugal. *Mar. Biol*. **127,** 455–61 (1997).

45. Yukihira, H., Klumpp, D. W. & Lucas, J. S. Comparative effects of microalgal species and food concentration on suspension feeding and energy budgets of the pearl oysters *Pinctada margaritifera* and *P. maxima* (Bivalvia: Pteriidae). *Mar. Ecol. Prog. Ser.* **171,** 71–84 (1998).
46. Häder, D. P., Kumar, H. D., Smith, R. C. & Worrest, R. C. Effects of solar UV radiation on aquatic ecosystems and interactions with climate change. *Photochem. Photobiol. Sci.* **6,** 267–285 (2007).
47. Zavatarelli, M., Raicich, F., Bregant, D., Russo, A. & Artegiani, A. Climatological biogeochemical characteristics of the Adriatic Sea. *J. Mar. Syst*. **18,** 227–263 (1998).
48. Beadman, H., Caldow, R., Kaiser, M. & Willows, R. How to toughen up your mussels: using mussel shell morphological plasticity to reduce predation losses. *Mar. Biol*. **142,** 487–494 (2003).
49. Leonard, G. H., Bertness, M. D. & Yund, P. O. Crab predation, waterborne cues, and inducible defenses in the blue mussel, *Mytilus edulis*. *Ecology*. **80,** 1–4 (1999).
50. Appleton, R. D. & Palmer, A. R. Water-borne stimuli released by predatory crabs and damaged prey induce more predator resistant shells in a marine gastropod. *Proc. Natl. Acad. Sci. USA* **85,** 4387–4391 (1988).
51. Dauphin, Y. & Denis, A. Structure and composition of the aragonitic crossed lamellar layers in six species of Bivalvia and Gastropoda. *Comp. Biochem. Physiol. Part A Mol. Integr. Physiol.* **126,** 367–377 (2000).
52. Kennedy, W. J., Taylor, J. D. & Hall, A. Environmental and biological controls on bivalve shell mineralogy. *Biol. Rev.* **44,** 499–530 (1969).
53. Sabbioni, L. Influence of Global Warming on Marine Calcifying Organisms. *MS Thesis, Department of Chemistry "Giacomo Ciamician"* (University of Bologna, Italy, 2012).
54. Grégoire, C. On submicroscopic structure of the Nautilus shell. *Bull. K. Belg. Inst. Nat. Wet.* **38,** 1–71 (1962).
55. Krampitz, G. P. Structure of the organic matrix in mollusc shells and avian eggshells in *Biological mineralization and demineralization* (ed. Nancollas, G. H.) 219–232 (Springer Berlin Heidelberg, 1982).
56. Reggi, M. *et al.* Biomineralization in Mediterranean corals: the role of the intraskeletal organic matrix. *Cryst. Growth Des.* **14,** 4310–4320 (2014).
57. Schneider, C. A., Rasband, W. S. & Eliceiri, K. W. NIH Image to ImageJ: 25 years of image analysis. *Nat. Methods*. **9,** 671–675 (2012).
58. Caroselli, E. *et al.* Environmental implications of skeletal micro-density and porosity variation in two scleractinian corals. *Zoology* **114,** 255–264 (2011).
59. Palmer, A. R. Growth in marine gastropods: A non-destructive technique for independently measuring shell and body weight. *Malacologia*. **23,** 63–73 (1982).
60. Potvin, C. & Roff, D. A. Distribution-free and robust statistical methods: viable alternatives to parametric statistics? *Ecology* **74,** 1617–1628 (1993).

Acknowledgements

We wish to thank Clam Fishery Consortia of Maritime Districts of Monfalcone, Chioggia, Goro, Cesenatico, San Benedetto and Capoiale for the sampling and their logistic support. We thank E. Caroselli, F. Prada, V. Airi and S. Branchini for manuscript proofreading.

Author Contributions

S.G., G.F. and C.P. conceived the research; F.G., M.G.C., G.A.S., A.M. and M.R. analyzed the data; S.G., G.F., C.P., F.G., S.F., M.S., P.F. and L.B. interpreted the results; F.G. and A.M. wrote the manuscript; S.G., G.F. and C.P. supervised the research. All authors discussed the results and commented on the manuscript.

Additional Information

Supplementary information accompanies this paper at http://www.nature.com/srep

Competing financial interests: The authors declare no competing financial interests.

How to cite this article: Gizzi, F. *et al.* Shell properties of commercial clam *Chamelea gallina* are influenced by temperature and solar radiation along a wide latitudinal gradient. *Sci. Rep.* **6**, 36420; doi: 10.1038/srep36420 (2016).

Publisher's note: Springer Nature remains neutral with regard to jurisdictional claims in published maps and institutional affiliations.

This work is licensed under a Creative Commons Attribution 4.0 International License. The images or other third party material in this article are included in the article's Creative Commons license, unless indicated otherwise in the credit line; if the material is not included under the Creative Commons license, users will need to obtain permission from the license holder to reproduce the material. To view a copy of this license, visit http://creativecommons.org/licenses/by/4.0/

© The Author(s) 2016

Supplementary information

Shell properties of commercial clam *Chamelea gallina* are influenced by temperature and solar radiation along a wide latitudinal gradient

Francesca Gizzi[1], Maria Giulia Caccia[1], Ginevra Allegra Simoncini[1], Arianna Mancuso[1,2], Michela Reggi[3], Simona Fermani[3], Leonardo Brizi[4,5], Paola Fantazzini[4,5], Marco Stagioni[2], Giuseppe Falini[3*], Corrado Piccinetti[2*], Stefano Goffredo[1*]

Tables

Table S1. Textural data of biogenic aragonite. Full width at half maximum (FWHM) of the X-ray powder diffraction peak (111) and normalized (over ν_3) intensities of the aragonite Fourier transform infrared (FTIR) bands ν_2 and ν_4. The angle (2θ) of the maximum of the diffraction peaks and wavenumbers of the maximum of the FTIR bands do not change among samples. n = number of samples; CI = 95% confidence interval. ν_2, ν_3 and ν_4 = characteristic calcium carbonate active vibrational modes.

Code	n	FWHM mean (CI)	ν_2/ν_3 mean (CI)	ν_4/ν_3 mean (CI)
MO	5	0.170 (0)	0.386 (0.014)	0.095 (0.005)
CH	5	0.180 (0)	0.345 (0.009)	0.058 (0.012)
GO	5	0.180 (0.006)	0.401 (0.014)	0.102 (0.015)
CE	5	0.172 (0.004)	0.388 (0.009)	0.100 (0.008)
SB	5	0.174 (0.005)	0.352 (0.014)	0.090 (0.007)
CA	5	0.188 (0.004)	0.369 (0.011)	0.075 (0.005)
K-W		***		

Values for each population, in decreasing order of latitude: MO (Monfalcone), CH (Chioggia), GO (Goro), CE (Cesenatico), SB (San Benedetto) and CA (Capoiale). K-W = Kruskal-Wallis equality-of-populations rank test, *** = $p < 0.001$.

Table S2. Intra-skeletal organic matrix content. Mean organic matrix (OM) percentage weight loss for each population of *C. gallina*. n = number of samples; CI = 95% confidence interval.

Code	n	OM (%) mean (CI)
MO	10	1.95 (0.09)
CH	10	1.86 (0.11)
GO	5	1.83 (0.16)
CE	5	1.93 (0.16)
SB	5	1.72 (0.13)
CA	10	1.97 (0.08)
K-W		NS

Values for each population, in decreasing order of latitude: MO (Monfalcone), CH (Chioggia), GO (Goro), CE (Cesenatico), SB (San Benedetto) and CA (Capoiale). K-W = Kruskal-Wallis equality-of-populations rank test, NS = not significant

PCA analysis

PCA analysis was obtained including bi-dimensional shell shape parameters, (perimeter, area, aspect ratio, solidity, circularity and roundness), and length and height, to observe the possible differences in bi-dimensional shell shape among populations, using R studio software[1]. Length, height, perimeter and area were related to the PC1, aspect ratio and roundness were related to the PC2, and together explained the 72.9% of the variance (Supplementary Fig. S2a). Circularity and solidity, closer to the centre of the plot, were related to the PC3, which was not considered in the analysis because of the low variance explained (18.7%; Supplementary Fig. S2a). PCA analysis resulted in a similar bi-dimensional outline shape in shells of *C. gallina* from six populations along the Italian Adriatic coast, due to the overlapping position of dots in the space (Supplementary Fig. S2b).

The result found using traditional morphometric analysis (PCA), was compared with the result of Palmer et al.[2], that studied the bi-dimensional shape of Mediterranean specimens of *C. gallina* by combining elliptic Fourier decomposition of the shell perimeter and canonical variate analysis. They find a geographical variability in bi-dimensional shell shape of *C. gallina*, by comparing samples from seven geographical groups with highly various environments, from Màlaga, Spain, to Venice, Italy[2]. The differences in bi-dimensional shell shape of *C. gallina* found by Palmer et al.[2] is not in contrast with our result, because we considered six population located along ~400 km in the Adriatic Sea, from Monfalcone (MO) to Capoiale (CA) and characterized by more similar environmental conditions. Nevertheless, differences in *C. gallina* shells among populations were obtained analysing the tri-dimensional shell biometric parameters (length, height, width, mass, volume, bulk-density and apparent porosity) not considered in Palmer et al.[2], but considered in this study (see main text). Analysing both, bi-dimensional shape shell parameters and tri-dimensional biometric shell parameters, it was possible to discriminate groups rather geographically close and revealed which shell parameters differed among populations.

Figures

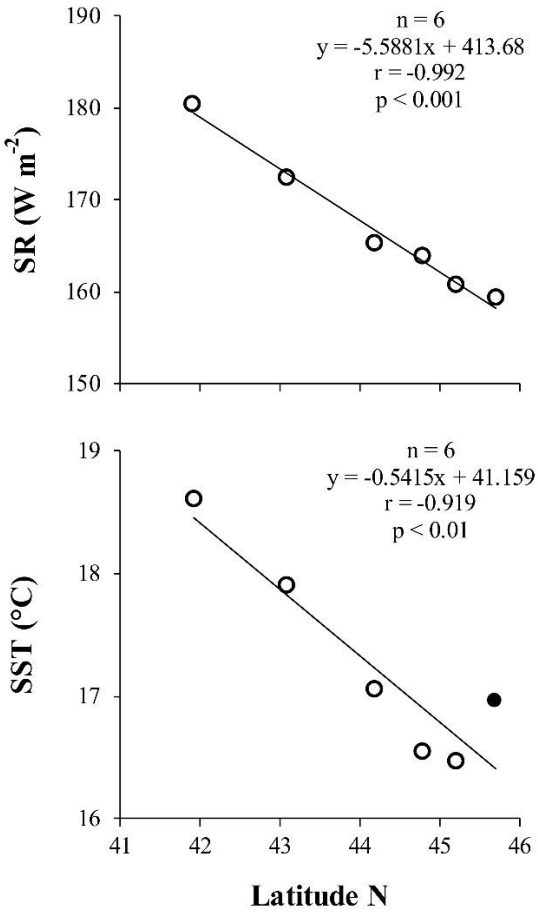

Figure S1. **Environmental parameters.** Relationship between environmental parameters (mean annual SR and SST) and the latitude of study sites along the coast of Italy. The black dot indicates the site of Monfalcone, which was characterized by higher temperature than expected at its latitude. n = number of stations; r = Pearson's correlation coefficient.

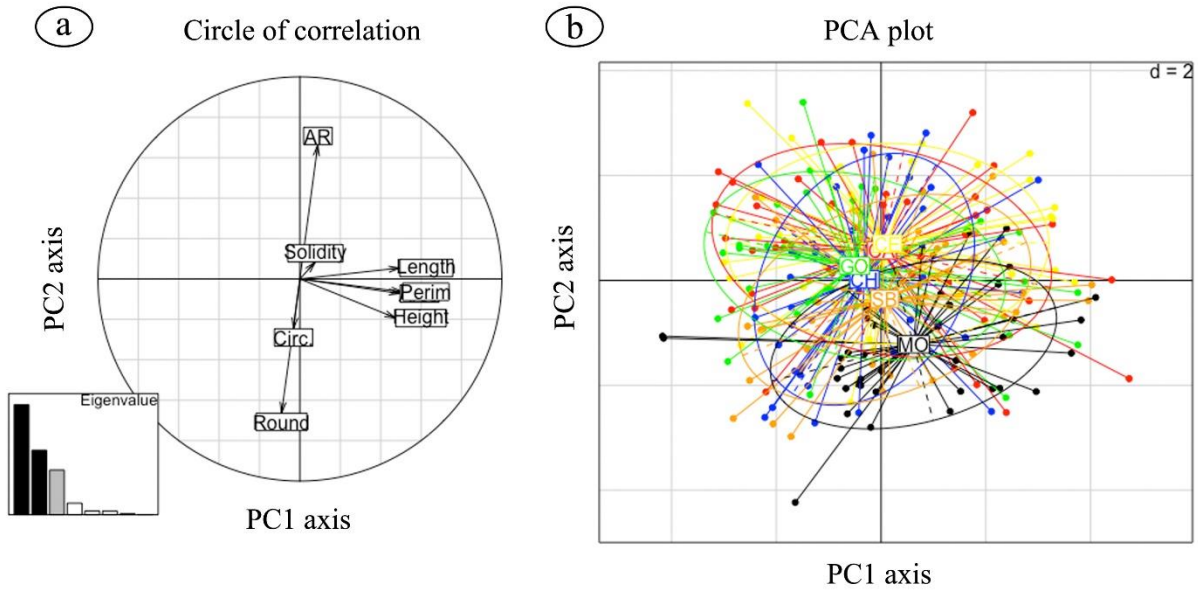

Figure S2. PCA analysis. (a) Circle of correlations between the bi-dimensional shell shape parameters and length and height and the first two principal components (PC1, PC2). Eigenvalues plot shows the percentage of explained variance for each component (PC1=46 %, PC2=26.9%, PC3=18.7%). Length, perimeter (Perim), height and area were related to PC1; the area variable is not visible, because covered by perimeter. Roundness (Round) and aspect ratio (AR) were related to PC2; solidity and circularity (Circ) were related to PC3. (b) PCA plot of the distribution of the dots in the space related to the bi-dimensional shell shape parameters and length and height, interpreted by PC1 and PC2. Each dot represents one *C. gallina* shell. MO (Monfalcone) in black; CH (Chioggia) in blue; GO (Goro) in green; CE (Cesenatico) in yellow; SB (San Benedetto) in orange; CA (Capoiale) in red.

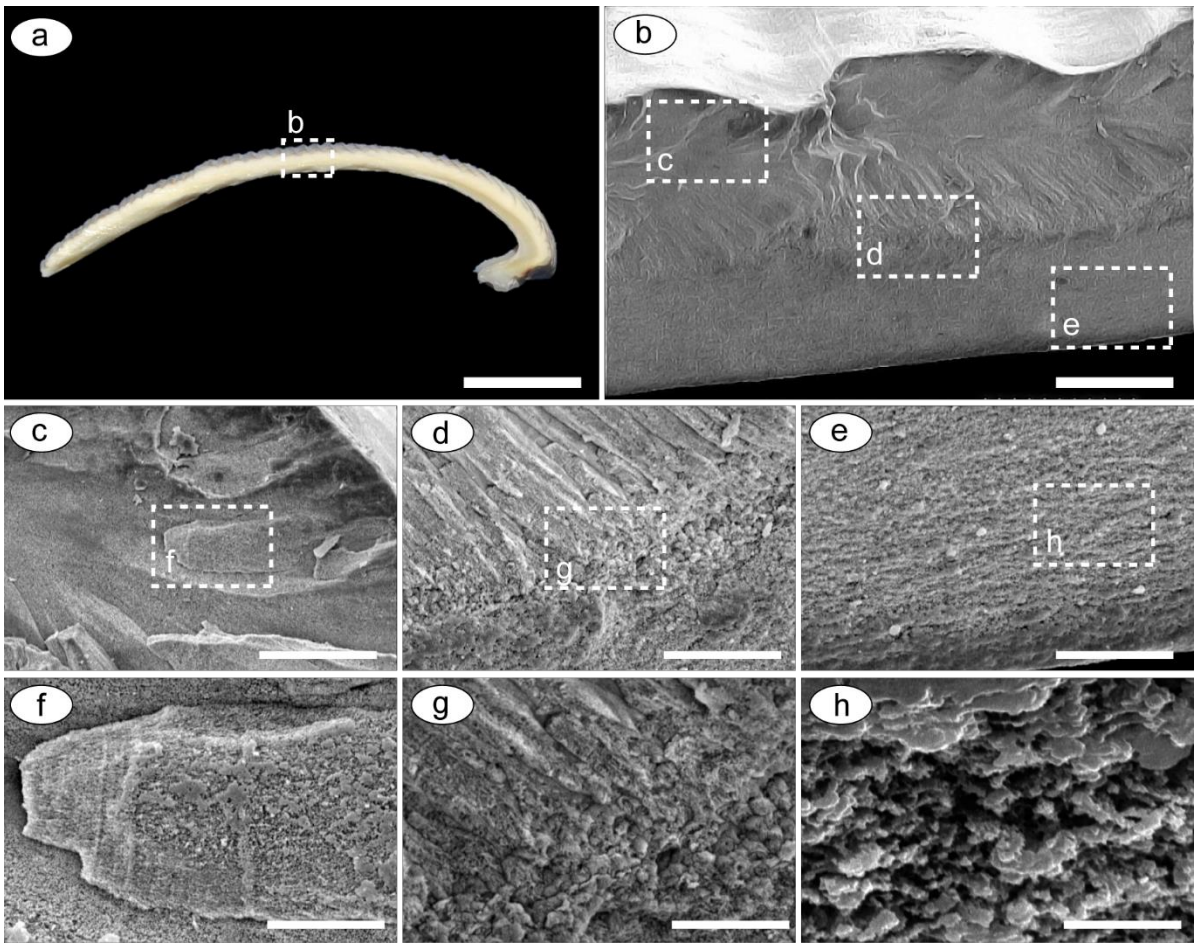

Figure S3. Scanning electron microscopy images. Skeletal morphology of *C. gallina* microstructure. The reported images are representative of all observed valves. (a, b) Images of the entire valve section. (a) Scale bar 5 mm. (b) Scale bar 0.3 mm. (c, d, e) Outer layer, transition layer and inner layer, respectively. Scale bars: 100, 50 and 50 μm, respectively. (f, g, h) Details of the outer layer, transition layer and inner layer, respectively. Scale bar 30, 20 and 5 μm, respectively. Outlined rectangles indicate areas of interest subject to higher magnifications in subsequent images.

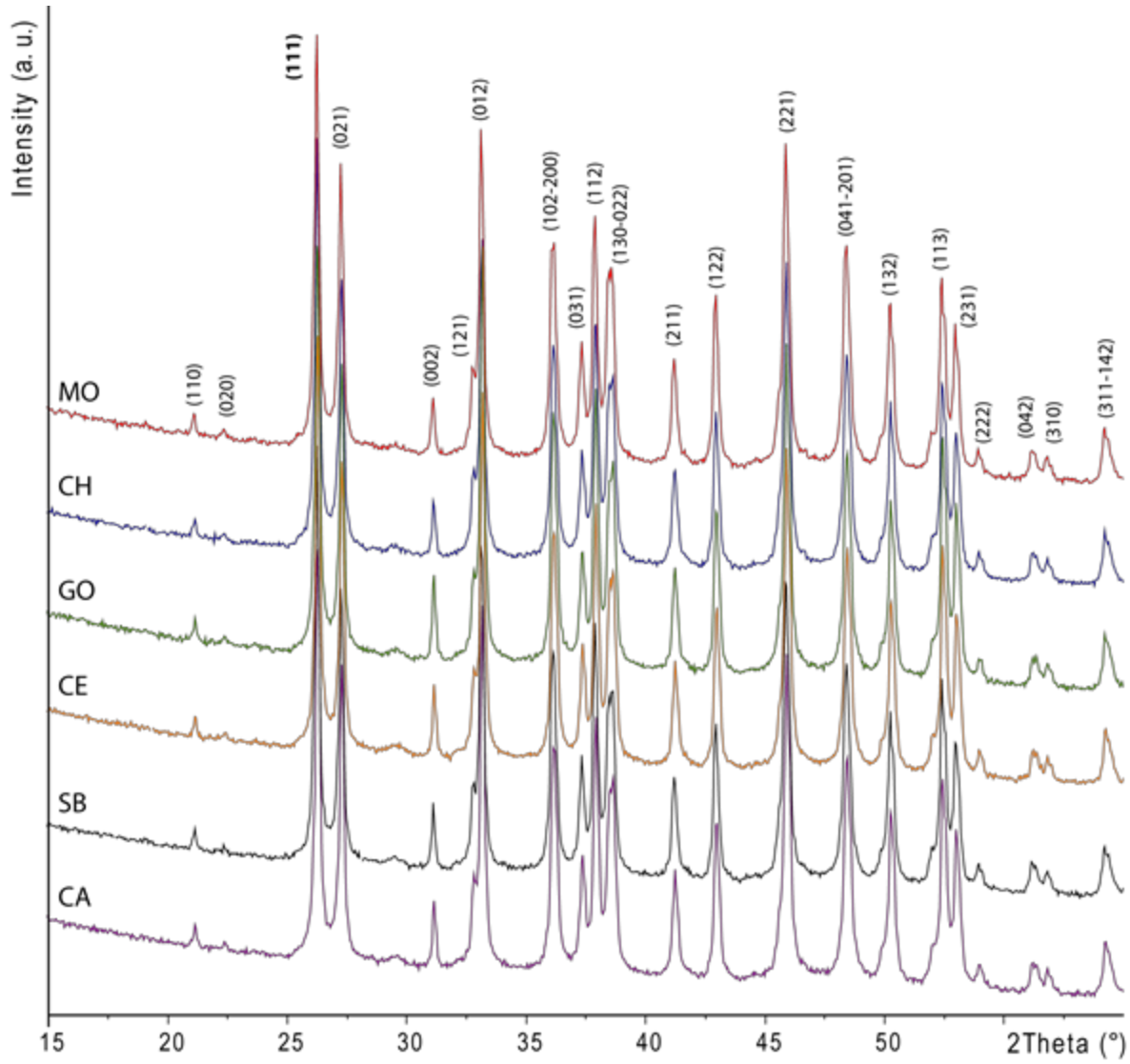

Figure S4. X-ray powder diffraction (XRD) patterns from ground shells of *C. gallina*. 5 diffractograms for each population were obtained. A representative diffraction pattern is shown for each population, in decreasing order of latitude: MO (Monfalcone), CH (Chioggia), GO (Goro), CE (Cesenatico), SB (San Benedetto) and CA (Capoiale). The diffraction peaks were labeled with the Miller index according to the PDF 01-075-2230[3]. All the peaks were assigned to aragonite. Diffraction patterns are offset to increase readability.

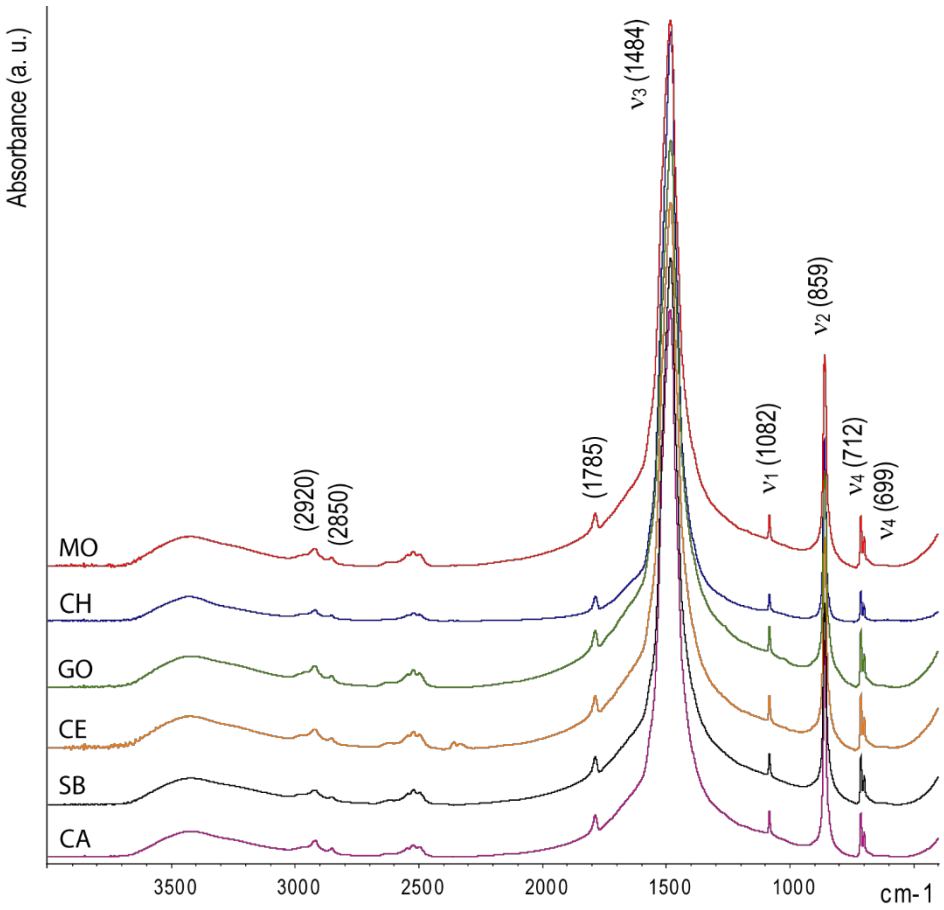

Figure S5. Fourier transform infrared (FTIR) spectra from ground shells of *C. gallina*. 5 spectra for each population were obtained. A representative FTIR spectrum is shown for each population, in decreasing order of latitude: MO (Monfalcone), CH (Chioggia), GO (Goro), CE (Cesenatico), SB (San Benedetto) and CA (Capoiale). Wavenumbers of the main absorption bands are indicated and those due to aragonite are assigned. Spectra are offset to increase readability.

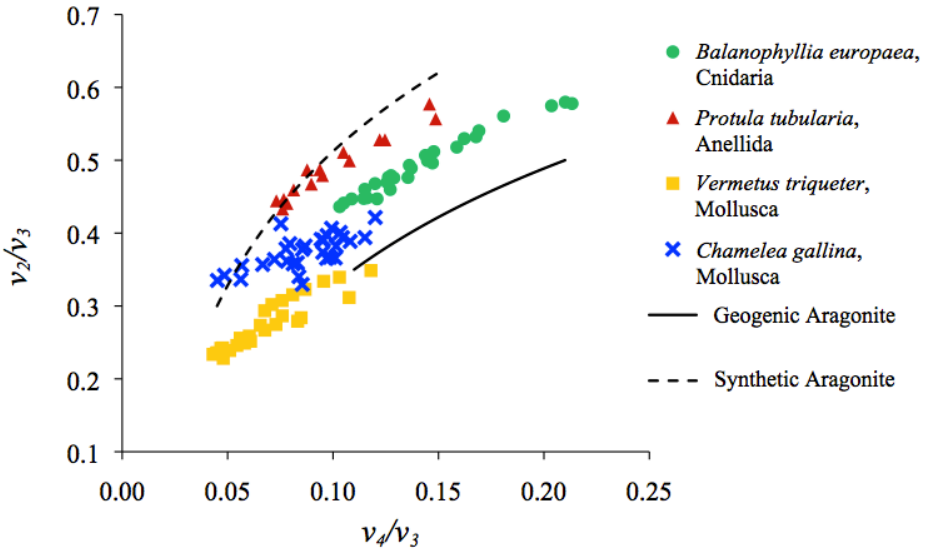

Figure S6. Evaluation of atomic order by FTIR grinding curves. Combined plots of the ν_4/ν_3 vs. ν_2/ν_3 band heights of *C. gallina* from this study, *B. europaea*, *P. tubularia* and *V. triqueter*[4] and fitted curves of the ν_4/ν_3 vs. ν_2/ν_3 peak heights of geogenic and synthetic aragonite[5].

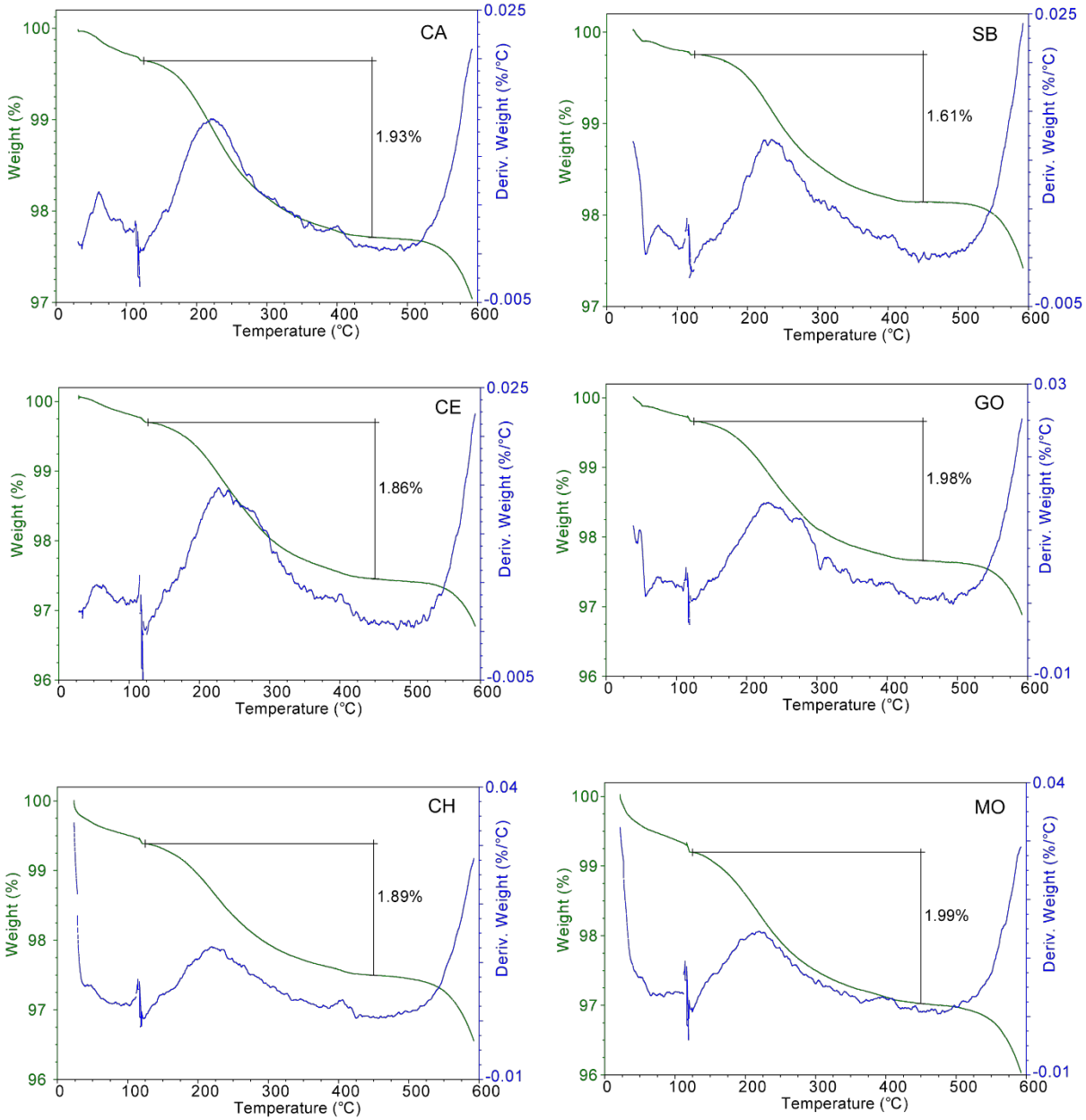

Figure S7. Intra-skeletal organic matrix content. A representative thermo gravimetrical profile is shown for each population, in increasing order of latitude: CA (Capoiale), SB (San Benedetto), CE (Cesenatico), GO (Goro), CH (Chioggia) and MO (Monfalcone). Weight lost (%) and derivate weight lost (%/°C) profiles are drown with black and blue lines, respectively.

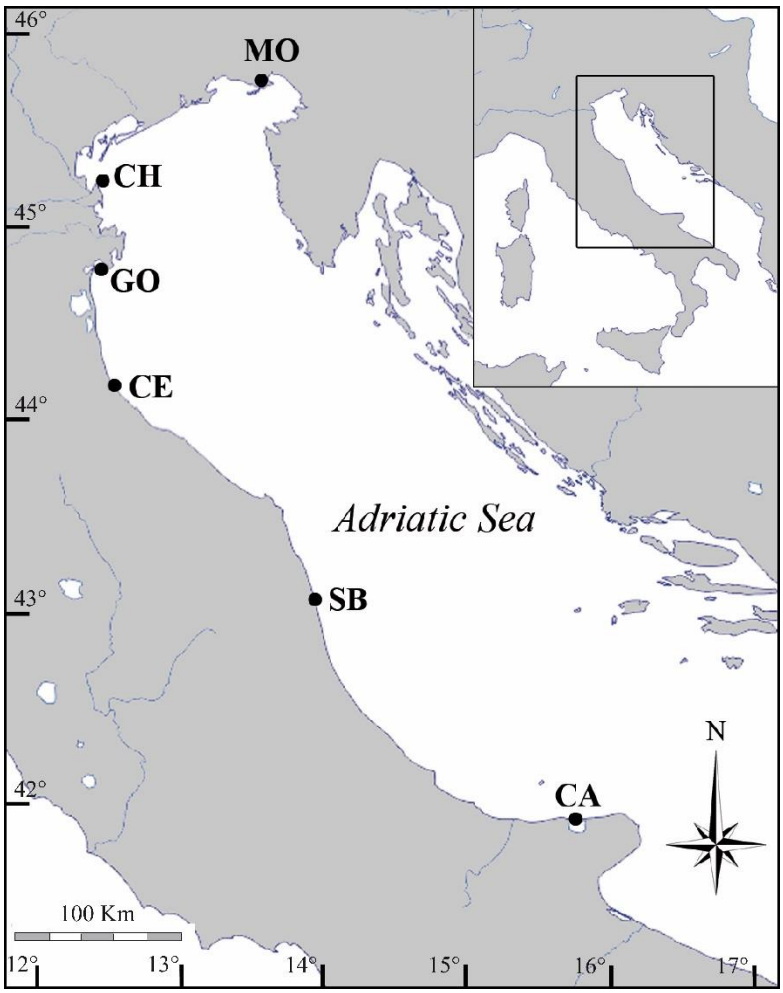

Figure S8. Map of the Adriatic coastline indicating the sites where the *C. gallina* clams were collected. Abbreviations and coordinates of the sites in decreasing order of latitude: MO, Monfalcone 45°42′N, 13°14′E; CH, Chioggia 45°12′N, 12°19′E; GO, Goro 44°47′N, 12°25′E; CE, Cesenatico 44°11′N, 12°26′E; SB, San Benedetto 43°5′N, 13°51′E; CA, Capoiale 41°55′N, 15°39′E. The map was downloaded from d-maps.com site (http://www.d-maps.com/carte.php?num_car=5993&lang=it) and modified with Adobe Photoshop CS4.

Supplementary references

1. Dray, S. & Dufour, A. B. The ade4 package: implementing the duality diagram for ecologists. *J. Stat. Softw.* **22,** 1-20 (2007).

2. Palmer, M., Pons, G. X. & Linde, M. Discriminating between geographical groups of a Mediterranean commercial clam (*Chamelea gallina* (L.): Veneridae) by shape analysis. *Fish. Res.* **67,** 93-98 (2004).

3. Jarosch, D. & Heger, G. Neutron diffraction refinement of the crystal structure of aragonite. *Tschermaks Mineral. Petrogr. Mitt*. **35,** 127-131 (1986).

4. Sabbioni, L. *Influence of Global Warming on Marine Calcifying Organisms.* MS Thesis, Department of Chemistry "Giacomo Ciamician" (University of Bologna, Italy, 2012).

5. Suzuki, M., Dauphin, Y., Addadi, L. & Weiner, S. Atomic order of aragonite crystals formed by mollusks. *Cryst. Eng. Comm.* **13,** 6780-6786 (2011).

Chapter 3

Inferred calcification rate in the bivalve *Chamelea gallina* along a latitudinal gradient in the Adriatic Sea

Submitted to Scientific Reports

Inferred calcification rate in the bivalve *Chamelea gallina* along a latitudinal gradient in the Adriatic Sea

Submitted to Scientific Reports

Arianna Mancuso[1,2], Marco Stagioni[2], Fiorella Prada[1], Daniele Scarponi[3], Corrado Piccinetti[2], Stefano Goffredo[1,2 *]

***corresponding author: E-mail s.goffredo@unibo.it**

[1]Marine Science Group, Department of Biological, Geological and Environmental Sciences, University of Bologna, Via Selmi 3, I-40126 Bologna, Italy, European Union

[2]Laboratory of Fisheries and Marine Biology at Fano, Department of Biological, Geological and Environmental Sciences, University of Bologna, Viale Adriatico 1/N, I-61032, Fano (PU), Italy, European Union

[3]Department of Biological, Geological and Environmental Sciences, University of Bologna, Via Selmi 3, I-40126 Bologna, Italy, European Union

ABSTRACT

Environmental variables are encoded in shells of marine organisms in the form of geochemical properties, shell growth rate and shell microstructure. Few studies have investigated how shell growth is affected by habitat conditions in natural populations of the commercial clam *Chamelea gallina*. Here, skeletal parameters (micro-density and apparent porosity) and growth parameters (bulk density, linear extension and net calcification rates) were investigated in relation to shell size and environmental parameters along a latitudinal gradient in the Adriatic Sea (400 km). Net calcification rates increased with increasing solar radiation, sea surface temperature and salinity and decreasing chlorophyll concentration in immature and mature shells. In immature shells, which are generally more porous than mature shells, enhanced calcification was due to an increase in bulk density. In mature shells, which show reduced extension rates compared to immature shells, increased calcification was due to an increase in linear extension rates. The presence of Po river in the Northern Adriatic Sea was likely the main driver of the fluctuations observed in environmental parameters, especially salinity and chlorophyll concentration, that seemed to negatively affect the growth of *C. gallina*.

Keywords: calcification, marine molluscs, Mediterranean Sea, salinity, shell properties

INTRODUCTION

Important ecological interactions between organisms and their environment can be unravelled through studies performed along latitudinal gradients, where varying environmental pressures can be explored on both biological and evolutionary processes[1]. Thermal conditions vary with latitude and the ability to understand the relationship between growth and temperature is important because global climate change will be a thermal challenge to most ectotherms[2].

Environmental variables are encoded in shells of marine organisms in the form of geochemical properties, shell growth rate and shell microstructure[3] and depending on the species and habitat, environmental or physiological factors are more relevant for shell growth[4,5]. Previous studies identified several drivers that influence the shell growth rate of bivalves including temperature[6,7], food supply and quality[8,9], salinity[10,11], latitude[1,12] and also reproduction[13]. Evidence for variation in growth in marine molluscs with the environment comes for example from the great scallop *Pecten maximus* along the Northeast Atlantic coast from Spain to Norway[1] and from the *Mytilus edulis* along the British coast in the Irish Sea[14].

Shell growth can be considered the result of the umbonal-ventral linear extension of the shell per unit time (cm yr^{-1}) and the calcification process ($CaCO_3$ growth rate;[15]). Net calcification rate is the product of shell bulk density (shell mass/volume ratio, including the volume of pores) and linear extension rate. Shell linear extension rates in bivalves decrease through ontogeny[16] and it might be influenced by seasonality or changes in environmental parameters[17]. Since decreasing linear extension rate is usually accompanied by an increasing in shell bulk density, variations in the total $CaCO_3$ precipitated by the animal and linear

extension rate may not necessarily correlate[17]. Therefore, differences in shell net calcification can result either from constant bulk density and non-continuous linear extension over the year, or varying bulk density and homogeneous linear extension rate.

Linear extension rates also indicate how much time is required to reach a certain marketable size[18] and the relationship between size and age is essential to implement appropriate management strategies[19]. The hard calcareous shell of many bivalves contains an ontogenetic record in the form of annually resolved growth increments[4]. Hence, bivalves sampled along well-known environmental gradients can provide reliable and accurate information on their individual ontogenetic life history, including their chronological age[20].

Bivalve age can be estimated using a variety of methods: mark and recapture experiments[21], analysis of size-frequency distributions[22], counting of annual growth marks or rings visible on the shell surface or in the microstructure of shell sections[23,24] and analysis of oxygen isotopic composition along the shell growth direction[19,25] Visible rings and banding patterns are often formed on the shells of bivalves when they undergo periods of reduced shell growth[26,27]. Ring formation has been associated with factors that probably affect the metabolic processes involved in growth, such as shifts in environmental conditions (e.g., temperature) or intrinsic conditions (e.g., spawning;[28]).

The present study investigated the shell growth of *Chamelea gallina* in six sites along a latitudinal environmental gradient in the Adriatic Sea (eastern coast of Italy). *C. gallina* (Linnaeus, 1758) is a bivalve species that occurs in the infralittoral zone and is distributed throughout the Black Sea and Mediterranean[29] and along the Algarve coast (Southern Portugal). Along the Adriatic coast of Italy, *C. gallina* has a

great economical relevance supporting an important commercial dredge fishery and is one of the most valuable bivalve resources, with a high market price (8-10 € per kg). Despite the economic importance of the clam, there have been few studies on the growth of *C. gallina* during its lifespan and in relation with environmental variation. A previous study investigated the effects of environmental parameters on shell features of commercial size (> 25 mm) at macro, micro and nanoscale levels, at the same six sites and showed that shells of the warmer and more irradiated populations were more porous and less resistant to breakage[30]. Water temperature has a dominant role in shell growth and metabolism of *C. gallina*[22,31]. Temperatures below 10 °C strongly slow or inhibit shell linear extension rates, whereas values above 28 °C reduce energy absorption and increase energy expenditure via respiration[22,31].

Previous studies on the age and shell linear extension rate of *Chamelea gallina* in the Mediterranean have employed length-frequency distributions[32], surface shell rings[33], shell thin sections[34,35] and acetate peels[22,36]. In this study, three different independent ageing methods were used: shell surface growth rings, shell internal bands (shell cross-sections and Mutvei's solution) and stable isotope composition. The method based on external rings appears to be fairly accurate in young shells[22], as *C. gallina* is, reaching 4 years in the Mediterranean Sea, while it becomes more difficult to make an accurate age determination with older and thicker shells[37]. Counting of internal bands in shell sections using Mutvei's solution is a new and easy-to-use technique that resolves annual and sub-annual growth structures in skeletons of a wide range of different organisms[38]. Shell oxygen isotope ($\delta^{18}O$) along the growth direction provides another clear method of ontogenetic age determination, in which age is directly indicated by the sequence of lower (summer)

and higher (winter) $\delta^{18}O$ values recorded by the shells[19,39].

The purposes of this investigation were to:

1) determine the growth functions for each site using three independent ageing methods;

2) measure shell linear extension and net calcification rates at each site comparing shell growth parameters along a latitudinal gradient of environmental variables in the Adriatic Sea.

While the previous study, along the same latitudinal gradient, considered only solar radiation (SR) and sea surface temperature (SST) and only shell of commercial size (>25 mm;[30]), here we investigated also sea surface salinity (SSS) and chlorophyll concentration (CHL) and we considered all shells size, from immature to mature clams.

RESULTS

SR, SST and SSS and CHL varied among sites along the latitudinal gradient (Kruskal-Wallis test, df=5, $p<0.001$; Table 1). SR, SST and SSS correlated negatively with latitude, while CHL showed the opposite trend ($p<0.001$; ESM, Fig. S1). SSS and CHL showed high variations among sites and Goro and Cesenatico located near the Po delta were the sites with higher data variability (ESM, Fig. S1a). All the environmental parameters were significantly correlated with each other, in particular SST with SR and SSS ($p<0.001$; ESM, Fig. S1b).

Shell lengths were homogeneous among sites (Kruskal-Wallis test, df=5 and $p>0.05$; ESM, Table S1). Also age did not differ among sites both for external rings and internal bands (Kruskal-Wallis test, df=5 and $p>0.05$; ESM, Table S1).

There were no significant differences among the growth curves obtained from the external and internal rings within each site (ESM, Table S2), therefore, a generalised VBG curve was obtained for each site (Fig. 3). The $\delta^{18}O$ values along the shell growth direction exhibited a roughly sinusoidal sequence of lower (summer) and higher (winter) values, and the number of observed seasons allowed to estimate the age. Age from $\delta^{18}O$ values validated the data from the other two ageing methods fitting the VBG curves (Fig. 3). A significant difference was observed comparing the generalised VBG function among sites (Kimura, $p<0.05$; ESM, Table S2).

At each site, shell skeletal and growth parameters were significantly correlated with shell length (Fig. 4). Bulk density and apparent porosity showed an opposite correlation with shell length and micro-density positively correlated with length in all sites (Fig. 4). At all sites, shell length correlated negatively with linear extension rates and net calcification rates (Fig. 4).

Variation of shell skeletal and growth parameters was then analysed in relation to environmental variables along the latitudinal gradient. Correlations were performed in the whole dataset of 84 shells for each site (Tables 2 and 3). Apparent porosity and bulk density not correlated with environmental parameters, while linear extension rate and net calcification showed significant positive correlations with SR, SST, SSS and negative correlations with CHL (Table 3). Correlations with the environment were also performed in the immature and mature shells separately and in a subgroup of the mature shells including only shells of commercial size (> 22 mm). In all groups, linear extension and net calcification were positively

correlated with SR, SST, SSS and were negatively correlated with CHL, except extension rate which did not correlate with SST in immature shells (Table 3; ESM, Figs S2-S3-S4). Micro-density, apparent porosity and bulk density showed no trends with SR in immature shells (Table 3; ESM, Fig. S2). In mature shells, apparent porosity showed no correlations with SST, SSS and CHL while bulk density correlated with SR, SST and CHL (Table 3; ESM, Fig. S3). In shells of commercial size apparent porosity positively correlated with SR, SST and negatively with CHL and bulk density correlated positively with CHL and negatively with SR, SST and SSS (Table 3; ESM, Fig. S4). Overall, comparing relationships between environmental and growth and skeletal parameters in shells of different size, environmental variables seemed to have a greater influence on shells of commercial size over 22 mm, in which we found 18 out 20 significant relationships (Table 3; ESM, Fig. S4).

DISCUSSION

In this study, we successfully used shell external and internal growth rings to estimate the age of *C. gallina* and build growth curves for this species at six sites along a wide latitudinal gradient. Both methods were validated by $\delta^{18}O$ profiles along shell growth direction, resulting to be appropriate and reasonably accurate for the age estimation of *C. gallina* specimens. This work was the first attempt to estimate the age from the internal shell section of *C. gallina* using the Mutvei's solution to highlight internal growth bands. Our values are in conformity with the

estimated maximum shell length and growth constant of *C. gallina* from previous studies in the Adriatic Sea[34], in the Western Mediterranean Sea[22] and in the Algarve coast[21]. The differences reported in maximum asymptotic length (L_{inf}) and von Bertalanffy growth constants (*K*) among sites (Table 3) are probably due to local environmental conditions, as already suggested by previous studies on the growth of *C. gallina* conducted in different areas. In previous studies, the eastern populations of this species, from the Marmara and Adriatic Sea, exhibited greater longevities than western populations in the Mediterranean (Spanish coast) and in the Atlantic (Algarve coast)[36].

As previously observed for molluscs and for other organisms[40,41], *C. gallina* extension rate decreased with increasing length. The reduction in net calcification rates with size was determined by decreasing linear extension rates, partly countered by increasing bulk density. A higher apparent porosity was observed in shells of small size and it sharply decreased to less than 20% approaching the length at sexual maturity (about 18 mm)[42]. High porosity influenced bulk density which was conversely lower in small size shells. This suggests that during the first year of life, *C. gallina* seems to promote porosity, enabling to keep higher linear extension rates in order to reach the size at sexual maturity. Although juveniles are more vulnerable than adults to most predators, a denser skeleton could limit the rate of body growth, increasing the time spent at smaller, not reproductive sizes, while more porous ones could lead to an increase in shell's linear extension rate allowing *C. gallina* to reach size at sexual maturity faster[43]. *C. gallina* is a gonochoric species with external spawning thus having a larger shell could mean more space available for gonads. From about 20 mm in length, *C. gallina* seems to change its biomineralization behavior, showing small variations in apparent porosity and bulk

density and a continuous decrease in linear extension rate and net calcification. Thus, bigger and older individuals could make denser shells to be less vulnerable to predators, while reducing the energetic cost expended in producing skeletal material by depressing linear extension rate[43].

A previous study conducted along the same latitudinal gradient in the Adriatic Sea showed that solar radiation and sea surface temperature directly affected shell skeletal properties in specimens of *C. gallina* of commercial size, showing more porous and less dense shells in the most irradiated and warm populations[30], but these trends were not analysed in specimens less than 25 mm long. This is the first study investigating shell skeletal and growth parameters during the lifespan of the clam *C. gallina* and in relation to solar radiation, temperature, salinity and chlorophyll concentration in both immature and mature shells. Environmental parameters seemed to have a greater influence on large shells over 22 mm long. Large shells with lower growth rates tend to have higher standard metabolic rates (SMR) as confirmed by the "principle of allocation" theory.[44]. Earlier studies in marine bivalves show that individuals with higher SMR are less resistant to environmental stress and this is in agreement with our findings that mature shells were more influenced by varying environmental variables than immature shells[44,45]. Individuals with higher SMR, like mature clams, must rely more on their reserves to maintain vital functions and support physiological responses to stress; in contrast, individuals with lower energetic requirements, like immature clams, have a surplus of energy with which to resist against stressful conditions[45].

Net calcification rates increased towards southern populations, with increasing SR, SST and SSS and lower CHL, in immature and mature shells. The former, which were generally more porous than the latter, allocated increased

calcification rates on bulk density. A possible explanation could be that denser clams could make them less vulnerable to predation, which often affects early life stages[46].This hypothesis is consistent with the general pattern of decreasing vulnerability with increasing prey size reported for example for decapods preying upon molluscs[47]. Predation likely depends on the ability of the predators to crush or perforate the valves and changes in shell characteristics to enhance strength, such as increase in bulk density, could lead to higher survival of small individuals[46]. In mature shells, which showed reduced extension rates and higher bulk density compared to immature shells, the increase in calcification rates towards Southern populations was invested on increasing linear extension rates, but we are not able to find a biological significance to this behaviour.

Since *C. gallina* is an infaunal bivalve, the effect of SR along the latitudinal gradient is probably related to other abiotic and/or biotic parameters, such as temperature and phytoplankton density. The increase in net calcification rates with increasing SST could be due to a decrease in the energetic costs of shell formation with increasing aragonite saturation state in warmer waters[48]. Studies on molluscs highlight that calcification increases with aragonite saturation state[49]. In this study, SST does not exceed 19°C of mean annual sea surface temperature in the southernmost site and producing carbonate shells could be less expensive than in colder sites with mean SST of 16°C.

Chlorophyll a concentration is a good food proxy for clams, based on the assumption that phytoplankton is the main component of suspension feeding bivalves diet[15]. Phytoplankton distribution in the Adriatic Sea is characterized by a generally decreasing trend of nutrient concentration from North to South[50]. Despite growth increases as a function of food concentration[51], in this study shell linear

extension and net calcification rates resulted to be lower with high CHL in all size shells, suggesting there could be other environmental parameters that synergistically affected the growth of *C. gallina*.

Here we show that in the northern sites under Po delta influence, in particular in the site of Goro, linear extension and calcification rates *of C. gallina* were negatively impacted. One possible explanation could be non-optimal salinity conditions (SSS<30). The Po river flow reduces salinity, exposing *C. gallina* to strong seasonal variations in salinity values with intense reductions in autumn and increases in summer[52], especially in the site of Goro, while the other sites show increasing salinity moving from Goro towards North and South. Suboptimal salinity may constitute a stressor leading to energy reallocation from shell production to cellular processes such as osmoregulation[53] and prolonged exposure to low salinity can stress the clams, reducing their shell growth and physiological condition. Moreover, a recent study demonstrated that lower calcification in mussels at low salinities resulted from the increased cost of calcification, rather than costs associated with osmotic stress[54]. Another possible explanation could depend on eutrophication. The enormous input of fine-grained matter by the Po river and the subsequent transport by surface currents have resulted in a well-defined clay belt along the Italian coast. The records of the Po river nutrient load[55], sea water transparency[56] and anoxic events of the past decades[57] all suggest that the anthropogenic nutrient input is increasingly affecting the marine environment. Slow growth rates associated with eutrophicated habitats have been recorded previously for the bivalve *Cerastoderma edule*[58] and for the bivalve *Austrovenus stutchburyi*[59] and these studies seem to confirm the results found for *C. gallina* that showed higher extension and calcification rates in oligotrophic conditions. Moreover, silt and clay

that characterise the bottom of the Po delta area could interfere with the feeding mechanism, leading to low extension and net calcification rates and growth rates were found to be higher in sand than mud[59]. Thus, the observed reduction in extension and calcification rates of *C. gallina* in those sites that are most influenced by the Po delta could depend on a number of factors acting synergistically. However, further studies are needed to test these hypotheses.

CONCLUSIONS

Differences found in shell skeletal parameters, especially apparent porosity and bulk density, with length could be due to different behaviour in biomineralization between immature and mature shells of *C. gallina.* Before reaching sexual maturity, *C. gallina* seemed to promote porosity enabling to keep higher linear extension rates in order to reach the size at sexual maturity faster, while after sexual maturity shells seemed to depress linear extension rate and make denser shells. reducing the energetic cost expended in producing skeletal material.

Moving far from the Po delta towards South, warmer seawater, low fluctuations in salinity and oligotrophic conditions suggested that these environmental conditions may be most favourable for the clam *C. gallina*, leading to net calcification rates. Net calcification rates were significantly reduced in sites around the Po delta, possibly as a result of reduced salinity and increased eutrophication and silt and clay of the bottom driven by the river discharges. The present study therefore points out the importance of considering multiple environmental parameters to investigate bivalve growth. In addition, knowledge of

the growth rates allows a proper management of bivalve fisheries. Given the great socio-economic relevance of *C. gallina* in all the Italian Adriatic coasts, studies like this one are crucial to guarantee a knowledge-based management of this important resource.

MATERIALS AND METHODS

Between August 2013 and April 2015, specimens of *C. gallina* were collected from six sites along a latitudinal gradient in the Adriatic Sea from 45°42′N to 41°55′N (electronic supplementary material ESM, Fig. 1). Clams were sampled at each site using hydraulic dredges at 3–5 m depth. 84 shells of different size from each site were used for the analyses. Shells were divided in three groups: immature (up to 18 mm), mature shells (over 18 mm;[60]) and commercial shells (over 22 mm, new commercial size adopted from January 2017).

Skeletal apparent porosity (ratio of the pore volume connected to the external surface; %) and micro-density (mass per unit volume of the material which composes the shell, excluding the volume of pores; g cm^{-3}) were measured by buoyant weight analysis (see[30] for calculation details). In addition, clam shell length (anterior-posterior maximum distance), was obtained with ImageJ software after data capture of each shell shape with a scanner and dry shell weight was measured using an analytical balance (±0.1 mg).

Bulk density (shell mass/volume ratio, including the volume of pores) was measured by buoyant weight analysis. Shell linear extension rates were obtained with the length/age ratio (cm y^{-1}), while the net calcification rate (mass of $CaCO_3$

deposited per year per unit area g y^{-1} cm^2) was calculated for each shell by the formula: net calcification (g cm^{-2} y^{-1}) = bulk density (g cm^{-3}) x shell extension (cm y^{-1})[61].

Age was measured in a subsample of 30 shells of different size in each site, by using three methods: shell surface growth rings (ESM, Fig. 2a), shell internal bands (shell cross-sections and Mutvei's solution; ESM, Fig. 2b) and stable $\delta^{18}O$ composition (see ESM for the three ageing methods details). By counting the total number of visible external and internal rings in each shell, the age-length keys were obtained for the two methods and fitted with the von Bertalanffy growth (VBG) functions, using a non-linear model that provides estimates of the parameters in the VBG equation[62] through bootstrap method:

$$L_t = L_{inf}[1 - e^{-k(t)}]$$

where L_t is individual length at age t, L_{inf} is asymptotic length (maximum expected length in the population), K is a growth constant, t is the age of the individual. Two growth curves for each sites were produced and a chi-square test of maximum likelihood ratios[63] was used to examine the significance of differences in growth functions between the two ageing method. Kimura's method allows the testing of several hypotheses to compare the two curves by analysing one or more growth parameters simultaneously. For these purposes, the FSA (Simple Fisheries Stock Assessment Methods) and the Fishmethods packages in R studio[64] were used. If no differences were revealed between VBG curves from shell surface growth rings and internal bands, generalised growth curves for each site were constructed by merging age-length keys from both methods and the resulted generalised VBG function for each site were taken into account for extrapolating age in all the 84 shells. Age were calculated from the inverse of generalised VBG function of each site:

$$t = \frac{1}{k * \ln\left(\frac{L_{inf}}{L_{inf} - L}\right)}$$

To validate the data from the two counting rings methods and the generalised VBG curves, oxygen isotopic measurements ($\delta^{18}O$) were carried out on "spot" samples collected in sequence along the shell growth direction. Age resulted from counting lighter $\delta^{18}O$ (summer) and heavier $\delta^{18}O$ (winter) peaks were then plotted with the age-length key from the two ageing methods. $\delta^{18}O$ analysis was conducted at The Godwin Laboratory for Palaeoclimate Research, Department of Earth Sciences, University of Cambridge.

Environmental parameters

Solar radiation (SR; W m^{-2}), Sea Surface Temperature (SST; °C) and Sea Surface Salinity (SSS; PSU) data were obtained for each site from the Euro-Mediterranean Center on Climate Change data banks (CMCC http://oceanlab.cmcc.it/afs/). Mean annual SR, SST and SSS were calculated from daily values measured from July 2011 to June 2015 (number of daily values = 1447 for each site, instead of 1460 days for 4 years for 13 days missing data), to enclose the almost full *C. gallina* lifespan of two-three years for the samples under investigation. For the same period, a mean annual chlorophyll concentration (CHL; mg/m^3) was calculated from monthly values of CHL, obtained for each site (48) from the *GlobColour data* (http://globcolour.info) by ACRI-ST, France (http://hermes.acri.fr).

REFERENCES

1. Chauvaud, L. *et al.* Variation in size and growth of the Great Scallop *Pecten maximus* along a latitudinal gradient. *PLoS One* (2012). doi:10.1371/journal.pone.0037717
2. Angilletta, M. J., Oufiero, C. E. & Leache, A. D. Direct and indirect effects of environmental temperature on the evolution of reproductive strategies: An information-theoretic approach. *Am. Nat.* (2006). doi:10.1086/507880
3. Purroy, A., Milano, S., Schöne, B. R., Thébault, J. & Peharda, M. Drivers of shell growth of the bivalve, *Callista chione* (L. 1758) – Combined environmental and biological factors. *Mar. Environ. Res.* 134, 138–149 (2018)
4. Richardson, C. A. Molluscs as archives of environmental change. *Oceanogr. Mar. Biol.* (2001)
5. Nishida, K., Ishimura, T., Suzuki, A. & Sasaki, T. Seasonal changes in the shell microstructure of the bloody clam, Scapharca broughtonii (Mollusca: Bivalvia: Arcidae). *Palaeogeogr. Palaeoclimatol. Palaeoecol.* 363–364, 99–108 (2012)
6. Brocas, W. M. *et al.* The dog cockle, *Glycymeris glycymeris* (L.), a new annually-resolved sclerochronological archive for the Irish Sea. *Palaeogeogr. Palaeoclimatol. Palaeoecol.* 373, 133–140 (2013)
7. Schone, B. R. *et al.* Daily Growth Rates in Shells of Arctica islandica: Assessing Sub-seasonal Environmental Controls on a Long-lived Bivalve Mollusk. *Palaios* 20, 78–92 (2005)
8. Broom, M. J. & Mason, J. Growth and spawning in the pectinid *Chlamys opercularis* in relation to temperature and phytoplankton concentration. *Mar. Biol.* 47, 277–285 (1978).
9. Sato, S. Shell microgrowth patterns of bivalves reflecting seasonal change of phytoplankton abundance. *Paleontol. Res.* 1, 260–266 (1997)
10. Koike, H. Microstructure of the growth increment in the shell of *Meretrix lusoria*. *Mech. Biominer. Anim. plants* (1980)
11. Marsden, I. & Pilkington, R. Spatial and temporal variations in the condition of *Austrovenus stutchburyi* Finlay, 1927 (Bivalvia: Veneridae) from the Avon-Heathcote estuary, Christchurch. *Nat. Sci.* 22, 57–67 (1995)

12. Hall, C. A., Dollase, W. A. & Corbató, C. E. Shell growth in *Tivela stultorum* (Mawe, 1823) and *Callista chione* (Linnaeus, 1758) (Bivalvia): annual periodicity, latitudinal differences, and diminution with age. *Palaeogeogr. Palaeoclimatol. Palaeoecol.* 15, 33–61 (1974).
13. Okaniwa, N., Miyaji, T., Sasaki, T. & Tanabe, K. Shell growth and reproductive cycle of the Mediterranean mussel *Mytilus galloprovincialis* in Tokyo Bay, Japan: relationship with environmental conditions. *Plankt. Benthos Res.* 5, 214–220 (2010)
14. Hiebenthal, C., Philipp, E. E. R., Eisenhauer, A. & Wahl, M. Effects of seawater pCO2and temperature on shell growth, shell stability, condition and cellular stress of Western Baltic Sea *Mytilus edulis* (L.) and *Arctica islandica* (L.). *Mar. Biol.* (2013). doi:10.1007/s00227-012-2080-9
15. Gillikin, D. P. *et al.* Strong biological controls on Sr/Ca ratios in aragonitic marine bivalve shells. *Geochemistry, Geophys. Geosystems* 6, n/a-n/a (2005)
16. Schöne, B. R., Lega, J., Flessa, K. W., Goodwin, D. H. & Dettman, D. L. Reconstructing daily temperatures from growth rates of the intertidal bivalve mollusk *Chione cortezi* (northern Gulf of California, Mexico). *Palaeogeogr. Palaeoclimatol. Palaeoecol.* (2002). doi:10.1016/S0031-0182(02)00252-3
17. Lorrain, A. *et al.* $\delta^{13}C$ variation in scallop shells: Increasing metabolic carbon contribution with body size? *Geochim. Cosmochim. Acta* 68, 3509–3519 (2004)
18. Urban, H.-J. Culture potential of the pearl oyster (*Pinctada imbricata*) from the Caribbean.: I. Gametogenic activity, growth, mortality and production of a natural population. *Aquaculture* 189, 361–373 (2000)
19. Keller, N., Del Piero, D. & Longinelli, A. Isotopic composition, growth rates and biological behaviour of *Chamelea gallina* and *Callista chione* from the Gulf of Trieste (Italy). *Mar. Biol.* 140, 9–15 (2002)
20. Austad, S. N. The uses of intraspecific variation in aging research. *Exp. Gerontol.* (1996). doi:10.1016/0531-5565(95)02068-3
21. Gaspar, M. B., Pereira, A. M., Vasconcelos, P. & Monteiro, C. C. Age and growth of *Chamelea gallina* from the Algarve Coast (Southern Portugal): influence of seawater temperature and gametogenic cycle on growth rate. *J. Molluscan Stud.* 70, 371–377 (2004)

22. Ramón, M. & Richardson, C. A. Age determination and shell growth of *Chamelea gallina* (Bivalvia: Veneridae) in the western Mediterranean. *Marine Ecology Progress Series* 89, 15–23 (1992)
23. Richardson, C. A., Seed, R. & Naylor, E. Use of internal growth bands for measuring individual and population growth rates in *Mytilus edulis* from offshore production platforms. *Mar. Ecol. Prog. Ser.* (1990). doi:10.3354/meps066259
24. Moura, P., Gaspar, M. & Monteiro, C. Age determination and growth rate of a *Callista chione* population from the southwestern coast of Portugal. *Aquat. Biol.* 5, 97–106 (2009).
25. Schöne, B. R. & Giere, O. Growth increments and stable isotope variation in shells of the deep-sea hydrothermal vent bivalve mollusk *Bathymodiolus brevior* from the North Fiji Basin, Pacific Ocean. *Deep. Res. Part I Oceanogr. Res. Pap.* 52, 1896–1910 (2005)
26. Stevenson, J. A. & Dickie, L. M. Annual Growth Rings and Rate of Growth of the Giant Scallop, *Placopecten magellanicus* (Gmelin) in the Digby Area of the Bay of Fundy. *J. Fish. Res. Board Canada* 11, 660–671 (1954)
27. Haag, W. R. & Commens-Carson, A. M. Testing the assumption of annual shell ring deposition in freshwater mussels. *Can. J. Fish. Aquat. Sci.* 65, 493–508 (2008)
28. Ropes, J. W. Modern Methods Used to Age Oceanic Bivalves. *Nautilus (Philadelphia).* (1985)
29. Poppe, GT and Goto, Y. European Seashells, vol. 2. *Verlag Christa Hemmen, Wiesbad.* 221 (1993)
30. Gizzi, F. *et al.* Shell properties of commercial clam *Chamelea gallina* are influenced by temperature and solar radiation along a wide latitudinal gradient. *Sci. Rep.* (2016). doi:10.1038/srep36420
31. Moschino, V. & Marin, M. G. Seasonal changes in physiological responses and evaluation of “well-being” in the Venus clam *Chamelea gallina* from the Northern Adriatic Sea. *Comp. Biochem. Physiol. Part A Mol. Integr. Physiol.* 145, 433–440 (2006)
32. Froglia, C. Osservazioni sull’accrescimento di *Chamelea gallina* (L.) ed *Ensis minor* (Chenu) nel medio Adriatico. *Quad. Lab. Tecnol. Pesca* 2, 37–48 (1975)

33. Deval, MC and Oray, I. The annual shell increments of Bivalvia *Chamelea gallina* L. 1758 in the northern Sea of Marmara. *Oebalia* 24, 93–109 (1998)
34. Arneri, E and Giannetti, G and Polenta, R and Antolini, B. Age and growth of *Chamelea gallina* (Bivalvia: Veneridae) in the Central Adriatic Sea obtained by thin sections. *Rapp. Comm. int. Mer Médit* 34, 17 (1995)
35. Arneri, E and Froglia, C and Polenta, R and Antolini, B. Growth of *Chamelea gallina* (Bivalvia: Veneridae) in the eastern Adriatic (Neretva river estuary). *Tisucu God. Prv. Spomena Ribar. u Hrvata* 597, 669–676 (1997)
36. Deval, M. C. Shell growth and biometry of the striped venus *Chamelea gallina* (L) in the Marmara Sea, Turkey. *J. Shellfish Res.* 20, 155–159 (2001)
37. MacDonald, B. A. & Thomas, M. L. H. Age determination of the soft-shell clam *Mya arenaria* using shell internal growth lines. *Mar. Biol.* 58, 105–109 (1980)
38. Schöne, B. R., Dunca, E., Fiebig, J. & Pfeiffer, M. Mutvei's solution: An ideal agent for resolving microgrowth structures of biogenic carbonates. *Palaeogeogr. Palaeoclimatol. Palaeoecol.* 228, 149–166 (2005)
39. Chute, A. S., Wainright, S. C. & Hart, D. R. Timing of shell ring formation and patterns of shell growth in the sea scallop placopecten magellanicus based on stable oxygen isotopes. *J. Shellfish Res.* (2012). doi:10.2983/035.031.0308
40. Caroselli, E. *et al.* Relationships between growth, population dynamics, and environmental parameters in the solitary non-zooxanthellate scleractinian coral *Caryophyllia inornata* along a latitudinal gradient in the Mediterranean Sea. *Coral Reefs* (2016). doi:10.1007/s00338-015-1393-9
41. Sebens, K. P. The Ecology of Indeterminate Growth in Animals. *Annu. Rev. Ecol. Syst.* 18, 371–407 (1987)
42. Cordisco CA, Trotta P, R. M. Spawning plasticity of baby clam *Chamela gallina*, Linnaeus 1758. *Biol. Mar. Mediterr.* 12, (2005)
43. Palmer A. Richard. Do carbonate skeletons limit the rate of body growth? *Nature* 292, (1981)
44. Steyermark, A. C. A high standard metabolic rate constrains juvenile growth. *Zoology* (2002). doi:10.1078/0944-2006-00055
45. Myrand, B., Tremblay, R. & Sévigny, J.-M. Selection against blue mussels (*Mytilus edulis* L.) homozygotes under various stressful conditions. *J. Hered.* (2002). doi:DOI 10.1093/jhered/93.4.238

46. Arsenault, D. J. & Himmelman, J. H. Size-related changes in vulnerability to predators and spatial refuge use by juvenile Iceland scallops *Chlamys islandica*. *Mar. Ecol. Prog. Ser.* (1996). doi:10.3354/meps140115
47. Juanes, F. Why do decapod crustaceans prefer small-sized molluscan prey? *Mar. Ecol. Prog. Ser.* (1992). doi:10.3354/meps087239
48. Clarke, A. Temperature and Extinction in the Sea: A Physiologist's View. *Paleobiology* 19, 499–518 (1993)
49. Ries, J. B., Cohen, A. L. & McCorkle, D. C. Marine calcifiers exhibit mixed responses to CO2-induced ocean acidification. *Geology* 37, 1131–1134 (2009)
50. Zavatarelli, M., Raicich, F., Bregant, D., Russo, A. & Artegiani, A. Climatological biogeochemical characteristics of the Adriatic Sea. *J. Mar. Syst.* 18, 227–263 (1998)
51. Iglesias, J. I. P., Navarro, E., Alvarez Jorna, P. & Armentina, I. Feeding, particle selection and absorption in cockles *Cerastoderma edule* (L.) exposed to variable conditions of food concentration and quality. *J. Exp. Mar. Bio. Ecol.* (1992). doi:10.1016/0022-0981(92)90200-T
52. Russo, A., Rabitti, S. & Bastianini, M. Decadal Climatic Anomalies in the Northern Adriatic Sea Inferred from a New Oceanographic Data Set. *Mar. Ecol.* 23, 340–351 (2002)
53. Hiebenthal, C., Philipp, E., Eisenhauer, A. & Wahl, M. Interactive effects of temperature and salinity on shell formation and general condition in Baltic Sea *Mytilus edulis* and *Arctica islandica*. *Aquat. Biol.* (2012). doi:10.3354/ab00405
54. Sanders, T., Schmittmann, L., Nascimento-Schulze, J. C. & Melzner, F. High Calcification Costs Limit Mussel Growth at Low Salinity. *Front. Mar. Sci.* (2018). doi:10.3389/fmars.2018.00352
55. Marchetti, R., Provini, A. & Crosa, G. Nutrient load carried by the River Po into the Adriatic Sea, 1968-1987. *Mar. Pollut. Bull.* (1989). doi:10.1016/0025-326X(89)90487-6
56. Justic, D. Trend in the transparency of the northern Adriatic Sea 1911-1982. *Mar. Pollut. Bull.* 19, (1988)
57. Justić, D. Long-term eutrophication of the Northern Adriatic Sea. *Mar. Pollut. Bull.* (1987). doi:10.1016/0025-326X(87)90505-4

58. Loo, L. O. & Rosenberg, R. Bivalve suspension-feeding dynamics and benthic-pelagic coupling in an eutrophicated marine bay. *J. Exp. Mar. Bio. Ecol.* (1989). doi:10.1016/0022-0981(89)90167-6
59. Marsden, I. Effects of reduced salinity and seston availability on growth of the New Zealand little-neck clam *Austrovenus stutchburyi*. *Mar. Ecol. Prog. Ser.* 266, 157–171 (2004)
60. Scarcella Giuseppe, C. A. M. *Research for PECH Committee - The Clam Fisheries Sector in the EU - The Adriatic Sea Case - Think Tank*. (2016)
61. Caroselli, E. *et al.* Inferred calcification rate of a Mediterranean azooxanthellate coral is uncoupled with sea surface temperature along an 8[degree sign] latitudinal gradient. *Front. Zool.* 9, 32 (2012)
62. von Bertalanffy Ludwig. A quantitative theory of organic growth (inquiries on growth laws. II. *Hum. Biol.* 10, 181–213 (1938)
63. Kimura, M. A simple method for estimating evolutionary rates of base substitutions through comparative studies of nucleotide sequences. *J. Mol. Evol.* 16, 111–120 (1980).
64. Ogle, D. *Introductory Fisheries Analyses with R*. 20155862, (Chapman and Hall/CRC, 2015)

Acknowledgements

We wish to thank Clam Fishery Consortia of Maritime Districts of Monfalcone, Chioggia, Goro, Cesenatico, San Benedetto and Capoiale for the sampling and their logistic support.

Authors' contributions

AM, SG and CP conceived the research; AM performed the analyses; AM and DS analysed the isotopic data; AM, MS, FP and SG interpreted the results; AM, FP and SG wrote the manuscript. All authors participated to the scientific discussion.

TABLES

Table 1. Environmental parameters. Mean annual values for solar radiation (SR), sea surface temperature (SST), sea surface salinity (SSS) and chlorophyll concentration (CHL) from 2011 to 2014. n = number of collected data, daily data for SR, SST and SSS and monthly data for CHL; CI = 95% confidence interval. Values for each site, in decreasing order of latitude: MO (Monfalcone), CH (Chioggia), GO (Goro), CE (Cesenatico), SB (San Benedetto), CA (Capoiale).

Code	Latitude (°)	n	SR (W/m^2) mean	CI	SST (°C) mean	CI	SSS (PSU) mean	CI	n	CHL (mg/m^3) mean	CI
MO	45.7	1447	159.44	155.45 - 164.43	16.96	16.58 - 17.34	35.43	35.37 - 35.49	48	4.50	4.11 - 4.89
CH	45.2	1447	160.76	155.82 - 165.70	16.47	16.09 - 16.85	30.89	30.72 - 31.06	48	2.88	2.45 - 3.31
GO	44.8	1447	163.78	158.74 - 168.82	16.54	16.17 - 16.91	28.52	28.36 - 28.68	48	4.98	4.21 - 5.75
CE	44.2	1447	165.17	160.18 - 170.16	17.05	16.65 - 17.45	34.19	34.11 - 34.27	48	6.23	5.03 - 7.43
SB	43.1	1447	172.39	167.39 - 177.39	17.90	17.52 - 18.28	36.29	36.24 - 36.34	48	2.09	1.54 - 2.64
CA	41.9	1447	180.44	175.36 - 185.52	18.60	18.27 - 18.93	37.43	37.40 - 37.46	48	1.21	0.85 - 1.57

Table 2. Shell skeletal and growth parameters. n = number of samples; CI = 95% confidence interval. Sites are arranged in order of decreasing latitude: MO (Monfalcone), CH (Chioggia), GO (Goro), CE (Cesenatico), SB (San Benedetto), CA (Capoiale). K-W = Kruskal-Wallis equality-of-populations rank test, NS = not significant, ** $p<0.01$, *** $p<0.001$.

Site	N	Length (mm)	CI	Micro-density (g/cm3)	CI	Apparent porosity (%)	CI	Bulk density (g/cm3)	CI	Linear extension rate (cm/y)	CI	Net calcification (g/cm2 y)	CI
MO	84	21.26	19.59 - 22.94	2.76	2.75 - 2.77	7.60	6.22 - 8.98	2.55	2.51 - 2.60	1.50	1.44 - 1.55	3.78	3.68 - 3.89
CH	84	21.90	20.33 - 23.48	2.79	2.78 - 2.80	7.85	6.64 - 9.05	2.57	2.53 - 2.61	1.46	1.40 - 1.52	3.72	3.61 - 3.83
GO	84	22.05	20.63 - 23.47	2.78	2.76 -2.80	9.60	7.46 - 11.74	2.52	2.45 - 2.59	1.41	1.36 - 1.47	3.51	3.42 - 3.60
CE	84	21.42	19.76 - 23.07	2.76	2.73 - 2.79	10.05	7.70 - 12.39	2.49	2.41 - 2.57	1.48	1.43 - 1.53	3.61	3.52 - 3.70
SB	84	21.59	19.86 - 23.31	2.78	2.75 - 2.80	7.39	6.19 - 8.60	2.57	2.53 - 2.62	1.47	1.43 - 1.52	3.76	3.68 - 3.84
CA	84	22.59	21.29 - 23.90	2.79	2.78 - 2.80	8.12	7.05 - 9.20	2.57	2.53 - 2.60	1.69	1.64 - 1.74	4.31	4.22 - 4.40
K-W		NS		***		**		***		***		***	

Table 3. Linear regression and correlation analysis between environmental and shell skeletal and growth parameters. rho, Spearman's rho coefficient. rho and p-value are shown only when Kruskal-Wallis test is significant. Regression parameters are shown only where the linear relationship is significant. SR, solar radiation; SST, sea surface temperature; SSS, sea surface salinity; CHL, chlorophyll concentration; SE, standard error.

	SR				SST				SSS				CHL			
	Slope (SE)	Intercept (SE)	rho	p	Slope (SE)	Intercept (SE)	rho	p	Slope (SE)	Intercept (SE)	rho	p	Slope (SE)	Intercept (SE)	rho	p
All samples, n = 504																
Micro-density	0.001 (0.001)	2.647 (0.087)	0.101	*	-	-	-0.029	NS	-	-	-0.063	NS	-	-	-0.024	NS
Apparent porosity	-	-	-	-	-	-	-	-	-	-	-	-	-	-	-	-
Bulk density	-	-	-	-	-	-	-	-	-	-	-	-	-	-	-	-
Linear extension rate	0.009 (0.002)	-0.055 (0.256)	0.217	***	0.096 (0.015)	-0.154 (0.252)	0.259	***	0.020 (0.004)	0.828 (0.122)	0.282	***	-0.031 (0.007)	1.616 (0.026)	-0.237	***
Net calcification rate	0.027 (0.003)	-0.701 (0.474)	0.259	***	0.281 (0.027)	-1.062 (0.46)	0.321	***	0.058 (0.007)	1.806 (0.227)	0.398	***	-0.011 (0.012)	4.186 (0.048)	-0.393	***
Immature samples (<18 mm), n = 150																
Micro-density	-	-	0.156	NS	0.019 (0.011)	2.401 (0.185)	0.182	*	0.005 (0.003)	2.558 (0.089)	0.283	***	-0.010 (0.005)	2.763 (0.018)	-0.360	***
Apparent porosity	-	-	-0.117	NS	-2.920 (1.004)	66.438 (17.328)	-0.183	*	-0.854 (0.242)	45.153 (8.259)	-0.276	***	1.903 (0.409)	9.008 (1.672)	0.297	***
Bulk density	-	-	0.141	NS	0.093 (0.030)	0.690 (0.520)	0.197	*	0.027 (0.007)	1.378 (0.248)	0.315	***	-0.058 (0.012)	2.507 (0.050)	-0.370	***
Linear extension rate	0.006 (0.001)	0.836 (0.238)	0.170	*	-	-	0.118	NS	0.007 (0.004)	1.587 (0.123)	0.170	*	-0.025 (0.006)	1.915 (0.025)	-0.276	***
Net calcification rate	0.025 (0.006)	0.030 (0.967)	0.189	*	0.301 (0.056)	-1.019 (0.962)	0.255	**	0.066 (0.014)	1.911 (0.473)	0.434	***	-0.167 (0.022)	4.788 (0.090)	-0.540	***
Mature samples (> 18 mm), n = 354																
Micro-density	-	-	0.049	NS	-0.001 (0.005)	2.822 (0.083)	-0.114	*	-0.002 (0.001)	2.858 (0.040)	-0.159	**	-	-	0.086	NS
Apparent porosity	0.087 (0.024)	-9.357 (4.032)	0.240	***	-	-	0.070	NS	-	-	-0.025	NS	-	-	-0.101	NS
Bulk density	-0.002 (0.001)	3.030 (0.143)	-0.141	**	-0.017 (0.008)	2.953 (0.139)	-0.117	*	-	-	-0.090	NS	0.005 (0.004)	2.636 (0.014)	0.118	*
Linear extension rate	0.013 (0.001)	-0.745 (0.162)	0.466	***	0.115 (0.009)	-0.613 (0.160)	0.446	***	0.020 (0.002)	0.682 (0.084)	0.440	***	-0.039 (0.004)	1.506 (0.018)	-0.411	***
Net calcification rate	0.030 (0.002)	-1.400 (0.388)	0.426	***	0.277 (0.022)	-1.169 (0.381)	0.422	***	0.051 (0.006)	1.917 (0.199)	0.438	***	-0.094 (0.011)	3.959 (0.043)	-0.419	***
Commercial samples (> 22 mm), n = 310																
Micro-density	-	-	0.033	NS	-0.004 (0.003)	2.871 (0.057)	-0.174	**	-0.002 (0.001)	2.884 (0.027)	-0.247	***	0.000 (0.001)	2.805 (0.006)	0.161	**
Apparent porosity	0.103 (0.021)	-12.594 (3.470)	0.303	***	0.757 (0.200)	-8.480 (3.467)	0.144	*	-	-	0.038	NS	-0.319 (0.089)	5.740 (0.358)	-0.145	*
Bulk density	-0.003 (0.001)	3.151 (0.110)	-0.182	**	-0.026 (0.006)	3.130 (0.108)	-0.201	***	-0.004 (0.002)	2.820 (0.053)	-0.176	**	0.009 (0.003)	2.643 (0.011)	0.172	**
Linear extension rate	0.013 (0.001)	-0.849 (0.140)	0.521	***	0.125 (0.008)	-0.820 (0.138)	0.554	***	0.023 (0.002)	0.555 (0.077)	0.552	***	-0.041 (0.004)	1.483 (0.017)	-0.486	***
Net calcification rate	0.030 (0.002)	-1.517 (0.375)	0.464	***	0.292 (0.021)	-1.475 (0.367)	0.503	***	0.055 (0.006)	1.711 (0.197)	0.519	***	-0.094 (0.011)	3.913 (0.043)	-0.460	***

FIGURES

Figure 1. Map of the Adriatic coastline indicating the sites where the *C. gallina* clams were collected. Abbreviations and coordinates of the sites in decreasing order of latitude: MO, Monfalcone 45°42'N, 13°14'E; CH, Chioggia 45°12'N, 12°19'E; GO, Goro 44°47'N, 12°25'E; CE, Cesenatico 44°11'N, 12°26'E; SB, San Benedetto 43°5'N, 13°51'E; CA, Capoiale 41°55'N, 15°39'E. The map was downloaded from d-maps.com site (http://www.d-maps.com) and modified with Adobe Photoshop CS4.

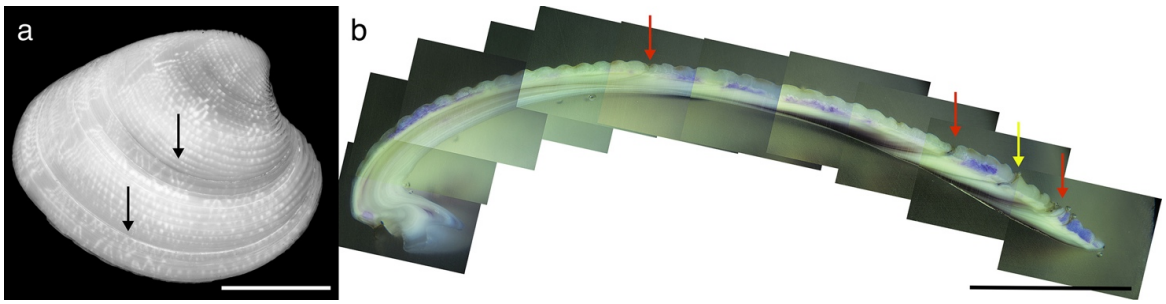

Figure 2. **Shell ageing methods.** a. External growth rings (black arrow) on the surface of *C. gallina* after shell scanning. Scale bar = 1 cm. b. Internal annual growth bands (red arrows) in the shell section of *C. gallina* from the umbo to the ventral margin after Mutvei's solution treatment. Yellow arrow indicates an ambiguous band, less marked and too close to the adjacent annual growth bands. Scale bar = 0.5 cm.

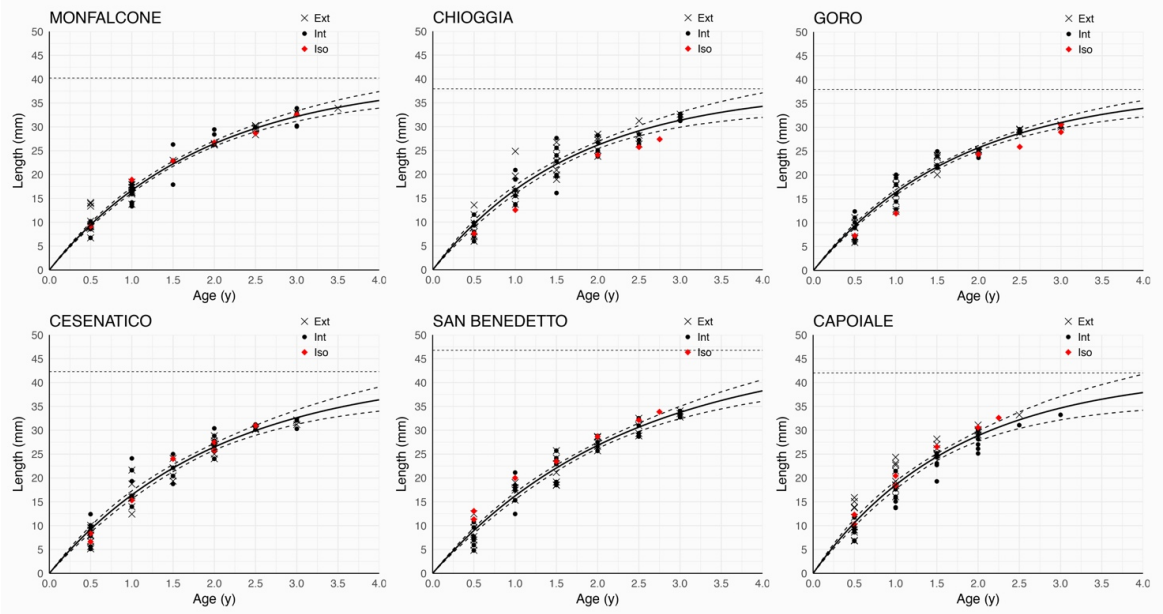

Figure 3. **Von Bertalanffy growth curves.** The generalised age-length von Bertalanffy growth curve in each site obtained by all data from the two ageing methods. Dotted lines indicate the maximum expected shell length (L_{inf}), dashed lines indicate the confidence intervals constructed through bootstrap method. Red points are the ages obtained from the $\delta^{18}O$ profiles along the shell growth axis.

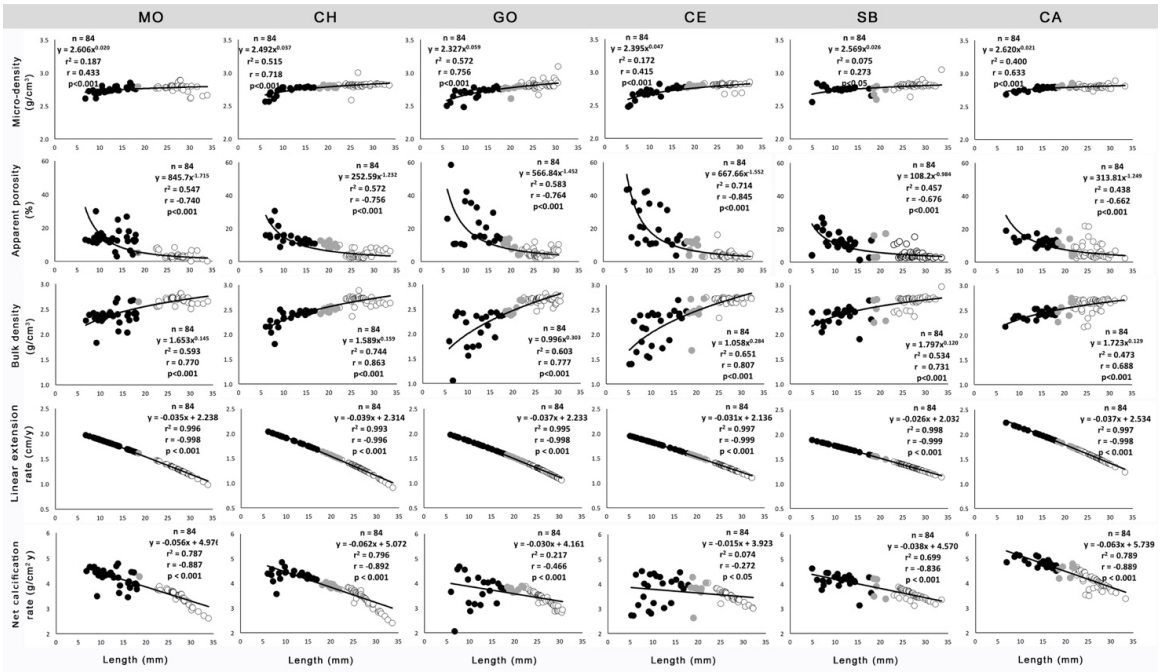

Figure. 4. Relationships between shell skeletal and growth parameters and length. Black dots are immature clams (length < 18 mm), grey dots are mature clams (> 18 mm) and white dots are the clams of commercial size (> 22 mm). n = number of individuals. r = Pearson's determination coefficient. Sites are arranged in order of decreasing latitude: MO (Monfalcone), CH (Chioggia), GO (Goro), CE (Cesenatico), SB (San Benedetto), CA (Capoiale).

Supplementary Material from

Inferred calcification rate in the bivalve *Chamelea gallina* along a latitudinal gradient in the Adriatic Sea

Arianna Mancuso[1,2], Marco Stagioni[2], Fiorella Prada[1], Daniele Scarponi[3], Corrado Piccinetti[2], Stefano Goffredo[1,2 *]

***corresponding author: E-mail s.goffredo@unibo.it**

[1]Marine Science Group, Department of Biological, Geological and Environmental Sciences, University of Bologna, Via Selmi 3, I-40126 Bologna, Italy, European Union

[2]Laboratory of Fisheries and Marine Biology at Fano, Department of Biological, Geological and Environmental Sciences, University of Bologna, Viale Adriatico 1/N, I-61032, Fano (PU), Italy, European Union

[3]Department of Biological, Geological and Environmental Sciences, University of Bologna, Via Selmi 3, I-40126 Bologna, Italy, European Union

METHODS

Shell ageing methods details

For counting surface external rings, shells were scanned in a transmitted light to enhance contrast of surface's ridge and highlight bands at different density that can be considered growth external rings (Fig. 2a). In order to estimate age by means of shell sectioning and Mutvei's solution, the valves were embedded in epoxy resin under vacuum at room temperature, followed by 24 h hardening. For counting internal bands, the shells were sectioned along the anterior-posterior axis, from the umbo to the ventral margin, using an electrodeposited diamond cutting blade (Fig. 2b). Sections were subsequently mounted on glass slides with Crystalbond 509 Clear, ground with SiC paper (600 and 2500 mesh) and polished with abrasive allumina compound (3M Perfect-it III Extrafine Pasta). Finally, the sections were ultrasonically cleaned, rinsed in purified water and dried. The original Mutvei's solution consists of 500 ml 1% acetic acid, 500 ml 25% glutaraldehyde and ca. 5 to 10 g alcian blue powder[1] while the solution used in this study was made of acetic acid, that removed the carbonate very gently and assisted formaldehyd in stabilizing the organic compounds, formaldehyd fixative that traps proteins and toluidine blue for staining. Shell sections were covered with some drops of Mutvei's solution for 30 minutes at 37–40°C and shaken with a vortex every five minutes to facilitate bubbles spill. Immediately after Mutvei's removal, the etched sections were carefully rinsed with purified water and allowed to air-dry. After Mutvei's solution shell sections with shadings of blue revealed three-dimensional growth structures, with annual growth lines stood out as etch-resistant ridges, while growth increments were etched. Shell sections were then examined under oblique light at low magnification and photographed with a digital camera (PowerShot G12; Canon, Tokyo, Japan), in order to identify internal growth bands (Fig. 2b).

To validate the data from the two counting rings methods, oxygen isotopic measurements ($\delta^{18}O$) were carried out on "spot" samples collected in sequence from the umbo to the ventral edge of the shells for each site. Between 50-200 micrograms of dried homogenized powdered samples were treated with CP grade helium then added an acidified solution consisting of 104% orthophosphoric acid, left to react for 1 hour at 70 degrees Celsius. Each sample was then analyzed using a Thermo

Gasbench preparation system attached to a Thermo Delta V Advantage mass spectrometer in continuous flow mode. Each run of samples was accompanied by 10 reference carbonates (Carrara Z) and 2 control samples (Fletton Clay). Carrara Z has been calibrated to VPDB using the international standard NBS19. Analyses were conducted at The Godwin Laboratory for Palaeoclimate Research, Department of Earth Sciences, University of Cambridge.

Statistical analyses

Levene's test was used for testing homogeneity of variance and Kolmogorov-Smirnov's test was used for testing normality of variance for both environmental and shell parameters. Since the assumptions for parametric statistics were not fulfilled, the non-parametric Kruskal-Wallis equality-of-populations rank test was used to test the significance of the differences among sites for environmental variables and shell parameters. Pearson's correlation coefficient (r) was used to correlate shell skeletal and growth parameters with respect to shell length in each site, while Spearman's rank correlation coefficient (rho) was used for the relationships between shell parameters and environmental parameters. All analyses were computed using R Studio Software (RStudio Team, 2016).

REFERENCES

1. Schöne, B. R., Dunca, E., Fiebig, J. & Pfeiffer, M. Mutvei's solution: An ideal agent for resolving microgrowth structures of biogenic carbonates. *Palaeogeogr. Palaeoclimatol. Palaeoecol.* 228, 149–166 (2005)

SUPPLEMENTAL FIGURES

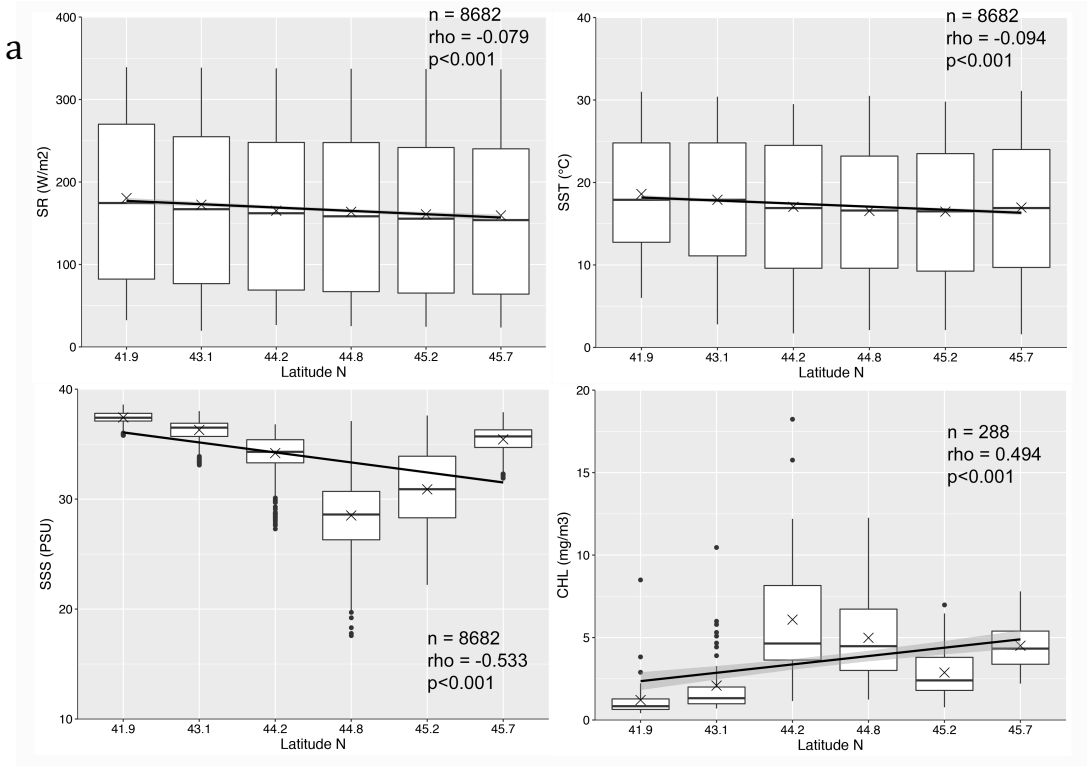

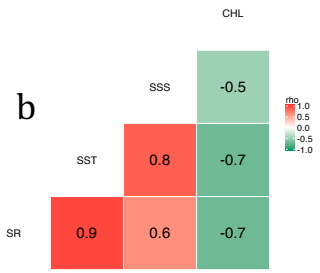

Figure S1. Environmental parameters.

a. Relationship between environmental parameters and the latitude of study sites along the coast of Italy. The crosses indicate the mean annual values. n = daily values for SR, SST and SSS and monthly values for CHL; rho = Spearman's correlation coefficient.

b. Correlations among environmental parameters. rho = Spearman's correlation coefficient. All the correlations are significant, p<0.001 (adjust p-values for multiple comparisons using correction of Holm, 1979. SR, solar radiation; SST, sea surface temperature; SSS, sea surface salinity; CHL, chlorophyll concentration.

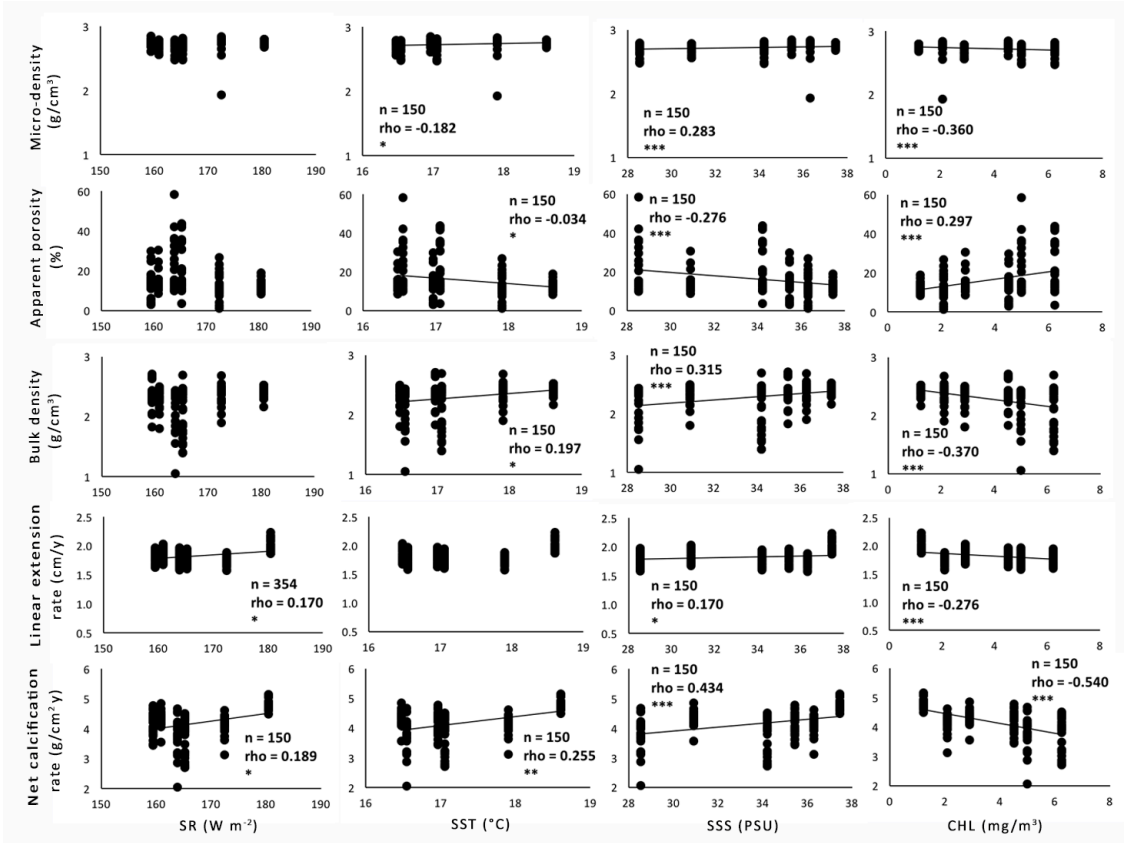

Fig. S2. Relationships between skeletal and growth parameters and environment in immature shells (< 18 mm). rho = Spearman's determination coefficient. Linear regression and correlations are listed in Table 4. n = number of individuals. SR, solar radiation; SST, sea surface temperature; SSS, sea surface salinity; CHL, chlorophyll concentration.

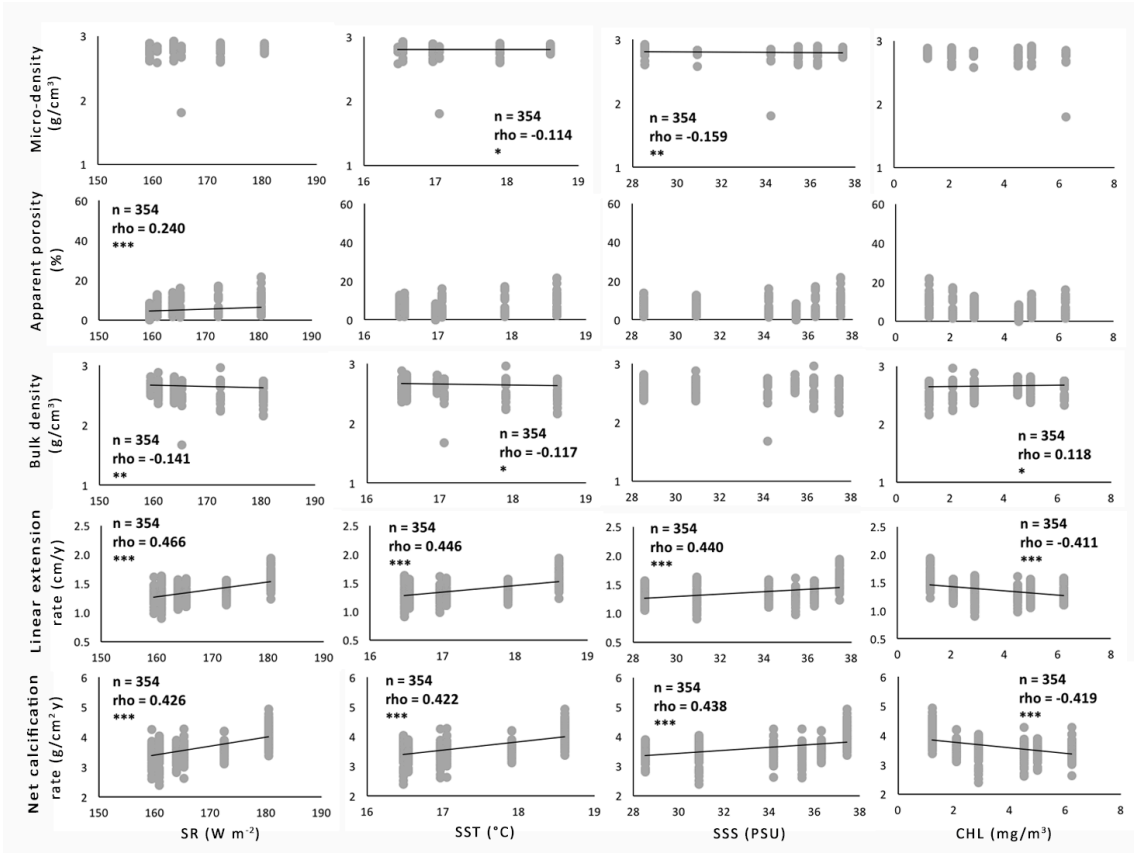

Fig. S3. Relationships between skeletal and growth parameters and environment in mature shells (> 18 mm). rho = Spearman's determination coefficient. Linear regression and correlations are listed in Table 4. n = number of individuals. SR, solar radiation; SST, sea surface temperature; SSS, sea surface salinity; CHL, chlorophyll concentration.

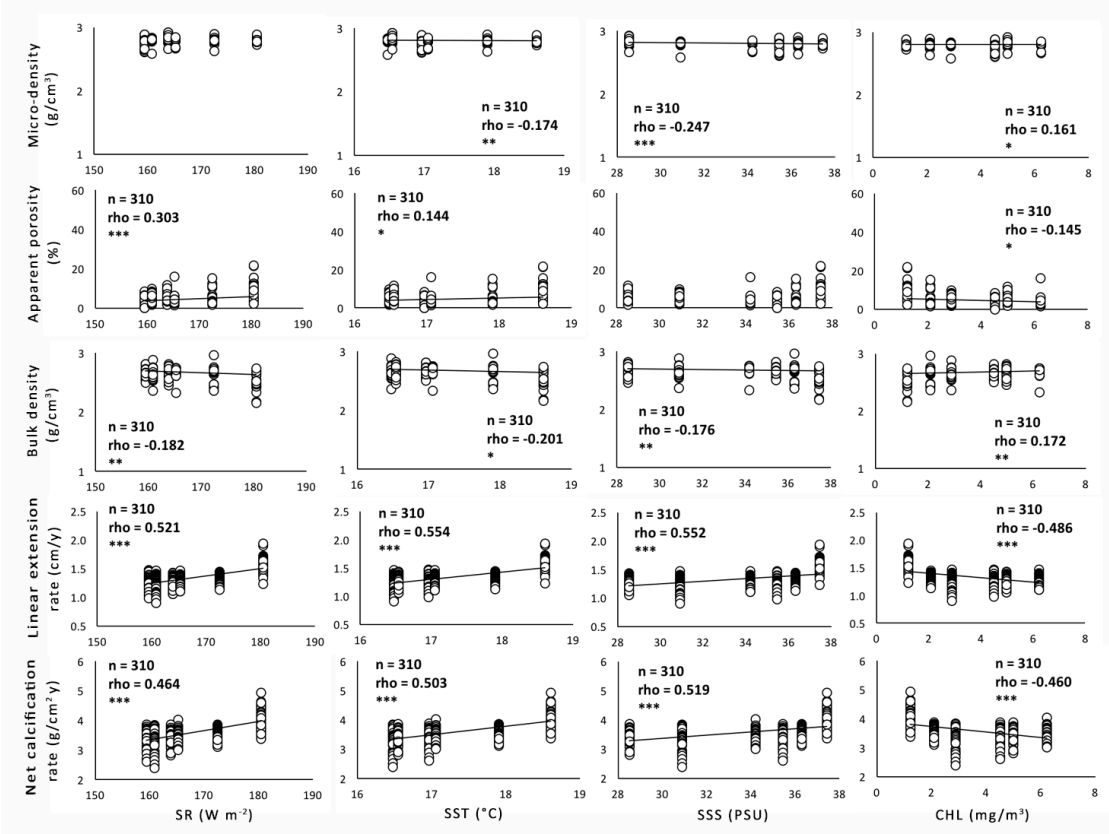

Fig. S4. Relationships between skeletal and growth parameters and environment in shells of commercial size (> 22 mm). rho = Spearman's determination coefficient. Linear regression and correlations are listed in Table 4. n = number of individuals. SR, solar radiation; SST, sea surface temperature; SSS, sea surface salinity; CHL, chlorophyll concentration.

SUPPLEMENTAL TABLES

Table S1. Length and age data. Mean length and age determined from the external rings and internal growth bands counting in each site. n = number of samples; CI = 95% confidence interval. Sites are arranged in order of decreasing latitude: MO (Monfalcone), CH (Chioggia), GO (Goro), CE (Cesenatico), SB (San Benedetto), CA (Capoiale). K-W = Kruskal-Wallis equality-of-populations rank test, NS = not significant.

Site	N	Mean Length (mm)	CI	Mean Age external rings (y)	CI	Mean Age internal bands (y)	CI
MO	30	19.33	16.29 - 22.37	1.37	1.03 - 1.70	1.40	1.09 - 1.71
CH	30	20.43	17.48 - 23.37	1.45	1.16 - 1.74	1.53	1.24 - 1.83
GO	30	19.18	16.20 - 22.16	1.43	1.13 - 1.74	1.42	1.10 - 1.73
CE	30	19.76	16.37 - 23.15	1.48	1.17 - 1.80	1.42	1.10 - 1.73
SB	30	21.24	17.90 - 24.58	1.57	1.26 - 1.88	1.57	1.26 - 1.87
CA	30	20.09	17.19 - 23.00	1.07	0.87 - 1.26	1.35	1.10 - 1.60
K-W		NS		NS		NS	

Table S2. Von Bertalanffy growth parameters. Linf and K estimated from the Von Bertalanffy growth function for external and internal bands and by pooling the data of the two methods (generalised). CI = 95% confidence interval. Sites are arranged in order of decreasing latitude: MO (Monfalcone), CH (Chioggia), GO (Goro), CE (Cesenatico), SB (San Benedetto), CA (Capoiale).

	External rings				Internal bands				Generalised			
Site	Linf	CI	K	CI	Linf	CI	K	CI	Linf	CI	K	CI
MO	**38.431**	35.334 - 43.153	**0.595**	0.489 - 0.701	**42.275**	37.277 - 50.244	**0.489**	0.376 - 0.601	**40.242**	37.208 - 44.175	**0.536**	0.460 - 0.618
CH	**37.253**	32.454 - 46.686	**0.621**	0.429 - 0.817	**38.950**	33.459 - 48.140	**0.544**	0.381 - 0.727	**37.931**	33.925 - 44.168	**0.584**	0.454 - 0.718
GO	**39.163**	34.631 - 45.266	**0.530**	0.423 - 0.656	**36.819**	32.972 - 42.043	**0.599**	0.480 - 0.738	**37.935**	34.750 - 41.589	**0.566**	0.484 - 0.664
CE	**44.766**	38.205 - 56.576	**0.439**	0.312 - 0.570	**40.321**	35.045 - 50.363	**0.547**	0.385 - 0.721	**42.298**	37.214 - 49.431	**0.492**	0.387 - 0.609
SB	**46.937**	39.929 - 58.661	**0.423**	0.304 - 0.559	**47.525**	40.167 - 62.085	**0.416**	0.282 - 0.555	**46.773**	41.247 - 54.883	**0.426**	0.334 - 0.522
CA	**41.649**	35.459 - 52.355	**0.649**	0.456 - 0.853	**46.462**	38.826 - 60.850	**0.451**	0.314 - 0.602	**42.010**	36.148 - 50.449	**0.581**	0.443 - 0.740

Chapter 4

Oxygen and carbon stable isotope composition in the shells of the bivalve *Chamelea gallina* in the Adriatic Sea

Manuscript in preparation

Oxygen and carbon stable isotope composition in the shells of the bivalve *Chamelea gallina* in the Adriatic Sea

Manuscript in preparation

Mancuso Arianna[1,2], Ruth Yam[2], Stefano Goffredo[1,2*], Aldo Shemesh[2*]

*corresponding authors: aldo.shemesh@weizmann.ac.il; s.goffredo@unibo.it

[1]Marine Science Group, Department of Biological, Geological and Environmental Sciences, University of Bologna, Via Selmi 3, I-40126 Bologna, Italy, European Union

[2]Laboratory of Fisheries and Marine Biology at Fano, Department of Biological, Geological and Environmental Sciences, University of Bologna, Viale Adriatico 1/N, I-61032, Fano (PU), Italy, European Union

[3]Department of Earth and Planetary Sciences, Weizmann Institute of Science, Rehovot, Israel.

ABSTRACT

Many calcifying organisms exert exquisite biological control over the construction and composition of biominerals which are thus generally depleted in oxygen-18 and carbon-13, relative to the isotopic ratios of aragonite. The shell $\delta^{18}O$ and $\delta^{13}C$ values of specimens of the clam *Chamelea gallina* were assessed in six sites along Eastern Italian coasts, spanning ~1.5 °C, ~21 W m^{-2} and ~9 PSU of annual average sea surface temperature, solar radiation and salinity, respectively. Seawater $\delta^{18}O$ and $\delta^{13}C_{DIC}$ were very different along the ~400 km latitudinal gradient and ~1.2‰ and ~1.8‰ variation in shell $\delta^{18}O$ and $\delta^{13}C$ respectively, was found among sites. Isotopic analyses on *C. gallina* allowed the following conclusions:

1. the calcium carbonate of *C. gallina* shells was not deposited under isotopic equilibrium conditions with the environmental variables;
2. only the sites near Po river showed positive $\delta^{18}O/\delta^{13}C$ correlations and heavy isotope depletions that could suggest the influence of metabolic and/or kinetic effects on precipitation of shell aragonite.
3. calcification rate, linear extension rate and shell density were unrelated to isotopic compositions.
4. the rate of calcium carbonate deposition decreased with increasing age;
5. the mean growth rate of the shells could be easily evaluated according to the oxygen isotopic composition of the spot measurements;
6. the sites towards South showed higher growth rates despite the site in the Northern Adriatic Sea

Furthermore, with this study that covers several sites and monitors ontogenic stages, we can have a better understanding whether vital/ontogenic process or environmental conditions govern the shell isotopic signature in the bivalve *C. gallina* and also improve their utilization in future paleo-environmental studies.

Keywords: stable isotopes, Adriatic Sea, mollusc shells, vital effects, kinetic isotope effects

INTRODUCTION

Mollusc shells contain many isotopic clues about calcification physiology and environmental conditions at the time of shell formation[1]. The potential utility of mollusc shells as paleo-environmental archives is due to their incremental deposition of carbonate material, such that they possess in their shell geochemical composition a temporal record of physical and chemical ambient conditions during growth[2–4]. In particular, intra-seasonal information can be gained from shells by analysing the oxygen and carbon isotope composition of successive growth increments of calcium carbonate along the direction of growth (known as sclerochronology), although it should be noted that shell growth is often not continuous and there may be significant seasonal cessations in growth [5].

Oxygen and carbon isotopic ratios of marine mollusc carbonates have been shown to be reliable proxies for water temperature, salinity and dissolved inorganic carbon isotopic composition ($\delta^{13}C_{DIC}$)[6–9]. It is a common view that the oxygen-isotope composition ($^{18}O/^{16}O$ ratios expressed as $\delta^{18}O$ values) of marine mollusc shell carbonate is deposited at, or near, isotopic equilibrium with the seawater solution from which precipitation occurs and hence reflects a combination of ambient temperature and the oxygen-isotope composition of seawater ($\delta^{18}O_{sw}$)[10,11]. However, $\delta^{18}O$ values lower than that predicted for equilibrium precipitation have been observed in some bivalve species[3,12–14]. Differences in isotopic composition between biogenic materials and compositions expected for thermodynamic equilibrium with their environment are due to the so-called vital effects[15,16]. Various explanations have been advanced for vital effects on the $\delta^{18}O$ of biogenic carbonates, one invoking kinetic isotope effects associated with processes such as the hydration and hydroxylation of CO_2 in solution or crystal growth rate[17]; a second set of explanations invokes an equilibrium isotope fractionation associated with the fractionation of isotopes between species of dissolved inorganic carbon, present in an organisms calcifying fluids (isotope fractionation between CO^{2-} and HCO^{-})[18–21]. Other models have invoked kinetic effects associated with element partitioning or isotope effects at the surface of a growing crystal, which is influenced by both crystal growth rate and dissolved inorganic carbon (DIC) speciation[21,22]. Temperature

dependence of $\delta^{18}O$ fractionation in biogenic carbonates can vary significantly, showing that the vital effects is species-dependent[11,23–26].

The interpretation of carbon stable isotope ratios ($^{13}C/^{12}C$ ratios expressed as $\delta^{13}C$ values) in marine biogenic carbonates is more complex than for $\delta^{18}O$ values. Some isotopic studies on shells have shown that $\delta^{13}C$ of the shell carbonate is governed by the ^{13}C of dissolved inorganic carbon ($^{13}C_{DIC}$) and therefore records changes in environmental variables such as pH, temperature, and salinity[27–30]. Under ideal conditions at controlled temperature and constant chemical and isotopic composition, shell carbonate would precipitate in equilibrium, resulting in calcite which is 1‰ enriched in comparison with bicarbonate, and aragonite that is 2.7‰ enriched[31]. On the other hand, shells $\delta^{13}C$ has been often found not to reflect the predicted equilibrium fractionation[32–35]. In general, shell $\delta^{13}C$ is more negative than predicted values and the offset is highly variable suggesting a significant and variable incorporation of metabolic carbon into the shell carbonate[32,36–38]. In bivalves there are varying degrees of $\delta^{13}C$ disequilibrium from $\delta^{13}C_{DIC}$. In some species, strong ontogenic decreases in $\delta^{13}C$ have been noted[6,14,39–41], whereas in others there is no discernable decrease[42–44]. Considerations of kinetic and metabolic effects, in addition to environmental conditions, therefore are paramount when interpreting $\delta^{13}C$ records obtained from mollusc specimens. Only one previous study investigated isotopic composition of the clam *Chamelea gallina* with considerations on its growth rates and biological behaviour, but it is restricted to a small area in the Northern Adriatic Sea, the Bay of Trieste[14]. Instead, the present study wants to investigate the variations of shell $\delta^{18}O$ and $\delta^{13}C$ and "vital effects" in *C. gallina* in six sites along a latitudinal gradient (~400km) in the Adriatic Sea, characterized by different environmental conditions. Physical features and water masses of the Adriatic Sea are well known[45] and they define a circulation pattern that is primarily controlled by horizontal density and salinity gradients which are derived from the mixing of southeast high-salinity waters and northwest riverine waters[46]. The presence of Po river delta plays an important role in the regional dynamics and in the biogeochemical processes of this basin, causing seasonal high fluctuations in salinity in the northern sites. We measured the surrounding seawater $\delta^{18}O$ and $\delta^{13}C_{DIC}$ to determine the fractionation between shells and seawater during

calcification. We also presented shell isotopic profiles of *C. gallina*, one for each site in order to study ontogenetic variations in shells $\delta^{18}O$ and $\delta^{13}C$ and to find out differences among sites. $\delta^{18}O$ and $\delta^{13}C$ and their relationships with the environmental parameters are of great value in obtaining a better insight into how the species can face variation of environmental factors among investigated locations. Furthermore, with this study that covers several sites and monitors ontogenic stages, we can have a better understanding whether vital/ontogenic process or environmental conditions govern the shell isotopic signature in the bivalve *C. gallina* and also improve their utilization in future paleo-environmental studies.

MATERIALS AND METHODS

Sample collection and treatment

Between August 2013 and April 2015, specimens of *C. gallina* of commercial size (>25 mm) were collected from six sites along a latitudinal gradient in the Adriatic Sea from 45°42′N to 41°55′N, spanning ~ 400 km (Fig. 1). Clams were sampled using hydraulic dredges on soft bottoms in the subtidal zone at 3–5 m depth along the Eastern Italian coasts. For each collected clam, the bivalve flesh was removed with a scalpel and the shell was cleaned with a tooth-brush and washed with purified water. Seawater samples were collected on board of clam hydraulic dredge both in summer and in winter season. Seawater samples were stored in plastic jars of 100 ml without additional treatments for $\delta^{18}O$, and in brown glass bottles with 1ml of saturated $HgCl_2$ for $\delta^{13}C_{DIC}$, in order to stop all biological activity. The bottles were kept in a refrigerator at 4°C until measurements were carried out. Seawater samples were collected in duplicate.

Carbon and oxygen isotopic compositions

For shell $\delta^{18}O$ and $\delta^{13}C$ analysis, 7-8 shells of each site were selected, treated with a solution of H_2O_2 (10% buffered with ammonium hydroxide) to clean the superficial

organic matter, rinsed with nanopure water and air-dried. The shells were sampled manually by means of a dental drill (0.5 mm diameter) in the outer shell layer. For isotope ratio comparison among sites, average powder samples, taken from combined powders drilled in many points along the shell growth axis, were collected in the whole shells along the maximum growth direction axis and each sample was replicated twice. Furthermore, $\delta^{18}O$ and $\delta^{13}C$ seasonal analysis was carried out on one shell for each site, except for Chioggia. "Spot" samples were drilled in sequence from the umbo to the ventral edge along the shell growth axis with ~1.4 mm mean spatial resolution. The necessity of roasting (350°C for 45 min in vacuo; Keller et al., 2002) was tested by analysing 12 random powder samples taken from all sites. Shell $CaCO_3$ samples of 180-250 µg of powder were flushed with helium gas and reacted with100% orthophosphoric acid and left to equilibrate at 25°C. The evolved CO_2 gas was analyzed using a Finnigan GasBench II connected in line to a Finnigan MAT252 isotope ratio mass spectrometer. Data are reported in per mil δ units versus the Pee Dee Belemnite (PDB) standard. Calibration was maintained by routine analyses of internal and international standards. The long-term precision of our internal laboratory standard is 0.05‰ and 0.08‰ for carbon and oxygen, respectively. Oxygen isotopes analysis of seawater ($\delta^{18}O_{sw}$) were carried out by equilibrating 0.5 ml of seawater with a mixture of 0.5% CO_2 in helium at 25°C for 24h. The CO_2 gas was analyzed using a Finnigan MAT 252 mass spectrometer connected online to a Gas- Bench II. The results are reported in per-mill relative to the Vienna Standard Mean Ocean Water (VSMOW) with 0.05‰ (±σ) long-term precision of laboratory working standard. For carbon isotopes analysis of seawater ($\delta^{13}C_{DIC}$), 1 ml of seawater was injected into gas vials pre-flushed with He, then acidified with 0.15 ml H_3PO_4 and left to react for 24h in 25°C. The samples were analysed on a GasBench II and Finnigan MAT 252. The results are reported relative to the international Vienna-PeeDee Belemnite (VPDB) standard with 0.08‰ (±σ) long-term precision of $NaHCO_3$ laboratory standard (chemically pure). All isotopic measurements indicated above were performed in stable isotope laboratory of prof. Aldo Shemesh, at the department of Earth and Planetary Sciences, Weizmann Institute of Science Israel. The isotopic value for a biological aragonite precipitated in quasi-equilibrium with ambient seawater along the latitudinal gradient is calculated from Grossman

and Ku equation[47] for oxygen [1] and Romanek equation[31] for carbon [2].

$$t = 21.8 - 4.69\ (\delta^{18}O_{shell} - \delta^{18}O_{seawater}) \quad [1]$$

$$\epsilon^{13}_{moll-DIC}(‰) = 2.66 - 0.131T\ (°C) \quad [2]$$

Diffractometric measurements

XRD analyses were performed in one specimen for each site. Diffraction patterns for each sample were collected using a D2 Phaser diffractometer with Lynxeye detector, using Cu-Kα radiation generated at 30 kV and 10 mA at the department of Earth and Planetary Sciences, in Weizmann Institute of Science Israel. Data were collected within the 2θ range from 15° to 60° with a step size (Δ2θ) of 0.02° and a counting time of 1500 s. XRD patterns were analyzed using the Diffract.Eva software.

Shell skeletal and growth parameters

Clam shell length (maximum distance on the anterior-posterior axis), was obtained with ImageJ software after data capture of each shell shape with a scanner (Acer Acerscan Prisa 620 ST 600 dpi, 0.04 mm/px) and dry shell weight was measured using an analytical balance (±0.1 mg). Skeletal apparent porosity (volume of the pores divided by volume of the shell including its pores; %), micro-density (mass per unit volume of the material which composes the shell, excluding volume pores; g cm^{-3}) and bulk density (shell mass divided by the total enclosed volume, including the volume of pores; g cm^{-3}) were measured by buoyant weight analysis (Jokiel et al., 1978), using a density determination kit Ohaus Explorer Pro balance (±0.1 mg; Ohaus Corp., Pine Brook, NJ, USA; see Gizzi et al., 2016[49] for calculation details). Age was calculated from the von Bertalanffy growth functions for each site, found in Mancuso et al. in preparation. Shell linear extension rates were obtained with the length/age ratio (cm y^{-1}), while the net calcification rate (mass of $CaCO_3$ deposited per year per unit area g y^{-1} cm^2) was calculated for each shell by the formula: net calcification (g cm^{-2} y^{-1}) = bulk density (g cm^{-3}) x shell extension (cm y^{-1})[50,51].

Environmental parameters

Solar radiation (SR; W m^{-2}), sea surface temperature (SST; °C) and sea surface

salinity (SSS; PSU) data were obtained for each site from the Euro-Mediterranean Center on Climate Change (CMCC http://oceanlab.cmcc.it/afs/) data banks. Mean annual SR, SST and SSS were calculated from daily values measured from July 2011 to June 2015, to enclose the almost full lifespan of two-three years for each sample. For the same period, monthly values of chlorophyll concentration (CHL; mg/m^3) was obtained for each site from the *GlobColour data* (http://globcolour.info) by ACRI-ST, France (http://hermes.acri.fr).

Statistical analyses

One-way analysis of variance (ANOVA) was then used to test the significance of the differences of environmental variables, seawater and shell isotopes data among sites. When assumptions for parametric statistics were not fulfilled, the non-parametric Kruskal-Wallis equality-of-populations rank test was used. Spearman's rank correlation coefficient was used to calculate the significance of the correlations between shell $\delta^{13}C$ and $\delta^{18}O$ and environmental parameters. Spearman's rank correlation coefficient is an alternative to Pearson's correlation coefficient; it is useful for data that are non-normally distributed, after applying Shapiro-Wilk test to check normality. All analyses were computed using R Studio Software (RStudio Team (2016). RStudio: Integrated Development for R. RStudio, Inc., Boston, MA).

RESULTS

Environmental parameters, $\delta^{18}O_{seawater}$ and $\delta^{13}C_{DIC}$

SR, SST and SSS and CHL, were significantly different among sites along the latitudinal gradient (Kruskal-Wallis test, $p<0.001$; Tables 1): SR, SST and SSS correlated negatively with latitude, while CHL showed opposite trend.

Significant differences in summer, winter and annual mean $\delta^{18}O_{sw}$ and $\delta^{13}C_{DIC}$ were found among sites (Kruskal-Wallis test, $p<0.001$, Table 2-3) and they showed correlations with latitude, except summer $\delta^{13}C_{DIC}$ (Fig. 2). $\delta^{18}O_{sw}$ showed positive values in summer season in four sites, while in Chioggia and Goro the $\delta^{18}O_{sw}$ shifted

towards negative values during the warm season (Table 2). In winter negative $\delta^{18}O_{sw}$ values were still found in Goro, together with Cesenatico and the resulted annual mean $\delta^{18}O_{sw}$ showed lighter values in Chioggia, Goro and Cesenatico (Table 2). Goro stood out for its deeply low values of $\delta^{13}C_{DIC}$ in both seasons; Capoiale was the only site with positive value of $\delta^{13}C_{DIC}$, both in summer and winter season (Table 3).

Shell $\delta^{18}O$ and $\delta^{13}C$

$CaCO_3$ of the analysed shells of *C. gallina* consisted of aragonite as indicated by XRD patterns obtained for six specimens (Fig. 3). The roasting test showed no differences in the $\delta^{18}O_{shell}$ and $\delta^{13}C_{shell}$ between roasted and not roasted powders, with a homogeneous distribution of values obtained from the two procedures ($p>0.05$; Fig. 4). Hence, additional roasting treatment was avoided.

Shell isotope data are presented as $\delta^{18}O_{shell}$ - $\delta^{18}O_{seawater}$ ($\delta^{18}O_{shell\ correct}$) and $\delta^{13}C_{shell}$ - $\delta^{13}C_{DIC}$ ($\delta^{13}C_{shell\ correct}$) in order to account for the isotopic composition of the local seawater in each site. A strong positive correlation between shell $\delta^{18}O_{shell\ correct}$ and $\delta^{13}C_{shell\ correct}$ was observed considering all the isotope dataset ($p<0.001$; Fig. 5) and only in two sites, Goro and Cesenatico ($p<0.05$; Fig. 5).

$\delta^{18}O_{shell\ correct}$ and $\delta^{13}C_{shell\ correct}$ were different among sites (Kruskal-Wallis test, $p<0.001$, Table 2); only $\delta^{18}O_{shell\ correct}$ correlated with latitude (Fig. 6). The site of Goro resulted to be completely separated from the other sites for both $\delta^{18}O_{shell\ correct}$ and $\delta^{13}C_{shell\ correct}$ (Fig. 6). Annual $\delta^{18}O_{shell\ correct}$ values showed more negative values for the southern sites, San Benedetto and Capoiale, and only the site of Goro showed positive value (Table 2; Fig.6). Annual values of $\delta^{13}C_{shell\ correct}$ showed the same trend of more negative values at South, while Goro and Cesenatico presented positive values (Table 2; Fig. 6). All the environmental parameters showed significant correlations with shell $\delta^{18}O_{shell\ correct}$ (Fig. 7). SST, SSS and CHL showed significant correlations with shell $\delta^{13}C_{shell\ correct}$ (Fig. 7). $\delta^{18}O_{shell\ correct}$ was negatively correlated with solar radiation, sea surface temperature and salinity and positively correlated with chlorophyll concentration; while $\delta^{13}C$ showed the same trends except for solar radiation that didn't show significant correlation (Fig. 7). No correlations were found between shell isotope values and growth parameters (net

calcification rate, linear extension rate and bulk density; Fig. 8). The Grossman and Ku equation[47] suggested temperatures of $CaCO_3$ precipitation in the shells of *C. gallina* not reasonable compatible with annual mean, winter and summer SST in the collected sites (Table 4). Only the site of Goro showed SST derived from the equation closer to real mean annual SST (Table 4). Considering winter SST, the equation reported high values not compatible with cold season, while considering summer SST the sites of Chioggia and more evident Goro reported very low values for warm season (Table 4).

Seasonal analysis obtained from the drilled spots along the shell growth axis revealed that the drilling method, with a mean spatial resolution of ~1.4 mm, resulted to be suitable to find out differences along the shells growth axis and detected the distinctive seasonal peaks in the $\delta^{18}O_{shell\ correct}$ (Fig. 9). Indeed, the oxygen isotope curves obtained from the spot samples in each shell exhibited a roughly sinusoidal sequence of lighter and heavier values that are consistent with seasonal variation in temperature. The age of five specimens could be easily defined by means of the isotopically lower (summer) and higher (winter) values and also the reduction of the growth rates could be detected with increasing age (Table 5; Fig. 9). There was a significant positive correlation between $\delta^{13}C_{shell\ correct}$ and annual growth rates (Table 5; Fig. 10). The shells from Monfalcone and Goro were probably born at the end of summer, while the shells from the other sites were born a little bit early in spring or at the beginning of summer, according with the first isotopes values of the curves (Fig. 9). $\delta^{13}C_{shell\ correct}$ of *C. gallina* were not homogeneous inside the shells and among sites, showing a decreasing trend from the umbo (oldest part of the shell) to the ventral edge (youngest part) in all shells and higher variability for $\delta^{13}C_{shell\ correct}$ in the shells from the northern sites (Fig. 9). The great variability in $\delta^{13}C_{shell\ correct}$ was observed especially over 30 mm and in the shells of Goro and Cesenatico considerable peaks of reduced carbon isotope values were depicted (-4.174 and -3.911 respectively; Fig. 9).

DISCUSSION

Both $\delta^{18}O_{sw}$ and $\delta^{13}C_{DIC}$ were remarkably different along the 400 km transect in the Adriatic Sea. Because of the salinity change from 28.52 to 37.43 PSU, evaporation could be the main factor controlling seawater $\delta^{18}O$ in this region. Variations in the annual $\delta^{13}C_{DIC}$ likely reflected chlorophyll concentration change from 1.21 to 6.23 mg/m^3, suggesting that local primary production could control the absolute value in each site. Marked environmental variations in salinity and chlorophyll concentration along the latitudinal gradient could be due to the influence of Po river delta in the Northern Adriatic Sea that completely changes the seawater chemistry with its freshwater flows. While today's marine water shows $\delta^{18}O$ values around 0‰ SMOW and $\delta^{13}C_{DIC}$ around 2‰ PDB[52], freshwater can exhibit a wide range of isotope compositions, although $\delta^{18}O$ and $\delta^{13}C_{DIC}$ values are commonly distinctly lower[53]. While evaporation processes tend to enrich surface water in heavy isotopes (Mediterranean Sea reaches an average value of +1‰ and the Red Sea an even higher one[54]), a depletion in heavy isotopes is caused by the inflow of continental runoff and atmospheric precipitation. The Po river is the largest Italian river (673 km long), supplies over 50% of the fresh water input to the northern Adriatic basin[55] and is characterized by two annual floods associated with increased rainfall in autumn and snow-melt in spring[56,57]. Thus, in the Northern Adriatic Sea, the extremely low $\delta^{18}O_{sw}$ values were related to considerably low salinity conditions (< 30 PSU) due to mixing with freshwater from the Po river ($\delta^{18}O$ of Po close to -10‰ according to[58]. At the opposite in the Southern sites there were positive $\delta^{18}O$ values, related to the inflow of the isotopically heavy and saltier water from the Southern Adriatic[59]. Also $\delta^{13}C_{DIC}$ can provide a proxy for salinity. Fluvial DIC is often isotopically lighter than oceanic $\delta^{13}C_{DIC}$, due to the input of CO_2 derived from the decomposition of terrestrial plants[1]. As rivers enter the sea, mollusc shells in coastal areas pick up the mixture of fluvial and marine DIC, so shell $\delta^{13}C_{DIC}$ reflects the mixture[43,60].

Together with salinity, $\delta^{13}C_{DIC}$ in seawater is affected by chlorophyll, especially in euphotic environments[61,62]. Chlorophyll concentration is considered the best proxy for phytoplankton biomass which represents the food source for

suspension feeding bivalves[63]. During photosynthesis molecular oxygen is released and carbon dioxide is absorbed and convert in organic carbon, altering $\delta^{13}C_{DIC}$ signature in seawater towards lighter values[61,64]. It is reasonable to hypothesize that regions of large chlorophyll blooms and high biological productivity may lower $\delta^{13}C_{DIC}$ signature in seawater. In this study, the sites with higher CHL concentrations showed marked negative $\delta^{13}C_{DIC}$ and they were located in the Northern Adriatic Sea. Po river is the most important contributor of OM and nutrients to the Mediterranean Sea[65] and in spring surface stratification, nutrient inputs from Po river and atmospheric precipitation give rise to phytoplankton blooms, which make the Northern Adriatic Sea a very productive area and a site of carbon uptake [46]. This river accounts for 50% of the total nutrient input[66] and the highest average primary production values were detected in the Northern region of the Adriatic Sea (588g C m^2 y^1). In contrast, production in the Middle and Southern regions of the Adriatic is significantly lower (137 and 97g C m^2 y^1, respectively), resulting in a strong eutrophic/oligotrophic gradient along the Eastern coasts of Italy from North to South[67]. The Southern site Capoiale was the only site with positive $\delta^{13}C_{DIC}$.

At thermodynamic equilibrium, shell $\delta^{18}O$ is a function of temperature and $\delta^{18}O_{sw}$ from which the shell deposited its $CaCO_3$[68]. In this study, shells $\delta^{18}O$ reflected huge differences in $\delta^{18}O_{sw}$ and followed the same above trends of lighter and heavier $\delta^{18}O_{sw}$ along the latitudinal gradient. The yearly average temperature variation along the transect was about 1.60 °C, yielding an expected shell $\delta^{18}O$ change of about 0.4 ‰ according to the shell aragonite temperature dependency (0.24 ‰ per 1 °C)[68]. Instead, a ~1.2 ‰ variation in shell $\delta^{18}O$ was observed in *C. gallina* among sites (Tables 2-3; Fig. 6). The shell $\delta^{13}C$, which derived mainly from feeding and seawater DIC[1] exhibited also a wide range of variation ~1.8 ‰ among sites. These ranges pointed either to the metabolic and/or kinetic effects as possible controlling factors of isotope variability of shell composition along the transect in the Adriatic Sea.

The full range of the isotope effect was presented in the $\delta^{18}O_{shell\ correct}$ vs. $\delta^{13}C_{shell\ correct}$ plot (Fig. 5). The key observations from this plot were:

1. The isotope range of Goro and Cesenatico was much larger than that of the other sites in both carbon and oxygen.

2. Significant correlation was found considering all the sites, while considering each site separately only Goro and Cesenatico showed significant correlations.
3. Only Goro exhibited values close to the equilibrium value as calculated for biogenic aragonite. Plus, isotopic features reminiscent of kinetic effects, observed in positive $\delta^{18}O/\delta^{13}C$ correlations seemed to be present in Goro and Cesenatico.
4. High $\delta^{18}O/\delta^{13}C$ ratio found in Northern sites close to Po delta resulted in lower calcification rates of *C. gallina* specimens and this resulted in agree with the previous study that indicated colder temperature, huge variations in salinity and high chlorophyll concentration as stressful environmental conditions that negatively affected linear extension and calcification rates (Mancuso et al. submitted to Scientific Reports).

Temperature derived from Grossman & Ku equation[47] showed mean winter temperatures consistently higher than the real winter water temperatures (Table 4). A mean winter temperature over 20 °C was obviously incompatible with mean winter temperature in these study areas. This inconsistency could be due to the fact that *C. gallina* could precipitate the shell carbonate preferentially during the warm period, considerably reducing its activity during the cold season[14,69]. According to these results, *C. gallina* seemed not precipitate the $CaCO_3$ of its shell in isotopic equilibrium with seawater, in agree with Keller et al., 2002[14]. In the case of most marine organisms, carbon isotope disequilibrium is the rule, with $\delta^{13}C$ values generally more negative than expected at equilibrium[14] (Fig. 5). This happens particularly in the case of benthic species, like *C. gallina*, where a correlation between $\delta^{13}C$ and food could cause a shift of the carbon isotope composition towards negative values, taking into account the very light carbon isotope composition of marin organic matter (close to -20‰)[14,69,70].

Net calcification rate, linear extension rate and shell bulk density were suggested as factors which impact the isotopic composition of calcareous organisms such as corals[17,71,72]. Our results showed that there was no correlation between any of these parameters and the measured isotope composition (Fig. 8). The lack of correlation between shell chemistry and linear extension and calcification rates

suggested that they could have minimal influence over shell chemistry and that their influence may be obscured by variation in environmental factors (temperature and salinity)[32].

From $\delta^{18}O$ and $\delta^{13}C$ profiles along the *C. gallina* growth direction we could derive considerations on growth rates along the latitudinal gradient in the Adriatic Sea. $\delta^{18}O$ profiles showed that samples of Cesenatico, San Benedetto and Capoiale were born in spring, while the samples of Monfalcone, the northern site was born in summer. $\delta^{18}O$ Goro showed a strange profile with a sinusoidal sequence of lighter and heavier values non consistent with seasonal variation in temperature. The reduced seasonal variability in the intra-shell $\delta^{18}O$ record, that not permitted to have winter and summer peaks, could be due to a seasonal cessation of shell growth in Goro or to the influence of salinity that masked seasonal changes in temperature. Except in Goro, in the other sites the shell accretion seemed to take place throughout the whole year, with a notable reduction in growth rates with increasing length (Fig. 9-10). Counting age from seasonal $\delta^{18}O$ peaks, in the Southern sites (San Benedetto and Capoiale) *C. gallina* reached a length of about 20 mm after 1 year, while reached the same age at length of about 13-15 mm in the sites of Monfalcone and Cesenatico (Fig. 9-10). *C. gallina* seemed to have higher linear extension rates toward South, in agree with the previous study that found out enhanced linear extension and calcification rates in the southern sites, while in the sites under the Po influence, growth resulted to be negatively affected (Mancuso et al. submitted to Scientific Reports). $\delta^{13}C$ profiles indicated a trend of lower values with increasing length, more pronounced in the Northern sites (Monfalcone, Goro and Cesenatico). Lorrain et al., 2004[41] showed that the ratio of respired to precipitated carbon, which represents the amount of metabolic carbon available relative to the carbon requirements for calcification, increased through ontogeny in scallops. This suggests that the decrease of $\delta^{13}C$ through ontogeny could be caused by increased utilization of this metabolic carbon to satisfy carbon requirements for calcification.

The high resolution profiles showed that the intra-annual variability of $\delta^{13}C$ could be large up to 2.4‰ between the umbo (the older part of shells) and the ventral margin (the youngest part of shells). Two possible explanations for this trend: a deeper position in the sediment of oldest specimens, that led to a large

availability in pore water of DIC produced by the oxidation of organic matter or the incorporation of larger amounts of respiratory CO_2[14,73]. Respired CO_2 and ambient inorganic carbon both contribute to mollusc shells formation and the relative importance of each source determine whether shell $\delta^{13}C$ records mainly dietary $\delta^{13}C$ or the $\delta^{13}C$ of ambient inorganic carbon[1]. McConnaughey et al., 1997[33] suggested that land snails and other air-breathing animals build their carbonates mainly from respired CO_2, while aquatic animals build their shells mainly from ambient inorganic carbon. The high dependency of calcification on external DIC from the ambient seawater was further supported by isotopic data which revealed only a minor fraction of metabolic CO_2 (5–15 %) but a large seawater signal in the shells of bivalves[1,74].

Isotope data of the *C. gallina* samples along the Adriatic coasts yielded a large range of values due to their origin from different environmental conditions. Some specimens clearly reflected the influence of Po river (in the sites of Chioggia, Goro and Cesenatico), others marine ingressions (in the site of Capoiale). Stable isotope investigations of *C. gallina* supported their usefulness as isotopic indicators for environmental parameters. Significant intra-shell variability in the stable isotope values was also an indication that shells retained their primary geochemical signature[75]. However, paleo-environmental interpretation of the $\delta^{18}O$ values was complicated because of an interplay between temperature, salinity and the $\delta^{18}O$ of the ambient water. Almost all the specimens exhibited shell $\delta^{18}O$ and $\delta^{13}C$ values depleted in comparison to the estimated isotopic equilibrium with ambient seawater, suggesting that this species cannot be used for thermometry-based seawater reconstruction. Being able to predict the contribution of metabolic carbon in the shell carbonate of molluscs would be of great value for reconstructing environmental conditions. Controlled laboratory experiments, where environmental parameters can be varied (such as $\delta^{13}C_{DIC}$, CO_2/O_2 ratios, $\delta^{13}C$ of food) and removed (such as a possible pore-water source) would be very beneficial to determine fractionations at each step from carbon source to shell.

REFERENCES

1. McConnaughey, T. A. & Gillikin, D. P. Carbon isotopes in mollusk shell carbonates. *Geo-Marine Lett.* 28, 287–299 (2008)
2. Jones, D. S. Sclerochronology: Reading the Record of the Molluscan Shell: Annual growth increments in the shells of bivalve molluscs record marine climatic changes and reveal surprising. *Am. Sci.* (1983)
3. Klein, R. T., Lohmann, K. C. & Thayer, C. W. Bivalve skeletons record sea-surface temperature and δ18O via Mg/Ca and18O/16O ratios. *Geology* 24, 415–418 (1996)
4. Richardson, C. A. Molluscs as archives of environmental change. *Oceanogr. Mar. Biol.* (2001)
5. Leng, M. J. & Lewis, J. P. Oxygen isotopes in Molluscan shell: Applications in environmental archaeology. *Environ. Archaeol.* 21, 295–306 (2016)
6. Krantz, D. E., Williams, D. F. & Jones, D. S. Ecological and paleoenvironmental information using stable isotope profiles from living and fossil molluscs. *Palaeogeogr. Palaeoclimatol. Palaeoecol.* 58, 249–266 (1987)
7. Bryan E. Bemis and Dana H. Geary. The Usefulness of Bivalve Stable Isotope Profiles as Environmental Indicators: Data from the Eastern Pacific Ocean and the Southern Caribbean Sea. *Palaios* 11, 328–339 (1996)
8. Hickson, J. A., Johnson, A. L. ., Heaton, T. H. . & Balson, P. S. The shell of the Queen Scallop Aequipecten opercularis (L.) as a promising tool for palaeoenvironmental reconstruction: evidence and reasons for equilibrium stable-isotope incorporation. *Palaeogeogr. Palaeoclimatol. Palaeoecol.* 154, 325–337 (1999)
9. GOODWIN, D. H., FLESSA, K. W., SCHONE, B. R. & DETTMAN, D. L. Cross-Calibration of Daily Growth Increments, Stable Isotope Variation, and Temperature in the Gulf of California Bivalve Mollusk Chione cortezi: Implications for Paleoenvironmental Analysis. *Palaios* 16, 387–398 (2001)
10. Epstein, S. & Mayeda, T. Variation of O18 content of waters from natural sources. *Geochim. Cosmochim. Acta* 4, 213–224 (1953)
11. Wefer, G. & Berger, W. H. Isotope paleontology: growth and composition of

extant calcareous species. *Mar. Geol.* 100, 207–248 (1991)

12. Tan, F. C., Cai, D. & Roddick, D. L. Oxygen Isotope Studies on Sea Scallops Placopecten-Magellanicus from Browns Bank Nova Scotia Canada. *Can. J. Fish. Aquat. Sci.* (1988)
13. KRANTZ, D. E., JONES, D. S. & WILLIAMS, D. F. GROWTH RATES OF THE SEA SCALLOP, *PLACOPECTEN MAGELLANICUS* , DETERMINED FROM THE ^{18}O/ ^{16}O RECORD IN SHELL CALCITE. *Biol. Bull.* 167, 186–199 (1984)
14. Keller, N., Del Piero, D. & Longinelli, A. Isotopic composition, growth rates and biological behaviour of Chamelea gallina and Callista chione from the Gulf of Trieste (Italy). *Mar. Biol.* 140, 9–15 (2002)
15. Weiner, S. & Dove, P. M. An Overview of Biomineralization Processes and the Problem of the Vital Effect. *Rev. Mineral. Geochemistry* 54, 1–29 (2003)
16. Eagle, R. A. *et al.* The influence of temperature and seawater carbonate saturation state on 13 C – 18 O bond ordering in bivalve mollusks. *Biogeosciences* 10, 4591–4606 (2013)
17. McConnaughey, T. 13C and18O isotopic disequilibrium in biological carbonates: I. Patterns. *Geochim. Cosmochim. Acta* (1989). doi:10.1016/0016-7037(89)90282-2
18. Spero, H. J., Bijma, J., Lea, D. W. & Bemis, B. E. Effect of seawater carbonate concentration on foraminiferal carbon and oxygen isotopes. *Nature* 390, 497–500 (1997)
19. Zeebe, R. E. An explanation of the effect of seawater carbonate concentration on foraminiferal oxygen isotopes. *Geochim. Cosmochim. Acta* 63, 2001–2007 (1999)
20. Adkins, J. F., Boyle, E. A., Curry, W. B. & Lutringer, A. Stable isotopes in deep-sea corals and a new mechanism for "vital effects". *Geochim. Cosmochim. Acta* 67, 1129–1143 (2003)
21. Tripati, A. K. *et al.* 13C–18O isotope signatures and 'clumped isotope' thermometry in foraminifera and coccoliths. *Geochim. Cosmochim. Acta* 74, 5697–5717 (2010)
22. Watson, E. B. A conceptual model for near-surface kinetic controls on the trace-element and stable isotope composition of abiogenic calcite crystals.

Geochim. Cosmochim. Acta 68, 1473–1488 (2004)

23. Böhm, F. *et al.* Oxygen isotope fractionation in marine aragonite of coralline sponges. *Geochim. Cosmochim. Acta* 64, 1695–1703 (2000)
24. Rahimpour-Bonab, H., Bone, Y. & Moussavi-Harami, R. Stable isotope aspects of modern molluscs, brachiopods, and marine cements from cool-water carbonates, Lacepede Shelf, South Australia. *Geochim. Cosmochim. Acta* 61, 207–218 (1997)
25. Bemis, B. E., Spero, H. J., Bijma, J. & Lea, D. W. Reevaluation of the oxygen isotopic composition of planktonic foraminifera: Experimental results and revised paleotemperature equations. *Paleoceanography* 13, 150–160 (1998).
26. Ziveri, P. *et al.* Stable isotope 'vital effects' in coccolith calcite. *Earth Planet. Sci. Lett.* 210, 137–149 (2003)
27. Craig, H. The geochemistry of the stable carbon isotopes. *Geochim. Cosmochim. Acta* 3, 53–92 (1953)
28. Keith, M. L., Anderson, G. M. & Eichler, R. Carbon and oxygen isotopic composition of mollusk shells from marine and fresh-water environments. *Geochim. Cosmochim. Acta* 28, 1757–1786 (1964)
29. Mook, W. G. Paleotemperatures and chlorinities from stable carbon and oxygen isotopes in shell carbonate. *Palaeogeogr. Palaeoclimatol. Palaeoecol.* 9, 245–263 (1971)
30. Donner, J. & Nord, A. G. Carbon and oxygen stable isotope values in shells of Mytilus edulis and Modiolus modiolus from holocene raised beaches at the outer coast of the varanger Peninsula, North Norway. *Palaeogeogr. Palaeoclimatol. Palaeoecol.* 56, 35–50 (1986)
31. Romanek, C. S., Grossman, E. L. & Morse, J. W. Carbon isotopic fractionation in synthetic aragonite and calcite: Effects of temperature and precipitation rate. *Geochim. Cosmochim. Acta* 56, 419–430 (1992)
32. Klein, R. T., Lohmann, K. C. & Thayer, C. W. Sr/Ca and 13C/12C ratios in skeletal calcite of Mytilus trossulus:covariation with metabolic rate, salinity, and carbon isotopic composition of seawater. *Geochim. Cosmochim. Acta* 60, 4207–4221 (1996)
33. McConnaughey, T. A., Burdett, J., Whelan, J. F. & Paull, C. K. Carbon isotopes in

biological carbonates: Respiration and photosynthesis. *Geochim. Cosmochim. Acta* 61, 611–622 (1997)

34. McConnaughey, T. A. Sub-equilibrium oxygen-18 and carbon-13 levels in biological carbonates: carbonate and kinetic models. *Coral Reefs* 22, 316–327 (2003)
35. Kaandorp, R. J. G. *et al.* Seasonal stable isotope variations of the modern Amazonian freshwater bivalve Anodontites trapesialis. *Palaeogeogr. Palaeoclimatol. Palaeoecol.* 194, 339–354 (2003)
36. Dettman, D. L., Reische, A. K. & Lohmann, K. C. Controls on the stable isotope composition of seasonal growth bands in aragonitic fresh-water bivalves (unionidae). *Geochim. Cosmochim. Acta* 63, 1049–1057 (1999)
37. Veinott, G. I. & Cornett, R. J. Carbon isotopic disequilibrium in the shell of the freshwater mussel Elliptio complanata. *Appl. Geochemistry* 13, 49–57 (1998)
38. Putten, E. Vander, Dehairs, F., Keppens, E. & Baeyens, W. High resolution distribution of trace elements in the calcite shell layer of modern mytilus edulis: environmental and biological controls. *Geochim. Cosmochim. Acta* 64, 997–1011 (2000)
39. Kennedy H, Richardson C, Duarte C & Kennedy D. Oxygen and carbon stable isotopic profiles of the fan mussel, Pinna nobilis , and reconstruction of sea surface temperatures in the Mediterranean. *Mar. Biol.* 139, 1115–1124 (2001)
40. Elliot, M., DeMenocal, P. B., Linsley, B. K. & Howe, S. S. Environmental controls on the stable isotopic composition of Mercenaria mercenaria: Potential application to paleoenvironmental studies. *Geochemistry, Geophys. Geosystems* (2003). doi:10.1029/2002GC000425
41. Lorrain, A. *et al.* δ13C variation in scallop shells: Increasing metabolic carbon contribution with body size? *Geochim. Cosmochim. Acta* 68, 3509–3519 (2004)
42. Buick, D. P. & Ivany, L. C. 100 years in the dark: Extreme longevity of Eocene bivalves from Antarctica. *Geology* 32, 921 (2004)
43. Gillikin, D. P., Lorrain, A., Bouillon, S., Willenz, P. & Dehairs, F. Stable carbon isotopic composition of Mytilus edulis shells: relation to metabolism, salinity,

δ13CDICand phytoplankton. *Org. Geochem.* 37, 1371–1382 (2006)

44. Surge, D. & Walker, K. J. Geochemical variation in microstructural shell layers of the southern quahog (Mercenaria campechiensis): Implications for reconstructing seasonality. *Palaeogeogr. Palaeoclimatol. Palaeoecol.* 237, 182–190 (2006)
45. Cushman-Roisin, B., Malačič, V. & Gačić, M. Tides, seiches and low-frequency oscillations. in *Physical Oceanography of the Adriatic Sea* 217–240 (Springer, 2001)
46. Catalano, G. *et al.* The carbon budget in the northern adriatic sea, a winter case study. *J. Geophys. Res. G Biogeosciences* (2014). doi:10.1002/2013JG002559
47. Grossman, E. L. & Ku, T. L. Oxygen and carbon isotope fractionation in biogenic aragonite: Temperature effects. *Chem. Geol. Isot. Geosci. Sect.* (1986). doi:10.1109/TEMC.2017.2764526
48. Jokiel, P.L. Maragos, J. E. Franzisket, L. Coral growth:buoyant weight technique. *UNESCO* (1978)
49. Gizzi, F. *et al.* Shell properties of commercial clam Chamelea gallina are influenced by temperature and solar radiation along a wide latitudinal gradient. *Sci. Rep.* 6, (2016)
50. Caroselli, E. *et al.* Inferred calcification rate of a Mediterranean azooxanthellate coral is uncoupled with sea surface temperature along an 8[degree sign] latitudinal gradient. *Front. Zool.* 9, 32 (2012)
51. Tortolero-Langarica, J. J. A., Rodríguez-Troncoso, A. P., Carricart-Ganivet, J. P. & Cupul-Magaña, A. L. Skeletal extension, density and calcification rates of massive free-living coral Porites lobata Dana, 1846. *J. Exp. Mar. Bio. Ecol.* 478, 68–76 (2016)
52. Kroopnick, P. The distribution of13C in the Atlantic Ocean. *Earth Planet. Sci. Lett.* 49, 469–484 (1980)
53. Latal, C., Piller, W. E. & Harzhauser, M. Shifts in oxygen and carbon isotope signals in marine molluscs from the Central Paratethys (Europe) around the Lower/Middle Miocene transition. *Palaeogeogr. Palaeoclimatol. Palaeoecol.* 231, 347–360 (2006)
54. Craig, H. Isotopic composition and origin of the Red Sea and Salton Sea

geothermal brines. *Science (80-.).* 154, 1544–1548 (1966)

55. Degobbis, D., Gilmartin, M. & Revelante, N. An annotated nitrogen budget calculation for the northern Adriatic Sea. *Mar. Chem.* 20, 159–177 (1986)
56. Flora, O. & Longinelli, A. Stable isotope hydrology of a classical karst area, Trieste, Italy. in *Isotope techniques in the study of the hydrology of fractured and fissured rocks* (1989)
57. Tesi, T. *et al.* Organic matter origin and distribution in suspended particulate materials and surficial sediments from the western Adriatic Sea (Italy). *Estuar. Coast. Shelf Sci.* 73, 431–446 (2007)
58. Bortolami, G., Fontes, J. C. & Panichi, C. Isotopes du milieu et circulations dans les aquiferes du sous-sol Vénitien. *Earth Planet. Sci. Lett.* (1973). doi:10.1016/0012-821X(73)90110-6
59. Stenni, B., Nichetto, P., Bregant, D., Scarazzato, P. & Longinelli, A. The Delta-O-18 signal of the northward flow of mediterranean waters in the adriatic sea. *Oceanol. acta* 18, 319–328 (1995)
60. Mook, W. G. & Vogel, J. C. Isotopic equilibrium between shells and their environment. *Science (80-.).* 159, 874–875 (1968)
61. Montes-Hugo, M. *et al.* Seasonal forcing of summer dissolved inorganic carbon and chlorophyll a on the western shelf of the Antarctic Peninsula. *J. Geophys. Res. Ocean.* 115, (2010)
62. Guo, X. S., Lü, Y. C., Sun, Z. G., Wang, C. Y. & Zhao, Q. S. Spatial-temporal distributions of dissolved inorganic carbon and its affecting factors in the Yellow River estuary. *Huan jing ke xue= Huanjing kexue* 36, 457–463 (2015)
63. Huot, Y. *et al.* Does chlorophyll a provide the best index of phytoplankton biomass for primary productivity studies? Does chlorophyll a provide the best index of phytoplankton biomass for primary productivity studies? Proxies of biomass for primary production Does chlorophyll a provide the best index of phytoplankton biomass for primary productivity studies? Proxies of biomass for primary production. *Biogeosciences Discuss. Biogeosciences Discuss* 4, 707–745 (2007)
64. Bennington, V., McKinley, G. A., Dutkiewicz, S. & Ullman, D. What does chlorophyll variability tell us about export and air-sea CO2 flux variability in

the North Atlantic? *Global Biogeochem. Cycles* 23, (2009)

65. Pettine, M., Patrolecco, L., Camusso, M. & Crescenzio, S. Transport of carbon and nitrogen to the northern Adriatic Sea by the Po River. *Estuar. Coast. Shelf Sci.* 46, 127–142 (1998)
66. Gilmartin, M., Degobbis, D., Revelante, N. & Smodlaka, N. The mechanism controlling plant nutrient concentrations in the northern Adriatic Sea. *Int. Rev. der gesamten Hydrobiol. und Hydrogr.* 75, 425–445 (1990)
67. Giordani, P. *et al.* Gradients of benthic–pelagic coupling and carbon budgets in the Adriatic and Northern Ionian Sea. *J. Mar. Syst.* 33, 365–387 (2002)
68. Craig, H. The measurement of oxygen isotope paleotemperatures. *Stable Isot. Oceanogr. Stud. Paleotemp. Cons. Naz. delle Richerche* 161–182 (1965)
69. Cespuglio, G., Piccinetti, C. & Longinelli, A. Oxygen and carbon isotope profiles from Nassa mutabilis shells (Gastropoda): accretion rates and biological behaviour. *Mar. Biol.* 135, 627–634 (1999)
70. Rau, G. H., Sweeney, R. E. & Kaplan, I. R. Plankton13C:12C ratio changes with latitude: differences between northern and southern oceans. *Deep Sea Res. Part A, Oceanogr. Res. Pap.* (1982). doi:10.1016/0198-0149(82)90026-7
71. Land, L. S., Lang, J. C. & Barnes, D. J. Extension rate: a primary control on the isotopic composition of West Indian (Jamaican) scleractinian reef coral skeletons. *Mar. Biol.* 33, 221–233 (1975)
72. Erez, J. Vital effect on stable-isotope composition seen in foraminifera and coral skeletons. *Nature* 273, 199 (1978)
73. Elliot, M., deMenocal, P. B., Linsley, B. K. & Howe, S. S. Environmental controls on the stable isotopic composition of *Mercenaria mercenaria* : Potential application to paleoenvironmental studies. *Geochemistry, Geophys. Geosystems* 4, (2003)
74. Waldbusser, G. G. *et al.* A developmental and energetic basis linking larval oyster shell formation to acidification sensitivity. *Geophys. Res. Lett.* 40, 2171–2176 (2013)
75. Tripati, A., Zachos, J., Marincovich, L. & Bice, K. Late Paleocene Arctic coastal climate inferred from molluscan stable and radiogenic isotope ratios. *Palaeogeogr. Palaeoclimatol. Palaeoecol.* 170, 101–113 (2001)

TABLES

Table 1. Environmental parameters. Annual mean values for solar radiation (SR), sea surface temperature (SST), sea surface salinity (SSS) and chlorophyll concentration (CHL) from 2011 to 2014. n = number of collected data, daily data for SR, SST and SSS and monthly data for CHL; CI = 95% confidence interval. Values in decreasing order of latitude.

Population	Code	Latitude (°)	n	SR (W/m^2) mean (CI)	SST (°C) mean (CI)	SSS (PSU) mean (CI)	n	CHL (mg/m^3) mean (CI)
Monfalcone	MO	45.7	1447	159 (5)	16.96 (0.38)	35.43 (0.06)	48	4.50 (0.39)
Chioggia	CH	45.2	1447	161 (5)	16.47 (0.38)	30.89 (0.17)	48	2.88 (0.43)
Goro	GO	44.8	1447	164 (5)	16.54 (0.37)	28.52 (0.16)	48	4.98 (0.77)
Cesenatico	CE	44.2	1447	165 (5)	17.05 (0.40)	34.19 (0.08)	48	6.23 (1.20)
San Benedetto	SB	43.1	1447	172 (5)	17.90 (0.38)	36.29 (0.05)	48	2.09 (0.55)
Capoiale	CA	41.9	1447	180 (5)	18.60 (0.33)	37.43 (0.03)	48	1.21 (0.36)

Table 2. Isotope data. $\delta^{18}O_{sw}$ (summer, winter and annual average seawater), shell $\delta^{18}O$ and $\delta^{18}O_{shell\ correct}$ (by subtracting summer, winter and annual seawater values from shell values). SD, standar deviation of the shell isotope values for each site. Values for each site, in decreasing order of latitude: MO (Monfalcone), CH (Chioggia), GO (Goro), CE (Cesenatico), SB (San Benedetto), CA (Capoiale).

Site	Latitude (°)	Summer $\delta^{18}O_{sw}$ (‰)	Winter $\delta^{18}O_{sw}$ (‰)	Annual $\delta^{18}O_{sw}$ (‰)	n	$\delta^{18}O$ shell (‰)	SD	$\delta^{18}O$ shell - Summer $\delta^{18}O_{sw}$ (‰)	$\delta^{18}O$ shell - Winter $\delta^{18}O_{sw}$ (‰)	$\delta^{18}O$ shell - Annual $\delta^{18}O_{sw}$ (‰)
MO	45.700	0.797	0.119	0.458	8	-0.307	0.348	-1.104	-0.426	-0.765
CH	45.200	-1.243	0.870	-0.187	7	-0.828	0.096	0.415	-1.698	-0.641
GO	44.783	-2.843	-0.648	-1.745	7	-0.981	0.526	1.862	-0.333	0.764
CE	44.183	0.474	-0.603	-0.064	7	-0.910	0.428	-1.384	-0.307	-0.846
SB	43.083	1.317	0.680	0.998	7	-0.079	0.284	-1.396	-0.759	-1.077
CA	41.917	1.632	1.414	1.523	7	0.240	0.208	-1.392	-1.174	-1.283

Table 3. Isotope data. $\delta^{13}C_{DIC}$ (summer, winter and annual average seawater), shell $\delta^{13}C$ and $\delta^{13}C_{shell\ correct}$ (by subtracting summer, winter and annual seawater values from shell values) values. SD, standar deviation of the shell isotope values for each site. Values for each site, in decreasing order of latitude: MO (Monfalcone), CH (Chioggia), GO (Goro), CE (Cesenatico), SB (San Benedetto), CA (Capoiale).

Site	Latitude (°)	Summer $\delta^{13}C_{DIC}$ (‰)	Winter $\delta^{13}C_{DIC}$ (‰)	Annual $\delta^{13}C_{DIC}$ (‰)	n	$\delta^{13}C$ shell (‰)	SD	$\delta^{13}C$ shell - Summer $\delta^{13}C_{DIC}$ (‰)	$\delta^{13}C$ shell - Winter $\delta^{13}C_{DIC}$ (‰)	$\delta^{13}C$ shell - Annual $\delta^{13}C_{DIC}$ (‰)
MO	45.700	-0.046	-1.914	-0.980	8	-1.467	0.324	-1.421	0.447	-0.487
CH	45.200	-0.731	-0.786	-0.759	7	-1.163	0.276	-0.432	-0.377	-0.404
GO	44.783	-3.541	-2.338	-2.939	7	-2.141	0.385	1.400	0.197	0.798
CE	44.183	-1.558	-1.882	-1.720	7	-1.618	0.298	-0.060	0.264	0.102
SB	43.083	-0.207	-0.794	-0.501	7	-1.196	0.243	-0.989	-0.402	-0.695
CA	41.917	0.283	0.115	0.199	7	-0.342	0.128	-0.625	-0.457	-0.541

Table. 4. Comparisons between derived temperatures from Grossman & Ku equation and real temperatures in the sites. Values for each site, in decreasing order of latitude: MO (Monfalcone), CH (Chioggia), GO (Goro), CE (Cesenatico), SB (San Benedetto), CA (Capoiale).

	Mean annual SST (°C)		Winter SST (°C)		Summer SST (°C)	
Site	Derived SST	Real SST	Derived SST	Real SST	Derived SST	Real SST
MO	25.39	16.96	23.80	10.34	26.97	23.52
CH	24.81	16.47	29.77	10.01	19.85	22.71
GO	18.21	16.54	23.36	10.17	13.07	22.70
CE	25.77	17.05	23.24	10.16	28.29	23.70
SB	26.85	17.90	25.36	11.39	28.35	24.19
CA	27.82	18.60	27.31	12.91	28.33	24.10

Table. 5. Annual growth rate calculated from length/age at each year. From the $\delta^{18}O_{shell\ correct}$ of Goro we could not count the seasonal peaks and calculate age. No $\delta^{18}O$ seasonal profile for Chioggia. Values for each site, in decreasing order of latitude: MO (Monfalcone), GO (Goro), CE (Cesenatico), SB (San Benedetto), CA (Capoiale).

Site	Length (mm)	Age (y)	Annual growth rate (mm/y)	$\delta^{18}O_{shell\ correct}$	$\delta^{13}C_{shell\ correct}$
MO	12.68	1	12.68	-2.050	-0.937
MO	24.06	2	11.38	-1.520	-2.334
MO	31.65	3	7.59	-2.042	-2.872
MO	33.54	3.25	1.89	-0.399	-2.835
GO	30.43	-	-	-	-
CE	15.1	1	15.1	-2.053	0.105
CE	27.08	2	11.98	-1.421	-1.025
CE	32.21	2.75	5.13	-1.896	-3.911
SB	20.00	1	20.00	-1.348	-0.638
SB	28.66	2	8.66	-1.311	-1.087
SB	33.86	2.75	5.20	0.095	-1.147
CA	20.44	1	20.44	-1.101	-0.131
CA	30.58	2	10.14	-0.810	-0.925
CA	32.61	2.25	2.03	-2.060	-1.643

FIGURES

Fig. 1. Map of the Adriatic coastline indicating the sampling sites of *C. gallina* clams. Abbreviations and coordinates of the sites in decreasing order of latitude: MO, Monfalcone 45°42'N, 13°14'E; CH, Chioggia 45°12'N, 12°19'E; GO, Goro 44°47'N, 12°25'E; CE, Cesenatico 44°11'N, 12°26'E; SB, San Benedetto 43°5'N, 13°51'E; CA, Capoiale 41°55'N, 15°39'E.

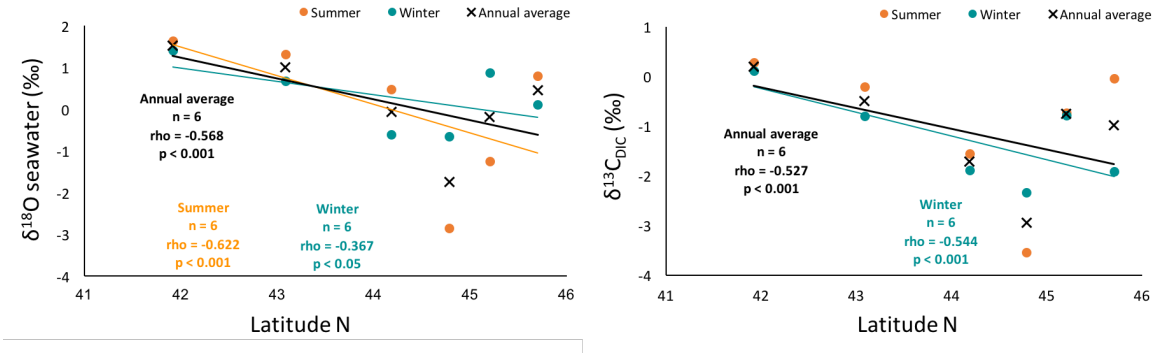

Figure 2. The relation between summer, winter and annual mean $\delta^{18}O_{seawater}$ and $\delta^{13}C_{DIC}$ with latitude in the 6 sites along the east coast of Italy (~400 km transect). Orange dots are summer values, green dots are the winter ones and black crosses are the annual isotope average between summer and winter. rho = Spearman's correlation coefficient.

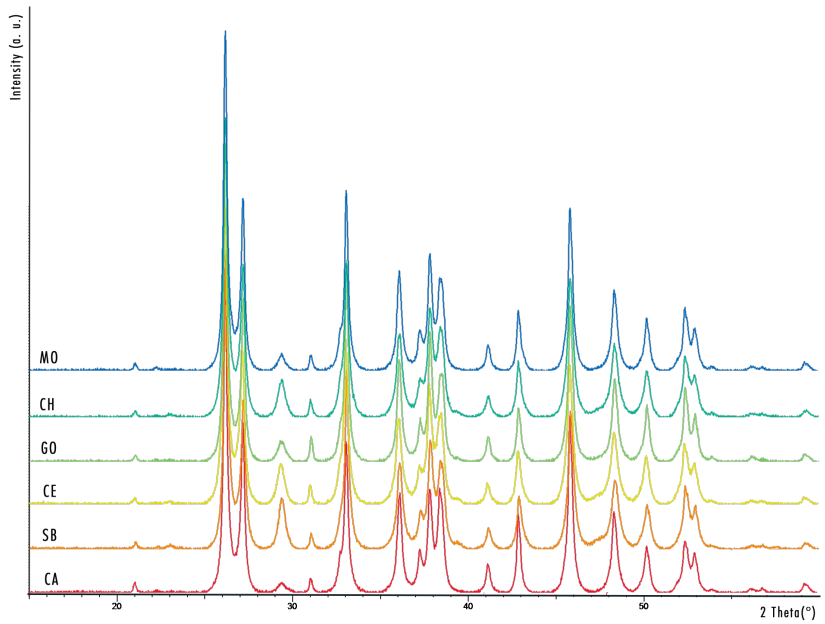

Fig. 3. X-ray powder diffraction (XRD) patterns from ground shells of *C. gallina*. A representative diffraction pattern is shown for each population, in decreasing order of latitude: MO (Monfalcone), CH (Chioggia), GO (Goro), CE (Cesenatico), SB (San Benedetto) and CA (Capoiale). All the peaks were assigned to aragonite.

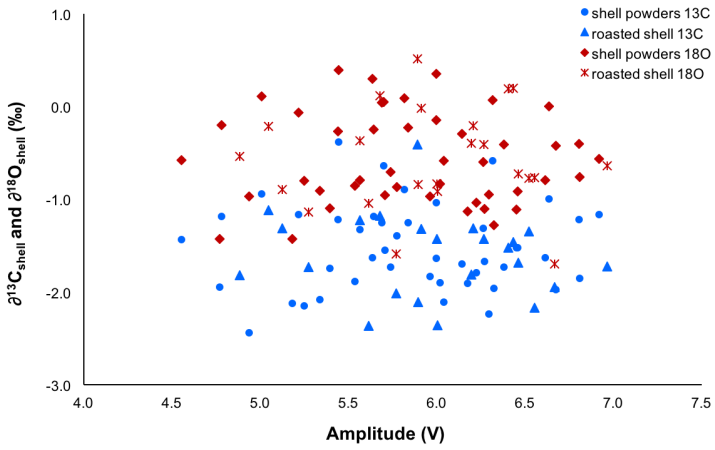

Fig. 4. Shell $\delta^{13}C$ and $\delta^{18}O$ values vs Amplitude (V). n=12 roasted and 12 not roasted samples.

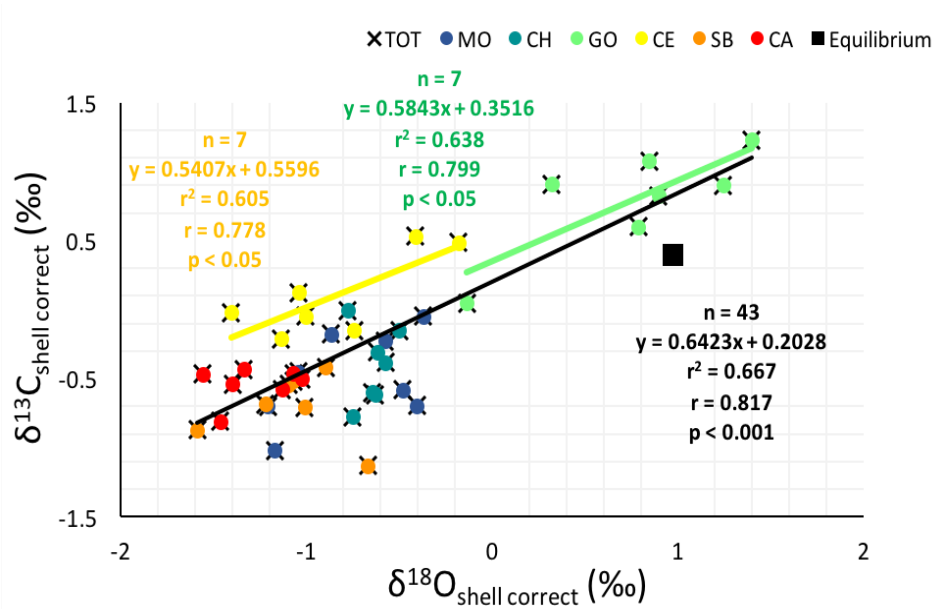

Fig. 5. Isotopic comparison among the six sites along the Adriatic coasts of Italy. MO (Monfalcone), CH (Chioggia), GO (Goro), CE (Cesenatico), SB (San Benedetto) and CA (Capoiale). Crosses depict the entire isotope dataset. r= Pearson's correlation coefficient. The black square indicates the estimated aragonite equilibrium value for average annual temperature for the 6 sites, using Grossman and Ku equation for oxygen and Romanek equation for carbon.

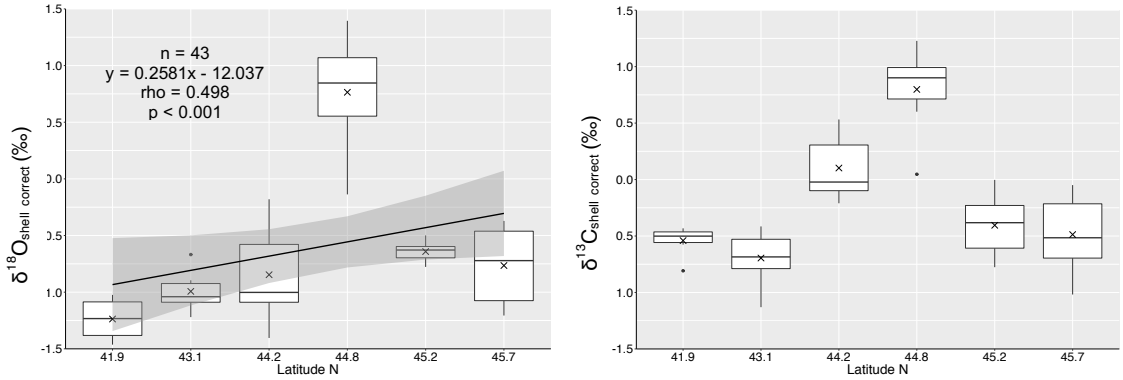

Fig. 6. The relation between shell $\delta^{18}O$ and $\delta^{13}C$ with latitude. n = 8 for Monfalcone, n = 7 for Chioggia, Goro, Cesenatico, San Benedetto and Capoiale. Crosses are the average values of each site. Grey ribbon depicts the 95% confidence interval. rho = Spearman's correlation coefficient.

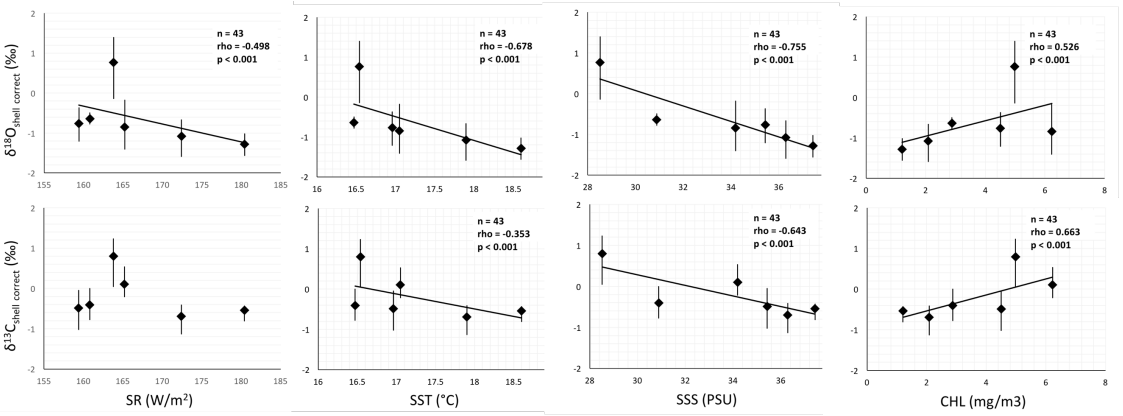

Fig. 7. Relations between $\delta^{18}O_{shell\ correct}$ and $\delta^{13}C_{shell\ correct}$ with environmental parameters. Diamonds depict average for each site. rho = Spearman's correlation coefficient.

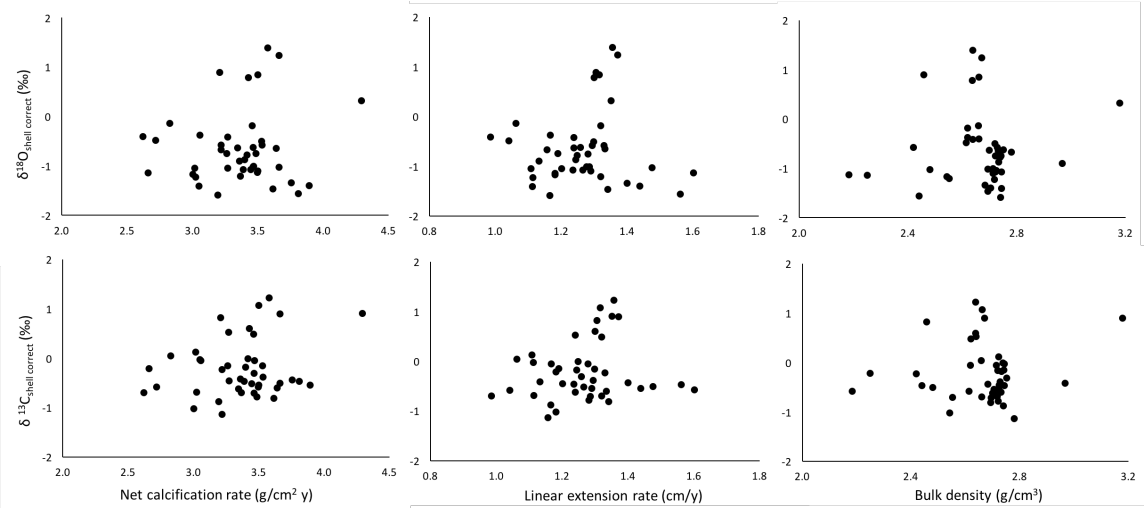

Fig. 8. The relations between $\delta^{18}O_{shell\ correct}$ and $\delta^{13}C_{shell\ correct}$ and net calcification rate (g/cm² y), linear extension rate (cm/y) and bulk density (g/cm³). Net calcification rate, linear extension rate and bulk density data were taken from Mancuso et al… (manuscript submitted to Scientific Reports.)

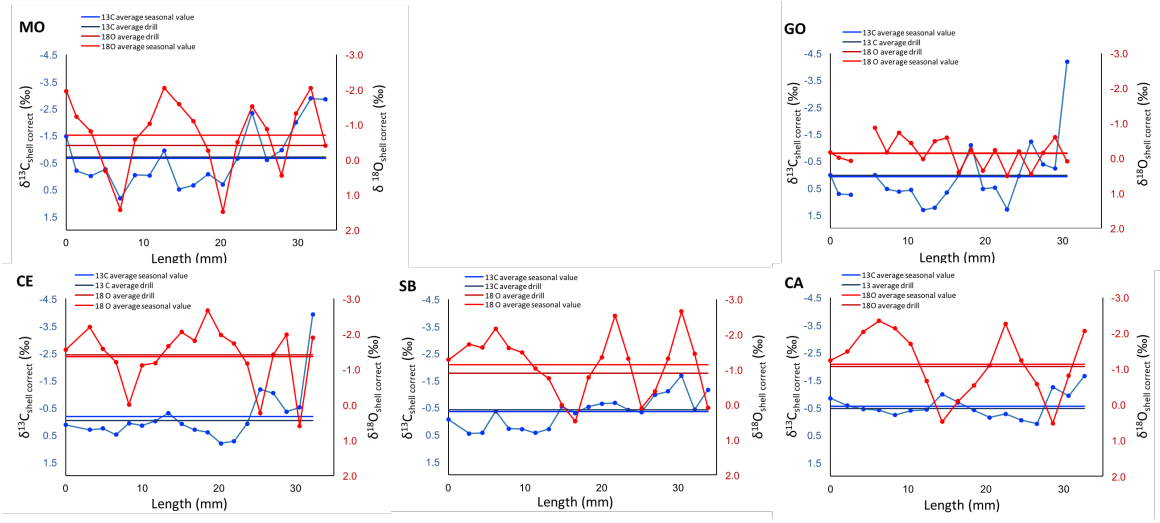

Fig. 9. $\delta^{18}O_{shell\ correct}$ and $\delta^{13}C_{shell\ correct}$ profiles along the shell growth axis. For each site are reported the average of seasonal values from spots along the growth axis and the value from drilling the entire shell. Blue lines represent $\delta^{13}C$ while red ones are $\delta^{18}O$. MO (Monfalcone), GO (Goro), CE (Cesenatico), SB (San Benedetto) and CA (Capoiale). Still no seasonal data for Chioggia.

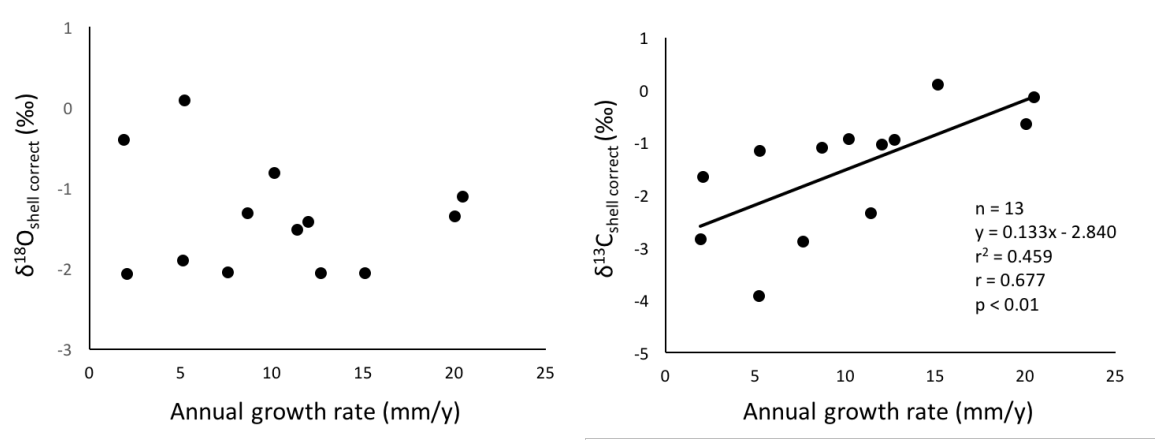

Fig. 10. Relationship between $\delta^{18}O_{shell\ correct}$ and $\delta^{13}C_{shell\ correct}$ and annual growth rates. Annual growth rates are calculated from the length and age at each year, by means of $\delta^{18}O$ profile along the shell growth axis.

Chapter 5

General conclusions

Environmental factors, such as solar radiation, temperature, salinity and food availability, all influence energy expenditure in marine organisms, especially in temperate seas, where marine organisms show marked seasonal patterns in growth, reproduction and abundance. To study the effect of environmental parameters on marine organisms, latitudinal gradients are useful natural laboratories, influencing variations in SR and SST and allowing to examine long-term effects on populations of the same species, adapted to different environmental conditions. Along the latitudinal gradient in the Adriatic Sea, the commercial clam *Chamelea gallina* was affected by different environmental conditions and variations found in shell parameters could be the outcome of phenotypic plasticity or a genetic adaptation of the populations subjected. Shell morphology of the most irradiated and warmest populations was characterized by lighter, thinner, more porous and fragile shells, leading to a modified shell resistance, likely affecting the economic aspects of fisheries and the survival of this species. At the same time, no effects of environment were detected on shell mineral composition and on the building blocks produced by the biomineralization process of the clam shells. *C. gallina* also showed variations in linear extension and net calcification along the latitudinal gradient and differences found in the growth rates among sites are probably due to local environmental conditions. Towards South, with higher temperatures, higher and steady salinity and oligotrophic conditions *C. gallina* enhanced linear extension and net calcification. At the opposite, prolonged exposure to low salinity, eutrophicated habitats and the presence of silt and clay in the substrate could stress the clams and negatively affect shell growth. These stressful habitat conditions heavily characterised the site under the influence of Po river delta in the Northern Adriatic Sea, as supported by high $\delta^{18}O/\delta^{13}C$ ratio found in Northern sites that confirmed lower calcification rates of *C. gallina* specimens in these sites. Shell isotope composition as a signature of environmental conditions, pointed out marked variations in shell $\delta^{18}O$ and $\delta^{13}C$ among sites and suggested that this species cannot be used for thermometry-based seawater reconstruction due to isotope depletion in comparison to the estimated isotopic equilibrium with ambient seawater.

Beside variations due to habitat conditions, differences were found in shell parameters during ontogeny and likely were the result of different biomineralization behaviour between immature and mature shells. *C. gallina* showed a marked decreasing extension rate with increasing length and clams of small size were more porous and less dense despite the bigger ones. Although these characteristics led to be more vulnerable to predators, they likely allowed to reach size at sexual maturity faster, promoting shell's linear extension rate. At the opposite, denser shells found in bigger and older individuals could be less vulnerable to predators, but the energetic cost expended in producing skeletal material was reduced by depressing linear extension rate.

This study highlights variations in shell properties and growth rates of the clam *Chamelea gallina* along a latitudinal gradient of environmental parameters and it can be considered a case study to gain further insight on the relationship between phenotype and growth and environment in calcifying marine organisms.

ACKOWLEDGMENTS

I would like to thank my supervisor Prof. Stefano Goffredo for inspiring me with his contagious passion for science and for his so precious suggestions and continuous support.

I thank also Prof Corrado Piccinetti to pass on interesting remarks of his extensive experience to me and for financial and logistic support.

Thanks to Prof Aldo Shemesh for giving me the opportunity to work at Weizmann Institute of Science and to his collaborators, especially Ruth Yam that took particular care to me like a mum and proposed important input for my abroad research. The months spent in Israel have been very formative and I could appreciate and enjoy the amazing country of Israel.

During these last three years I could count on my colleagues of the Lab in Fano and of MSG Lab in Bologna; they were always available for helping me and exchanging ideas.

Thank you to my family and friends, for encouraging me and giving funny and carefree moments during my PhD thesis writing… boogie dancing nights, beach volley challenges, relaxing on the beach.

Five years ago, when I arrived in this town, I couldn't imagine that I would have think to Fano like home. For this, I have to say a huge thank to my friends that welcome me and from the first moments together I understood they were exactly the friends I would have to find out. Ele, you were my first true friend here and you still are a fixed point on which I can rely on, grazie.

And to my friends from Lacchiarella, despite the distance, I know to can always enjoy and trust you. RdP, thanks to be patient, I would share more time with you, drinking cosmopolitan and chattering.

To Leo, that is getting to become almost wiser than me: "La differenza non è nelle cose che succedono, ma nel come reagiamo ad esse".

And last to you,

Mammut and Paput, who grew me with the idea that we can always do better and we don't give up. You taught me to be curious and wonder about the things around me, to desire exploring and thinking over. So grateful for encouraging me with positive attitude and open-mind.

To all of you,

Be bold and passionate!